

APPLIED SUPERCONDUCTIVITY (Industrial Applications)

Enzo Palmieri

ISTITUTO NAZIONALE DI FISICA NUCLEARE
Laboratori Nazionali di Legnaro

and

PADUA UNIVERSITY
Material Science and Engineering

CERN, Academic Training, Jan 18 2007

Lecture 2 of 3

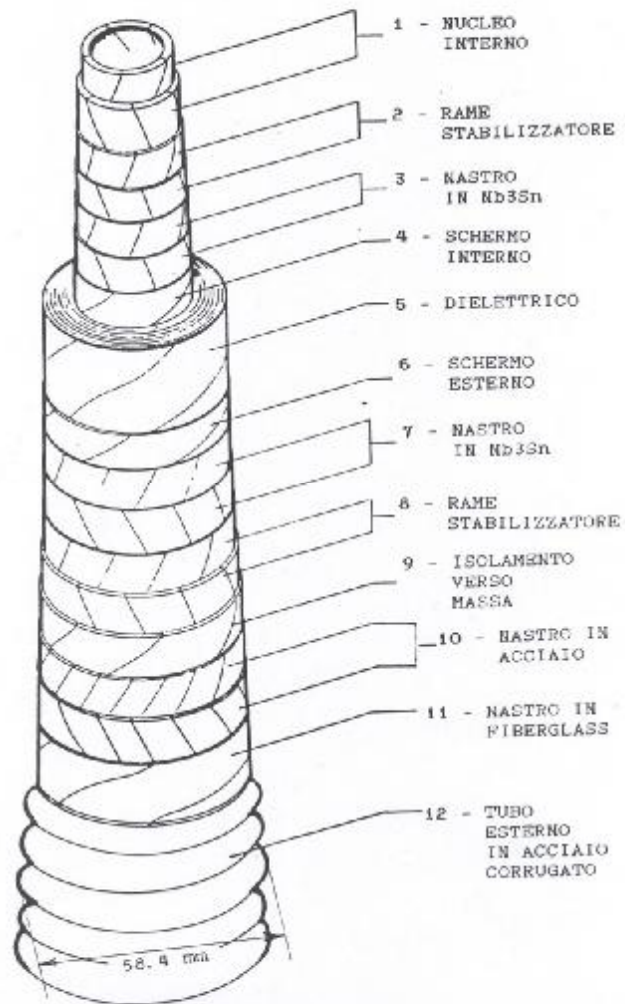


Fig.5 - Cavo flessibile superconduttore da 80 kV, 333 MVA [7.9]

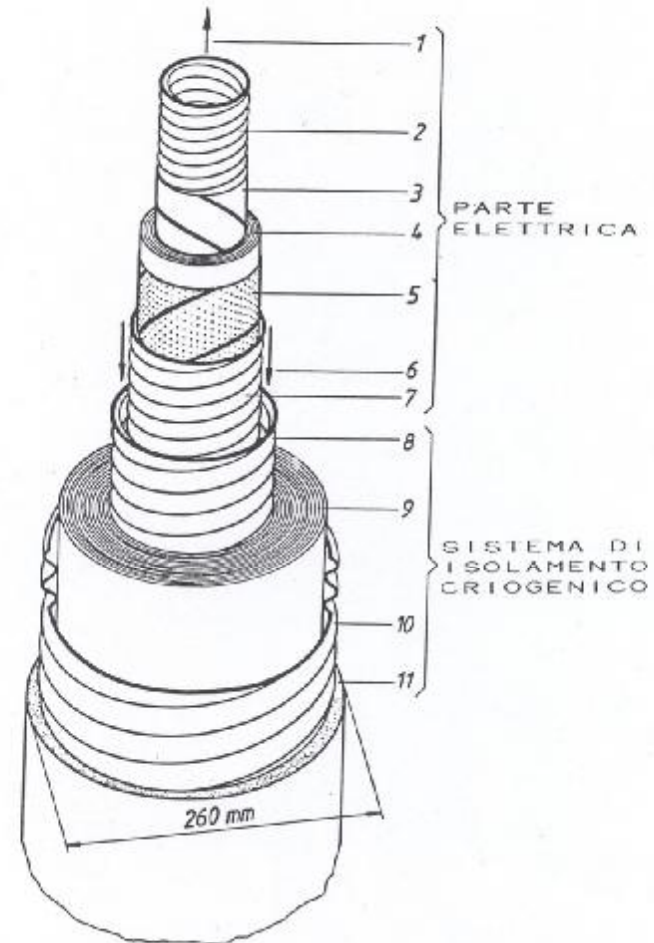


Fig.3 - Cavo superconduttore completamente flessibile da 110 kV, 333 MVA [5].
 1 e 6 elio supercritico di raffreddamento
 2 e 7 tubo in rame corrugato ricoperto di niobio
 strato livellatore
 3
 4 isolamento elettrico in nastro di carta impregnato d'elio
 5 schermo elettrostatico
 8 e 10 tubo metallico corrugato
 9 isolamento criogenico sotto vuoto
 11 foglie di EVC

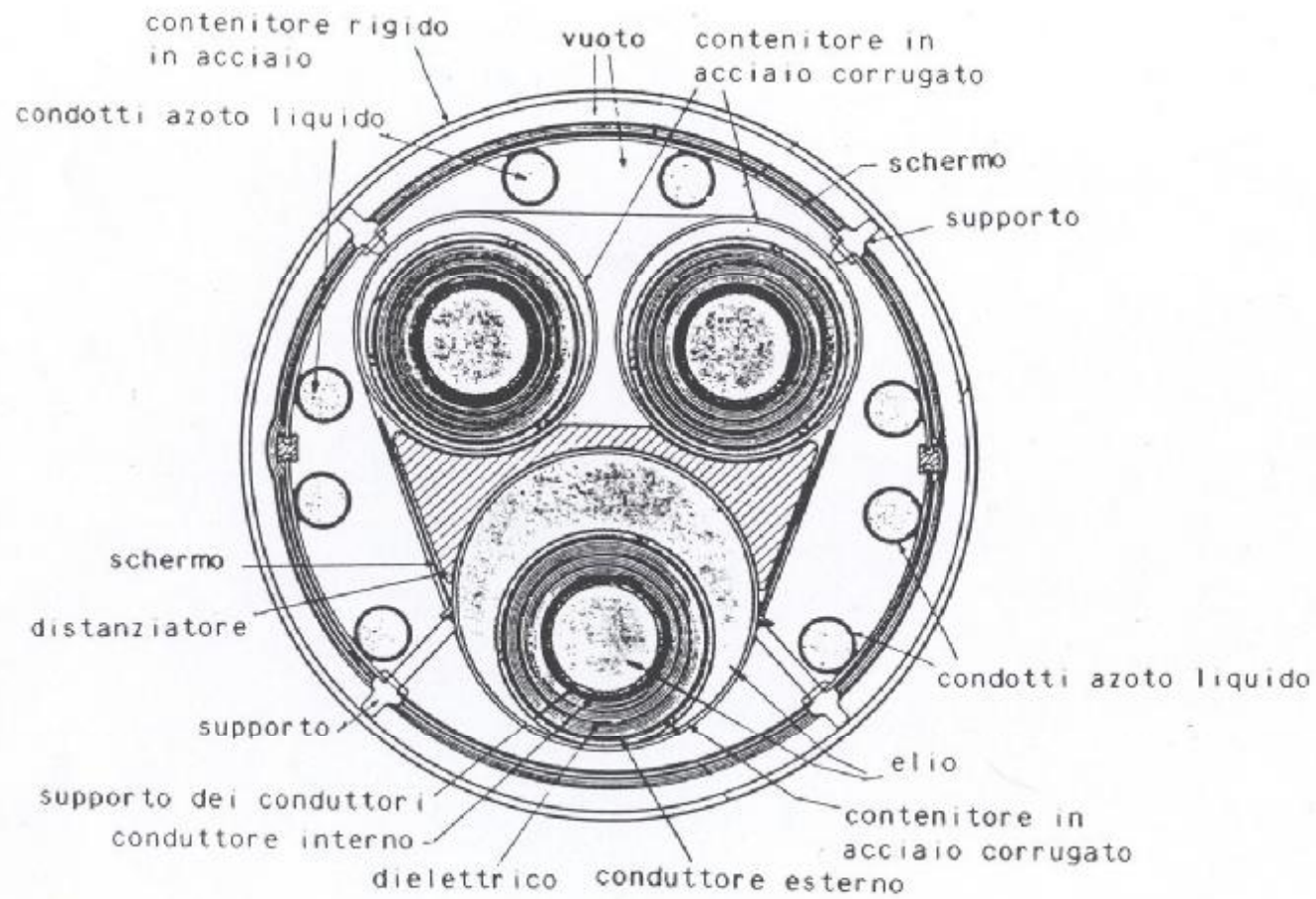
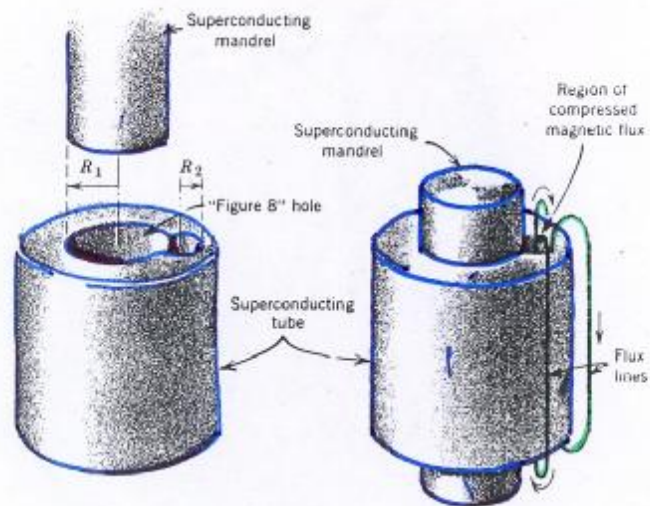
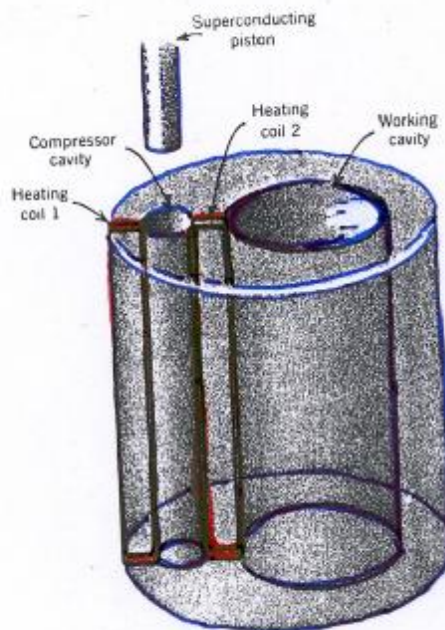


Fig.1 - Sezione schematica di un cavo flessibile superconduttore da 400 kV, 5 GW [14].

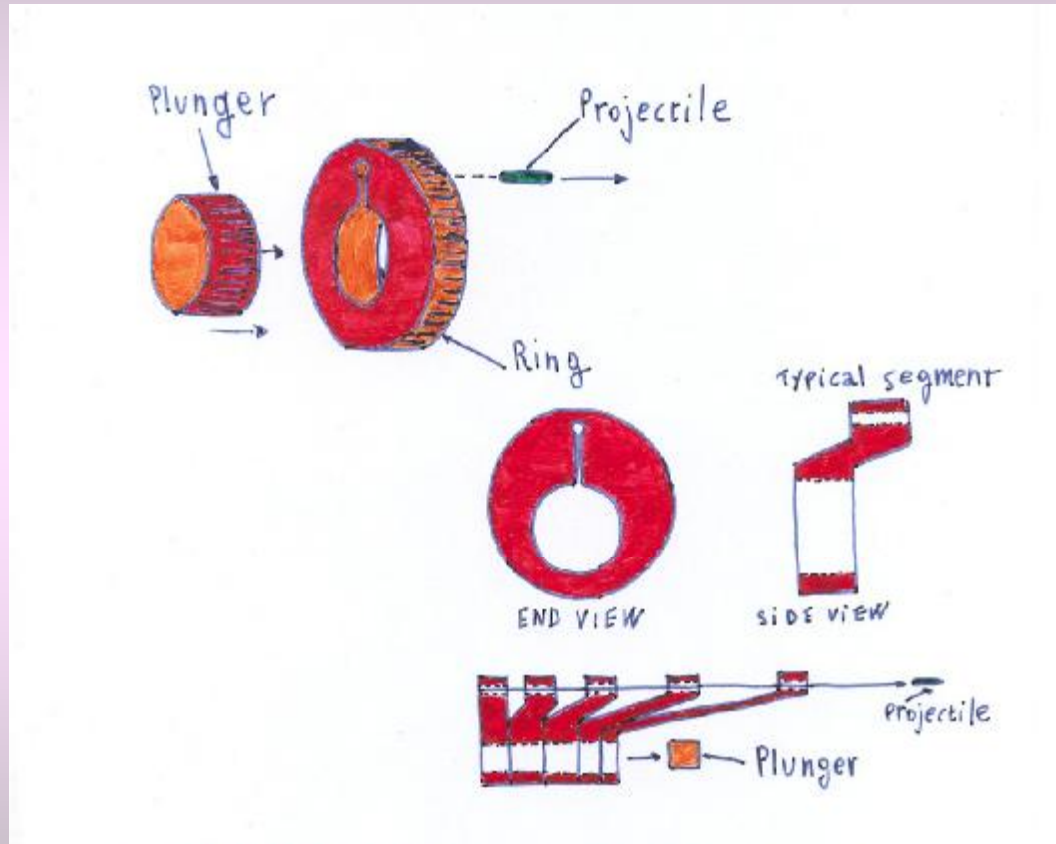


A flux compressor (Swartz and Rosner, 1962).



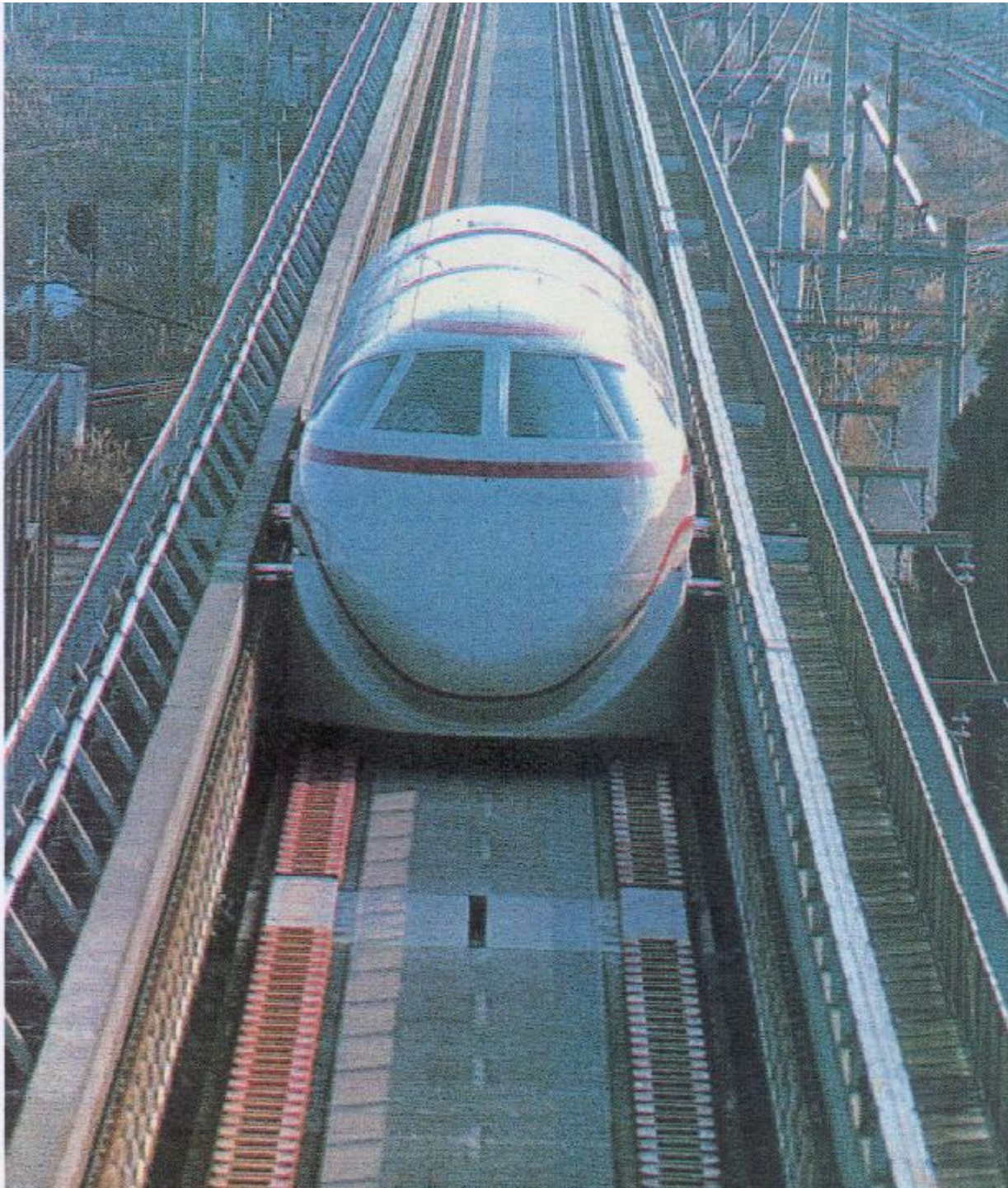
Cyclical flux pump.

The **MAGNETIC PROJECTILE LAUNCHER** would use magnetic flux compressed by a superconducting plunger in order to accelerate superconducting projectiles

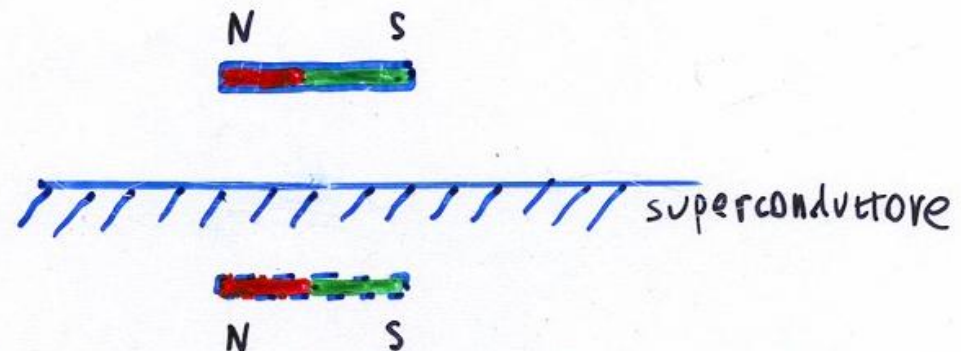


A MULTISEGMENT LAUNCHER would transfer a larger fraction of the total kinetic energy of the plunger to the projectile

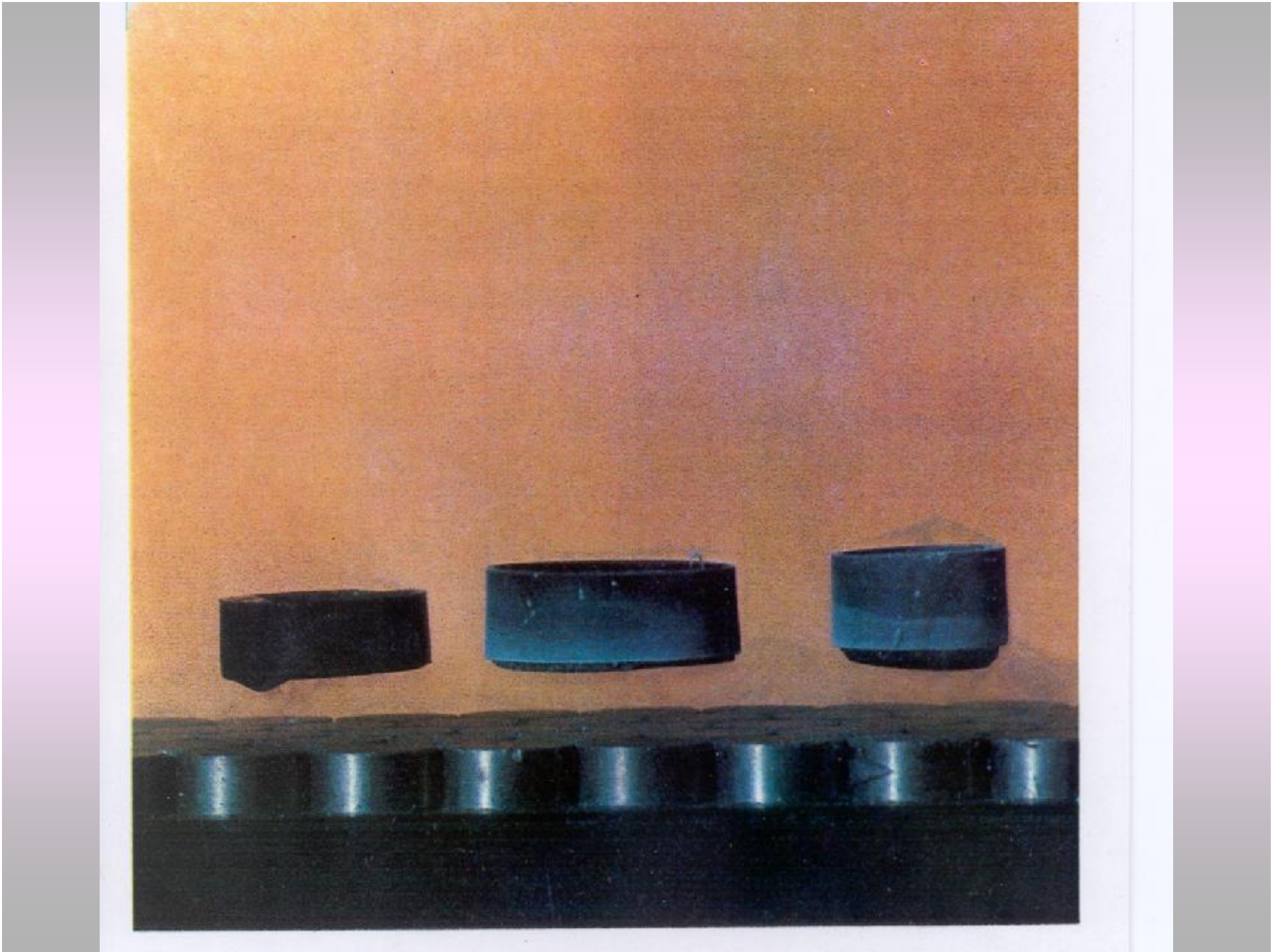
NASA, Tech brief., March 91

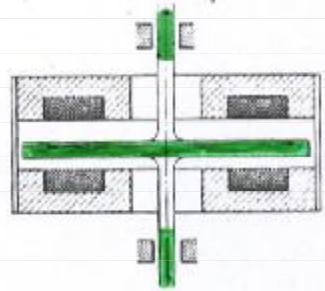


Magnetic Levitation

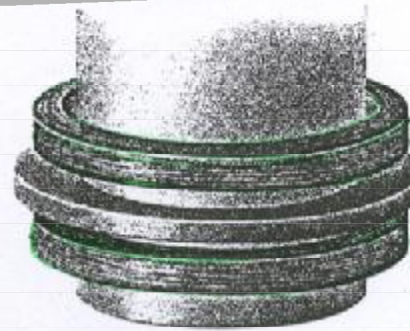


In absence of a superconductor, the magnet and its image produce the same field distribution

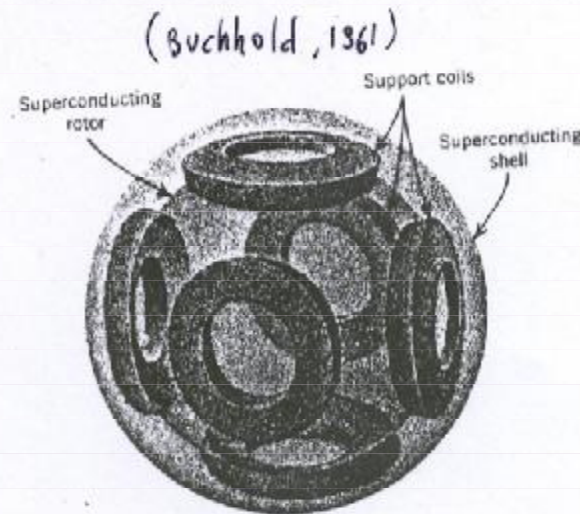
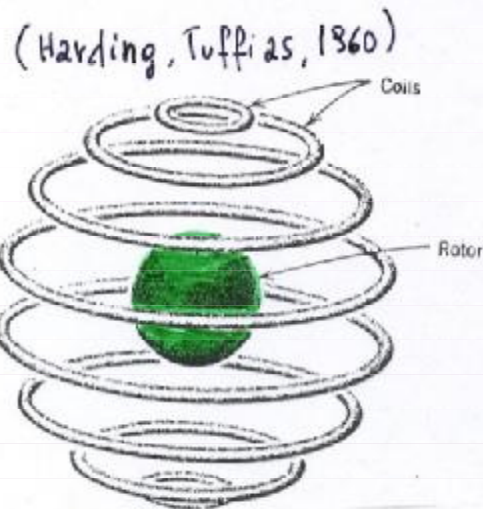




(Buchhold, 1961)
Supercond. Bearing



Ultra high vacuum, radiation cooling
losses due to magnetic flux trapping



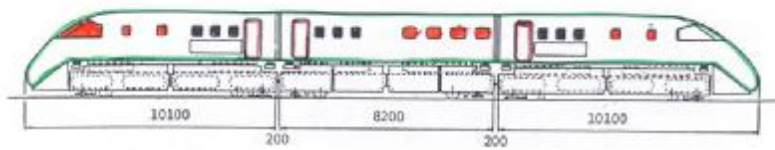
levitating trains do not work on the
principle of Meissner effect.

In 1842, Samuel Earnshaw proved what is now called Earnshaw's Theorem, which states that **there is no stable and static configuration of levitating permanent magnets.**

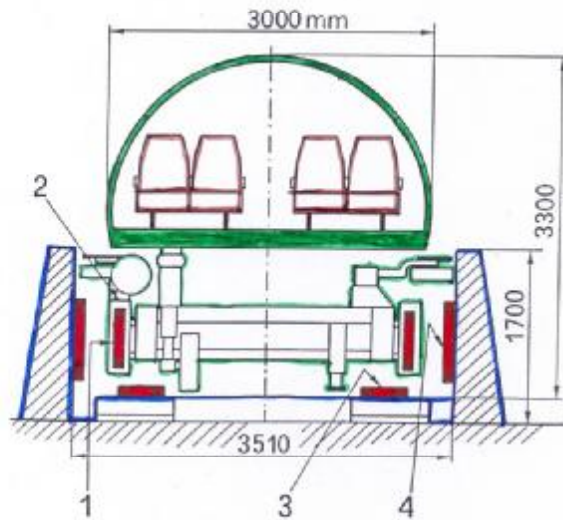
(See Earnshaw, S., On the nature of the molecular forces which regulate the constitution of the luminiferous ether., 1842, Trans. Camb. Phil. Soc., 7, pp 97-112.)



[NIST_Maglevwww.boulder.nist.gov...index.html](http://www.boulder.nist.gov...index.html).mov



a



b

Fig. 5 - Convoglio sperimentale MLU001 [8].
 (a) Profilo del convoglio e lunghezze dei tre veicoli interconnessi.
 (b) Sezione trasversale e principali dimensioni di uno dei tre veicoli e della pista a U.
 [1] - Bobine superconduttive in Nb-Ti; 2 - Criostato; 3 - Bobine di reazione; 4 - Bobina per la propulsione e la guida].

9

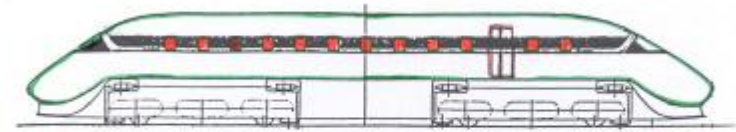
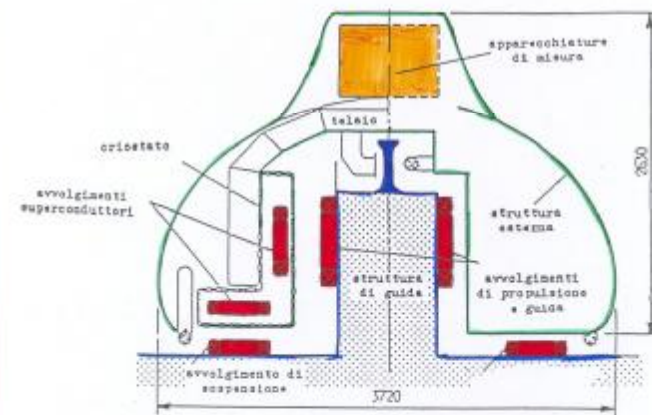


Fig. 7 - Profilo del veicolo sperimentale MLU002 [14,17].

Convoglio	
Dimensioni (lungh. x largh. x alt.) (m)	22,0 x 3,0 x 3,7
Peso (ton)	17
Posti a sedere	44
Bobine s.c.	12
Velocità (km/h)	420
Sospensione elettrodinamica	
Forza di levitazione (kN)	196
Altezza di levitazione (tra le bobine) (mm)	210
Franco effettivo (mm)	110
Motore LSM	
Forza di propulsione (kN)	80
Fasi	3
Frequenza (Hz)	0-28
Tensione (V)	5400
Corrente (A)	900

Tab. IV - Principali caratteristiche del prototipo MLU002 [9,14,17].



- Sezione trasversale del veicolo sperimentale ML500 e della pista a T.

Convoglio	
Dimensioni (lungh. x largh. x alt.) (m)	28.4 x 3.0 x 3.3
Peso (ton)	10
Posti a sedere	32
Bobine s.c. per veicolo	8
Velocità (un veicolo) (km/h)	400
Sospensione elettrodinamica	
Forza di levitazione (kN)	98
Altezza di levitazione (tra le bobine) (mm)	240
Franco effettivo (mm)	100
Motore LSM	
Forza di propulsione (per veicolo) (kN)	51
Fasi	3
Frequenza (Hz)	0+27
Tensione (V)	3000
Corrente (A)	1100
Pista	
Lunghezza (km)	7
Bobine di reazione	
dimensioni (m)	0.45 x 0.33
passo (m)	0.7
Bobine di armatura	
dimensioni (m)	1.1 x 0.7
passo (m)	1.4
Sezione (m)	42

Tab.II - Principali caratteristiche del prototipo MLU001 [7+9].



Transrapid Test Facility in Emsland, Germany

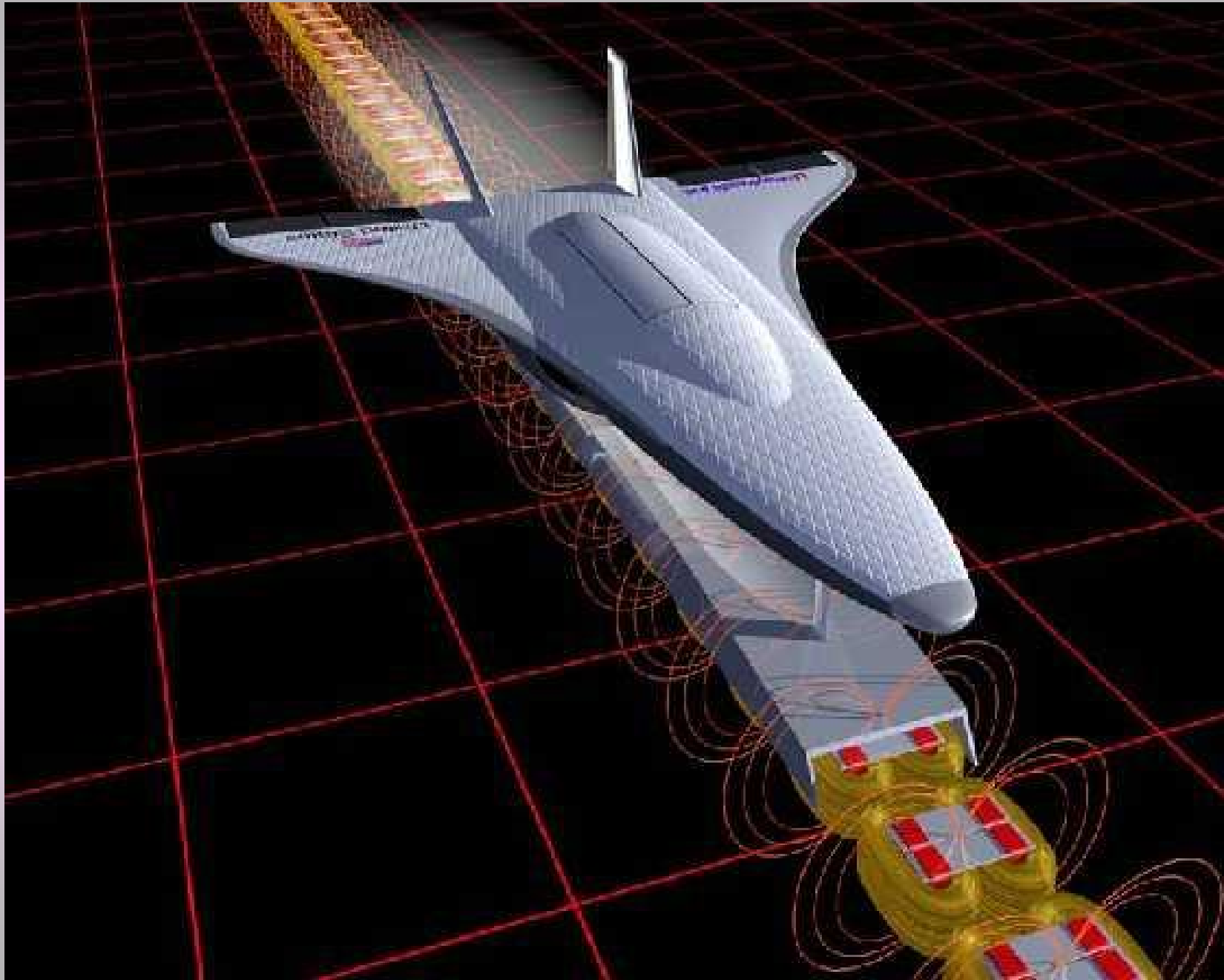


The Transrapid Test Facility first opened in 1984 at Emsland, Germany. Several generations of Transrapid trains have been tested on the 31.5-km track since then. The Transrapid 07 has covered a distance of more than 550,000 km at Emsland. More than 220,000 paying passengers from all over the world have ridden Transrapid on demonstration runs at speeds of up to 420 km/h. On June 10, 1993, the Transrapid 07 established a world record for passenger-carrying maglev vehicles when it reached a speed of 450 km/h (279mph). The Transrapid 08, a 3-section, passenger train began operating in 1999 and was built to obtain the type approval certification required for commercial operations. Designed for 550 km/h operation, the new train is lighter, more aerodynamic and quieter than its predecessor, the Transrapid 07.



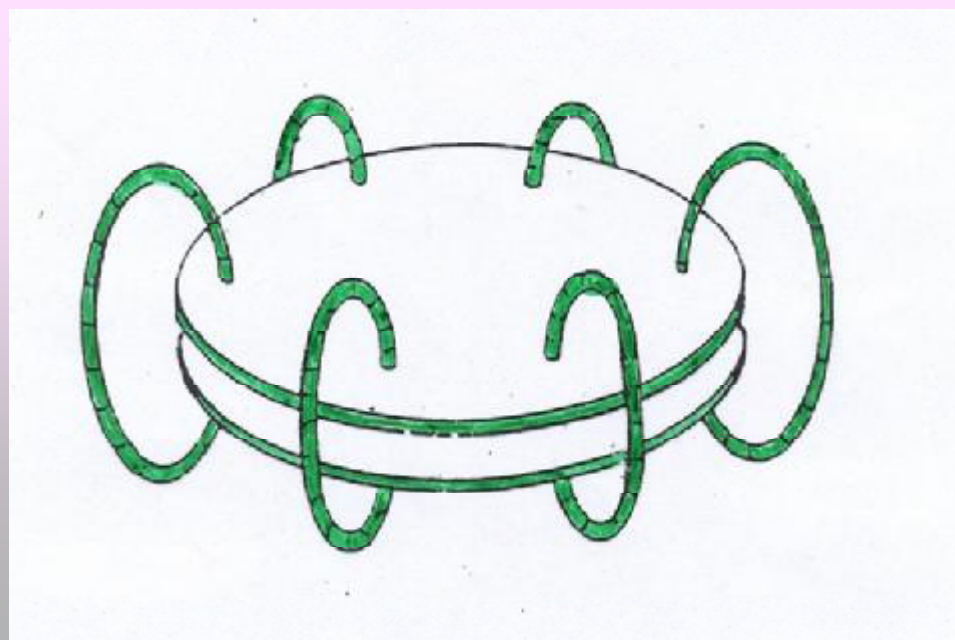
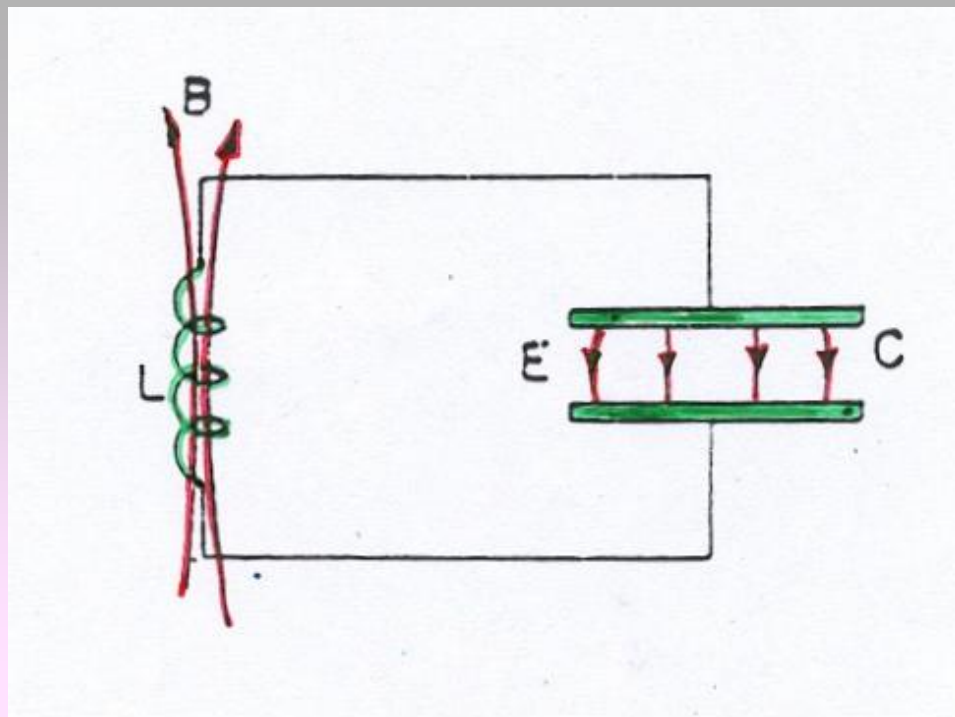
Maglev trains that wrap around their guideway are Maglev Monorails

(photo courtesy of Transrapid)

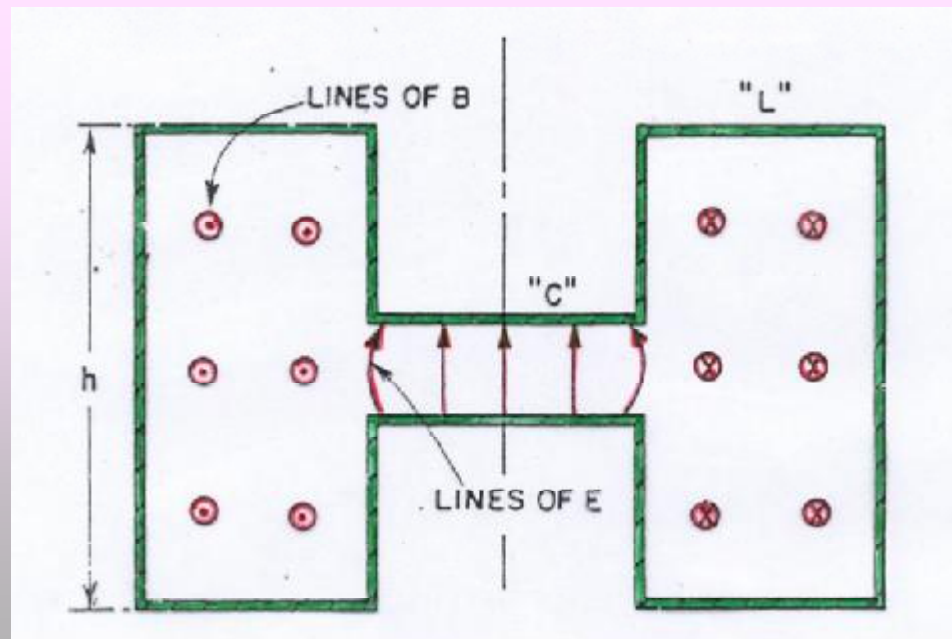
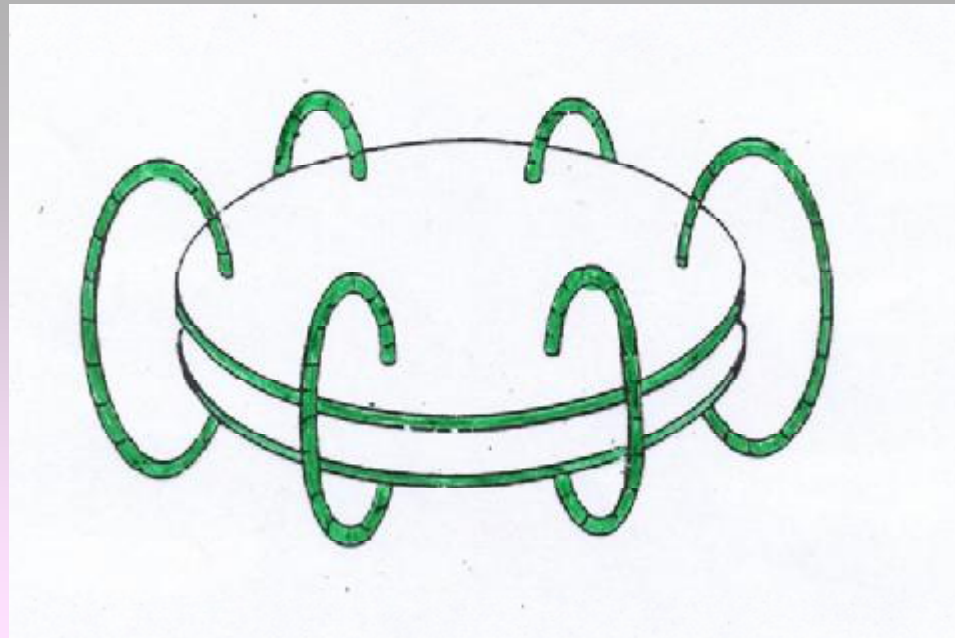




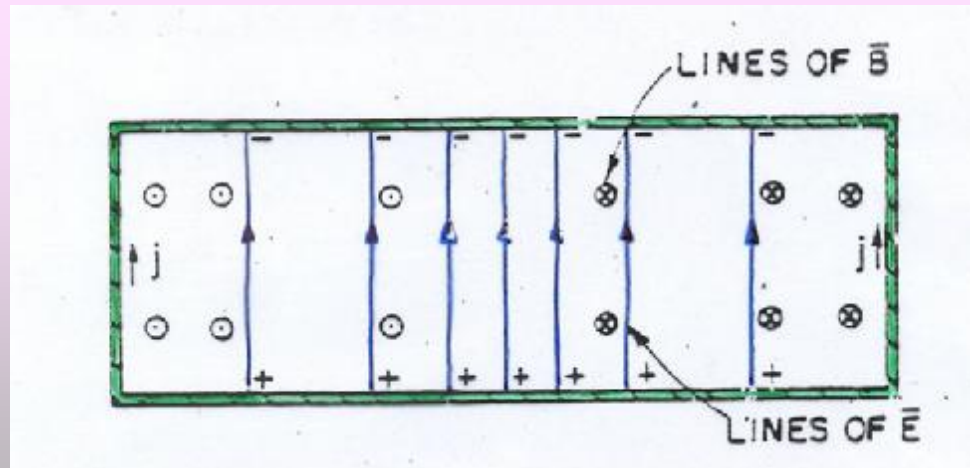
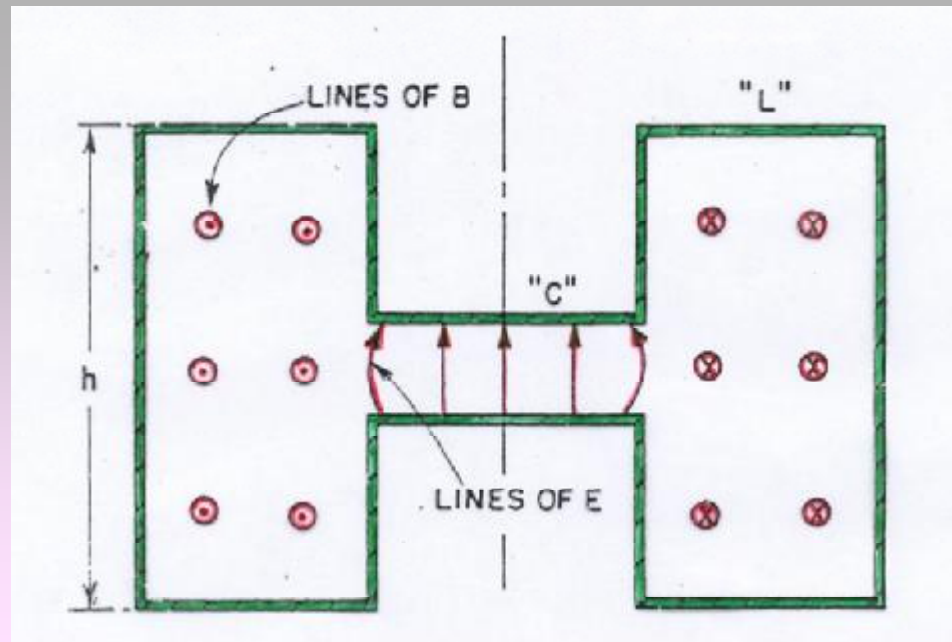
$$W = \frac{1}{\sqrt{LC}}$$

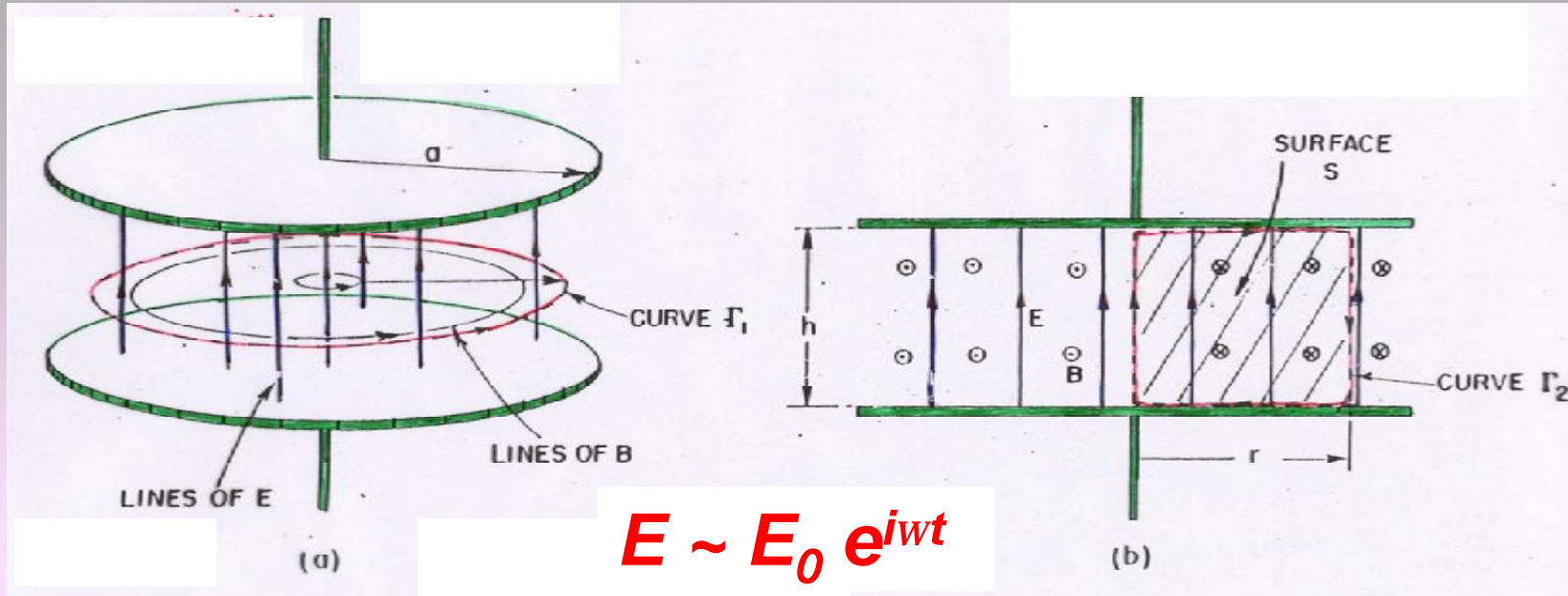


$$W = \frac{1}{\sqrt{LC}}$$



$$W = \frac{1}{\sqrt{LC}}$$





$$E \sim E_0 e^{i\omega t}$$

$$\oint_{\Gamma_1} \mathbf{B} \cdot d\mathbf{s} = \frac{1}{c^2} \cdot \frac{\partial}{\partial t} \int_{S_1} \mathbf{E} \cdot \mathbf{n} da$$

$$\oint_{\Gamma_2} \mathbf{E} \cdot d\mathbf{s} = -\frac{\partial}{\partial t} \int_{S_2} \mathbf{B} \cdot \mathbf{n} da$$

$$B = \frac{i\omega\Gamma}{2c^2} \cdot E_0 e^{i\omega t}$$

$$-E_1(r)h = -h \frac{\partial}{\partial t} \int B_1(r) dr$$

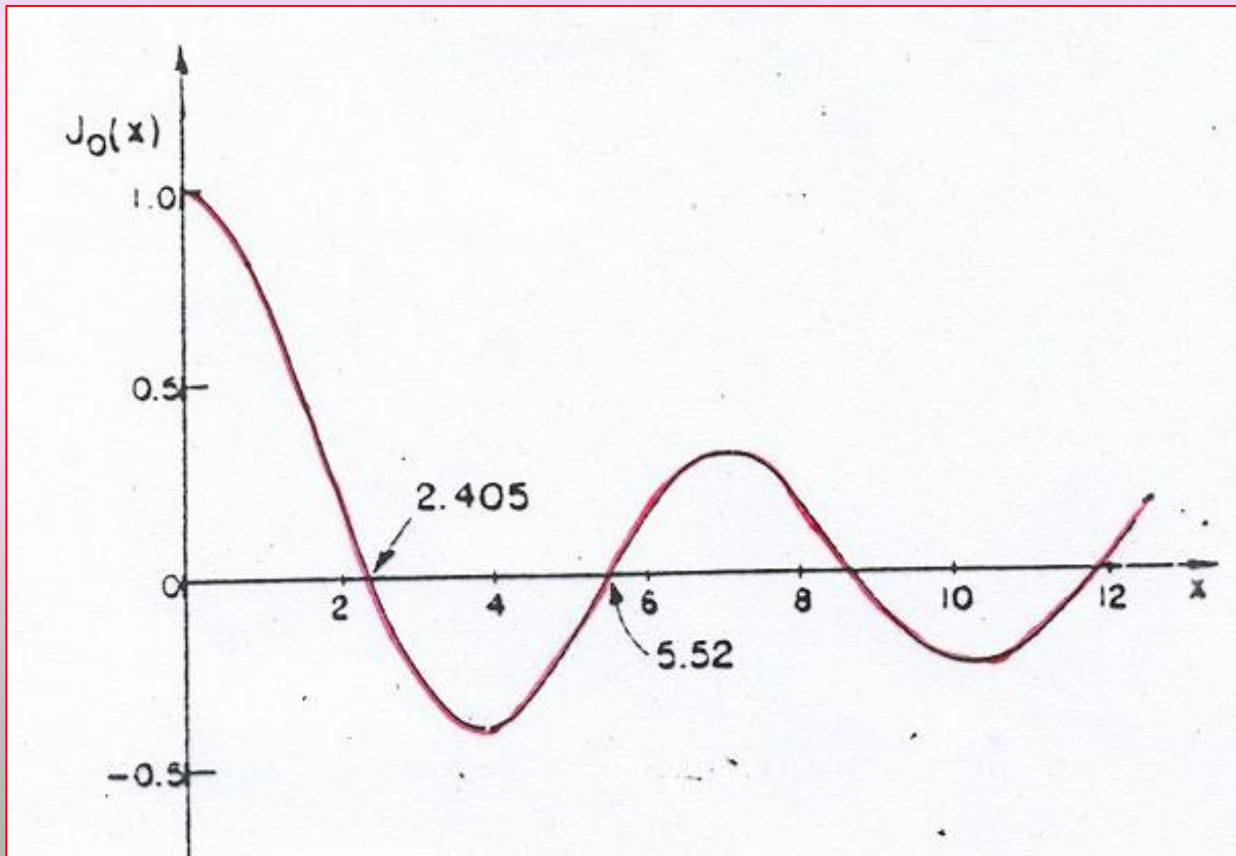
$E_0 \rightarrow B_0 \rightarrow E_0 + E_1 \rightarrow B_0 + B_1 \rightarrow E_0 + E_1 + E_2 \rightarrow$

$$E = E_0 e^{i\omega t} \left[1 - \frac{1}{(1!)^2} \left(\frac{\omega r}{2c} \right)^2 + \frac{1}{(2!)^2} \left(\frac{\omega r}{2c} \right)^4 + \frac{1}{(3!)^2} \left(\frac{\omega r}{2c} \right)^6 + \dots \right]$$

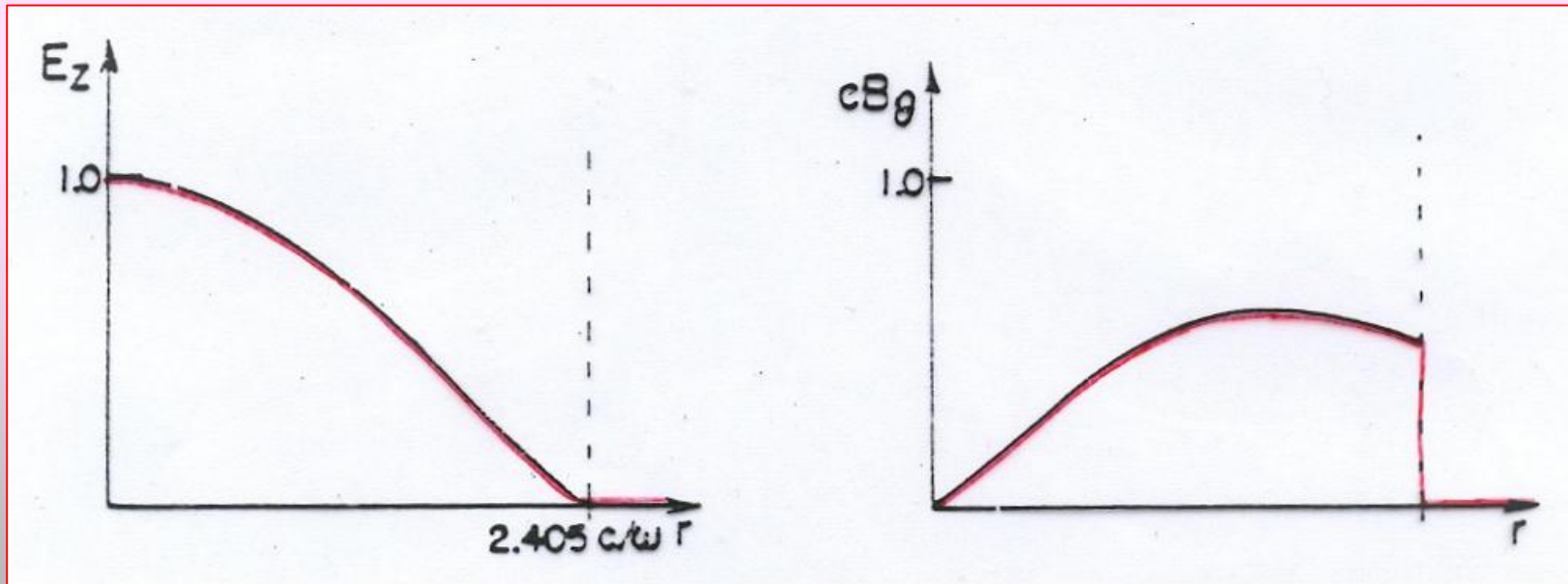
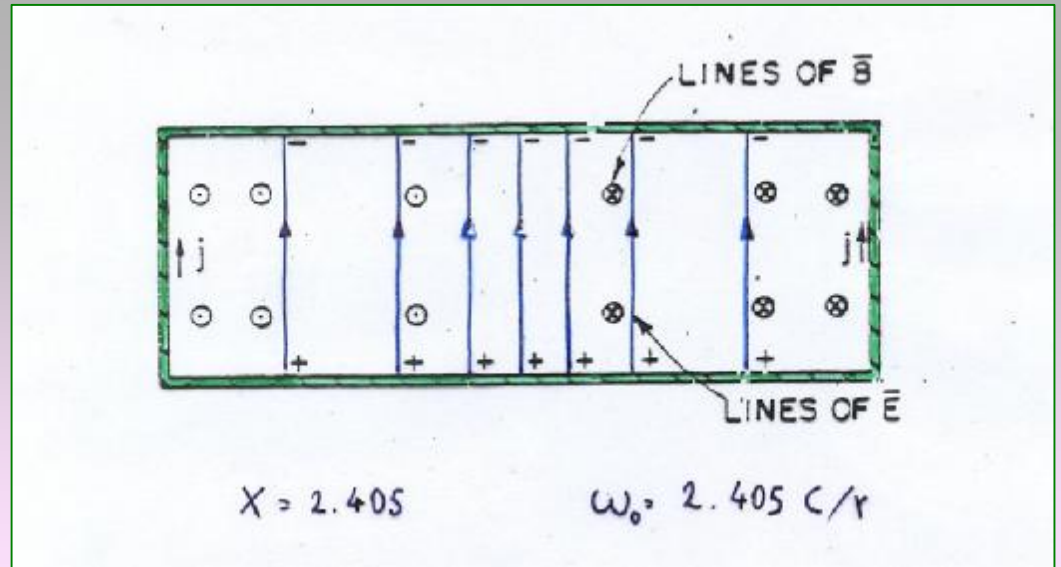
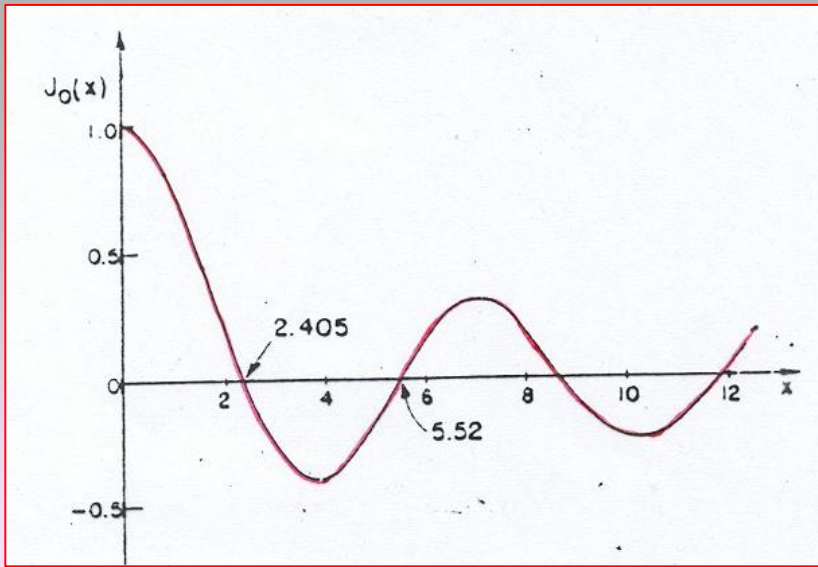
$$E = E_0 e^{i\omega t} \left[1 - \frac{1}{(1!)^2} \left(\frac{\omega r}{2c} \right)^2 + \frac{1}{(2!)^2} \left(\frac{\omega r}{2c} \right)^4 + \frac{1}{(3!)^2} \left(\frac{\omega r}{2c} \right)^6 + \dots \right]$$

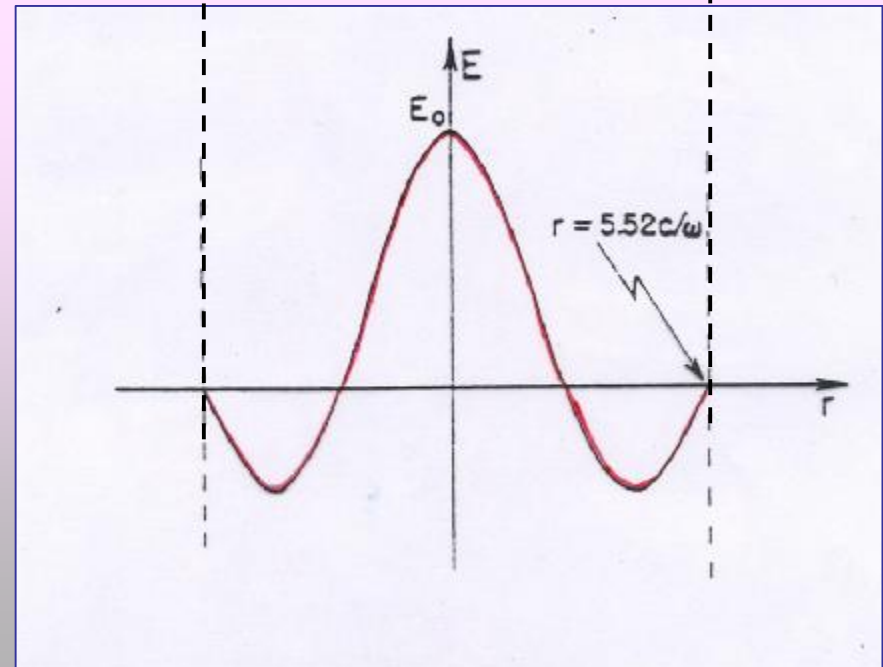
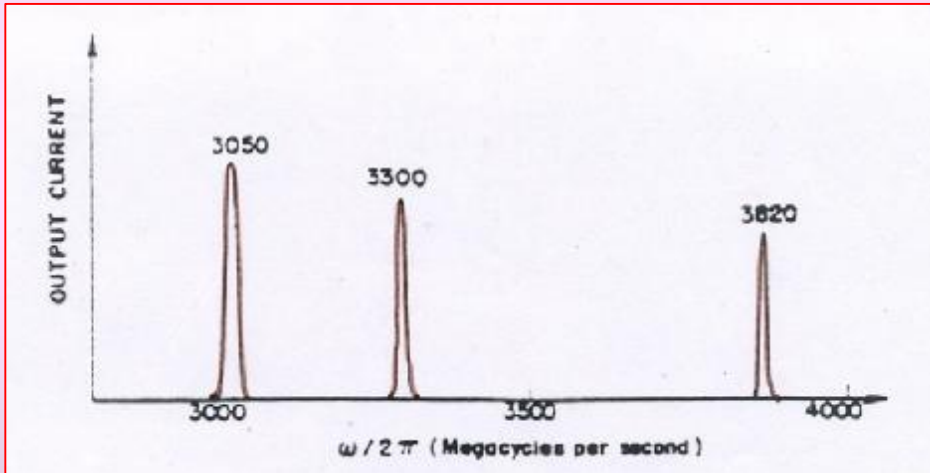
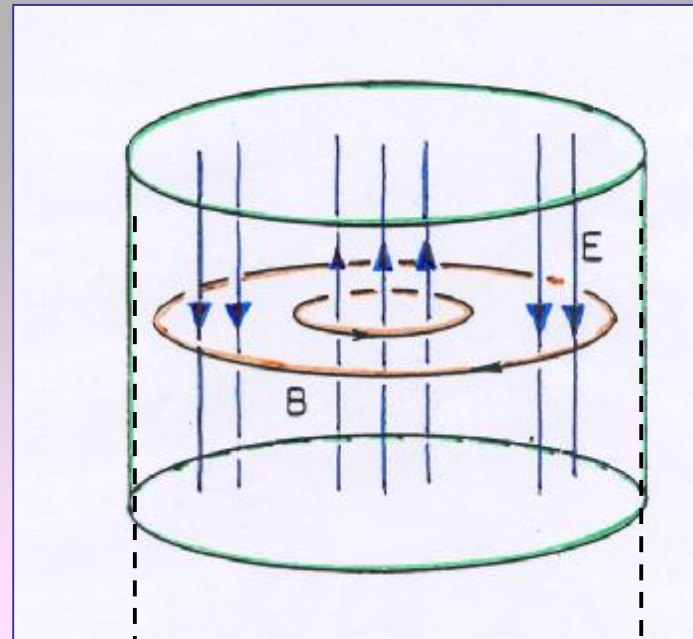
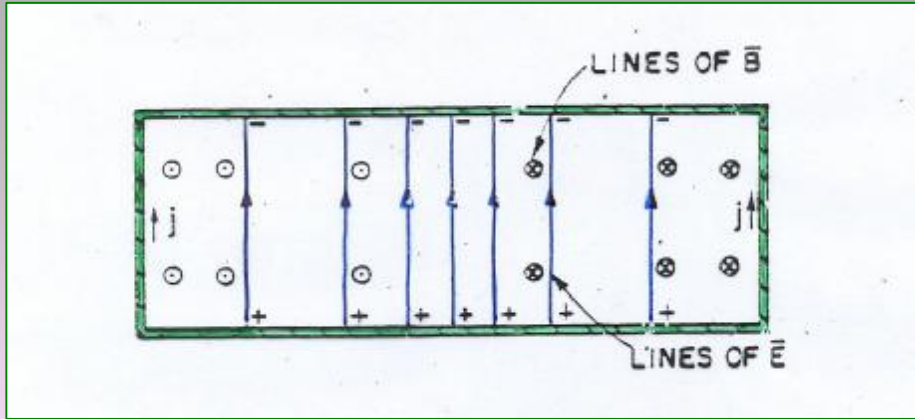
$$J_0(x) = \left[1 - \frac{1}{(1!)^2} \left(\frac{x}{2} \right)^2 + \frac{1}{(2!)^2} \left(\frac{x}{2} \right)^4 + \frac{1}{(3!)^2} \left(\frac{x}{2} \right)^6 + \dots \right]$$

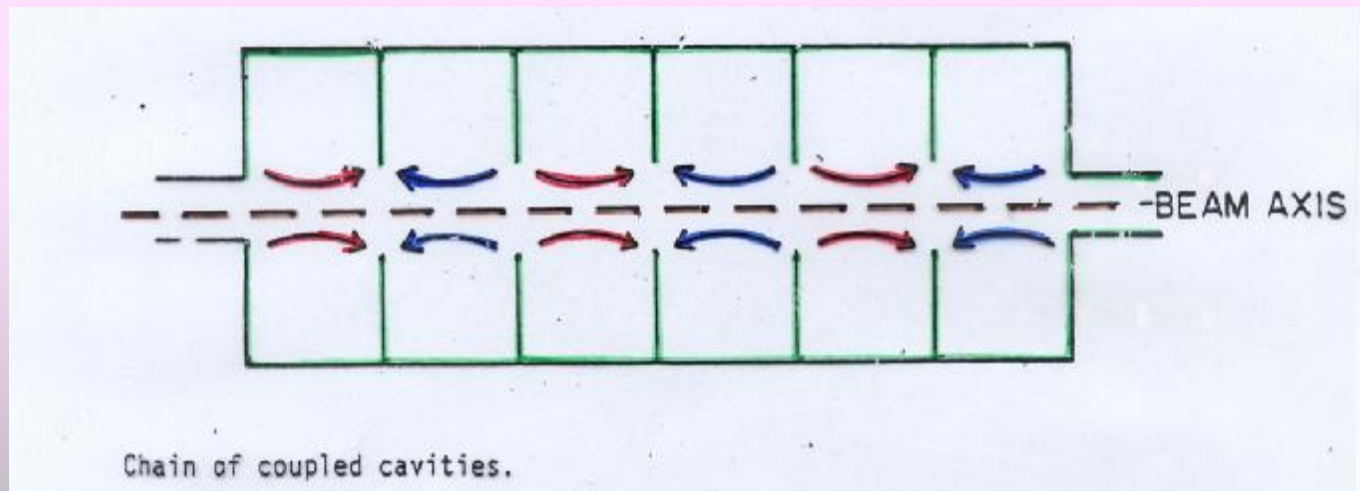
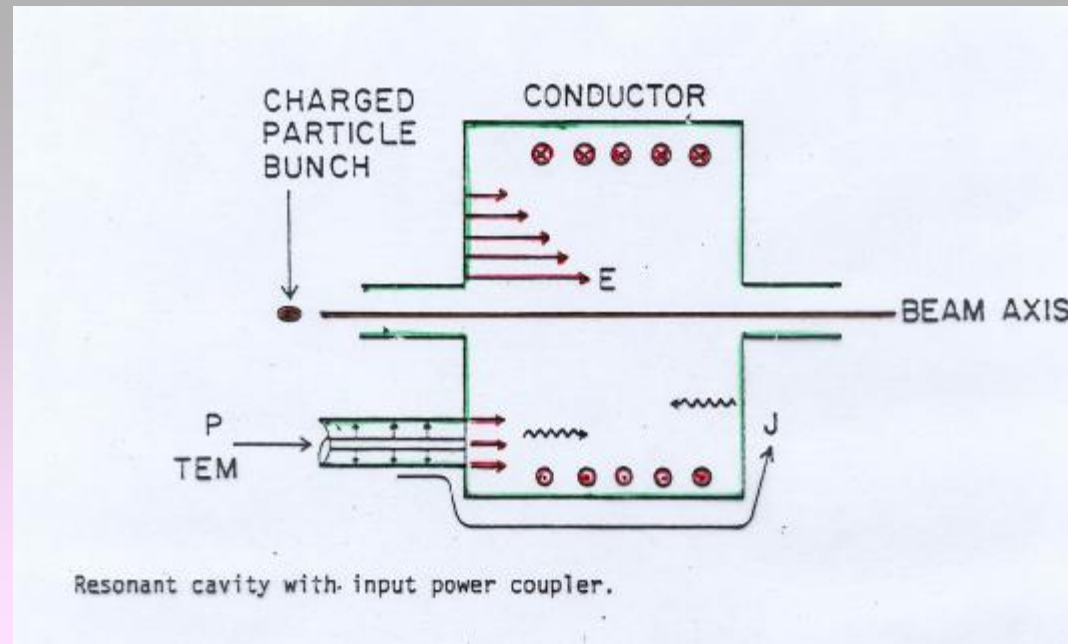
$$x = \frac{\omega r}{c}$$



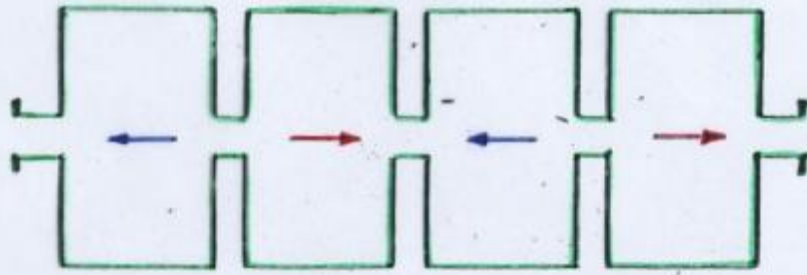
$$E(r, \omega) = J_0 \left(\frac{\omega r}{c} \right)$$



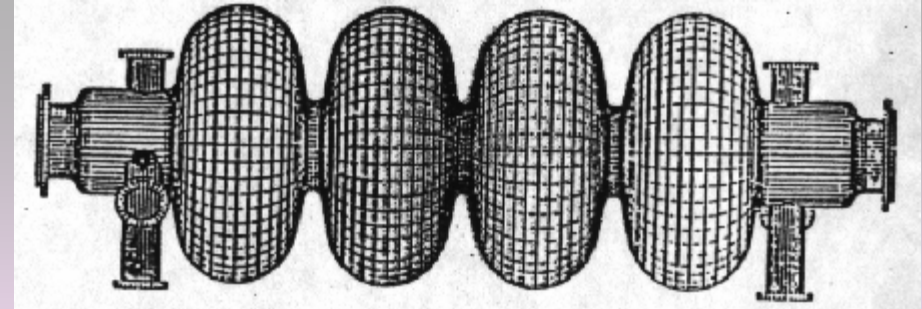




By **Radiofrequency** one can accelerate particles to high energy without the need of the **equivalent high static fields**



Chain of weakly coupled pill-box cavities representing an accelerator module

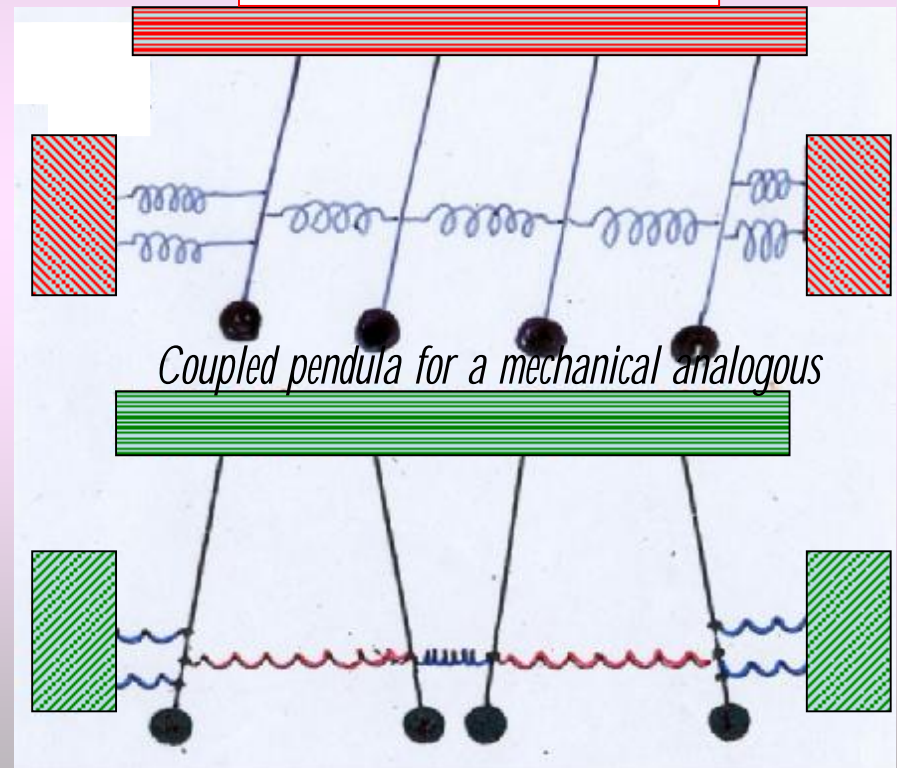


There are N eigen-modes for such an oscillating system

$$w_q = w_0 \cdot \left(1 + k(1 - \cos a_q) \right)$$

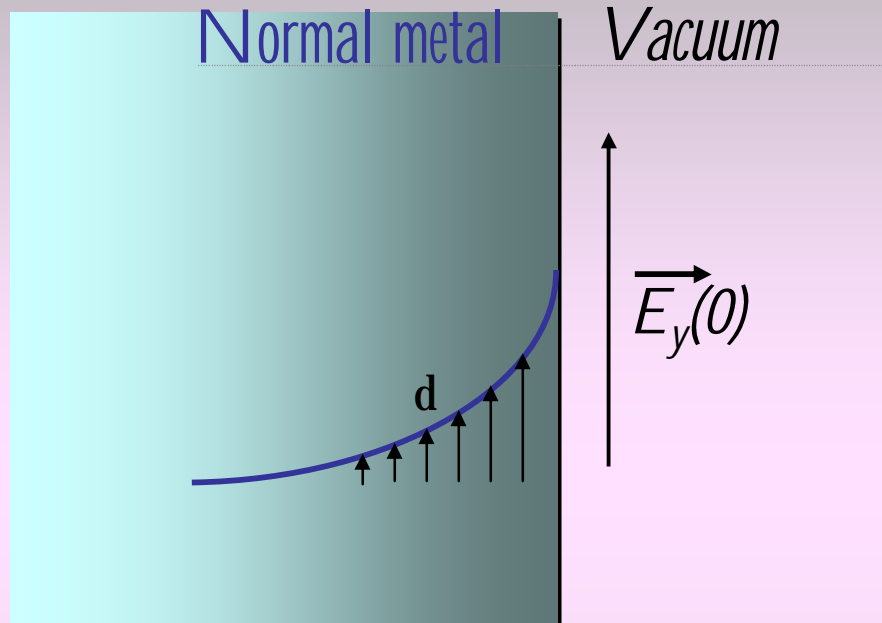
The smallest RF losses

Zero mode



p-mode

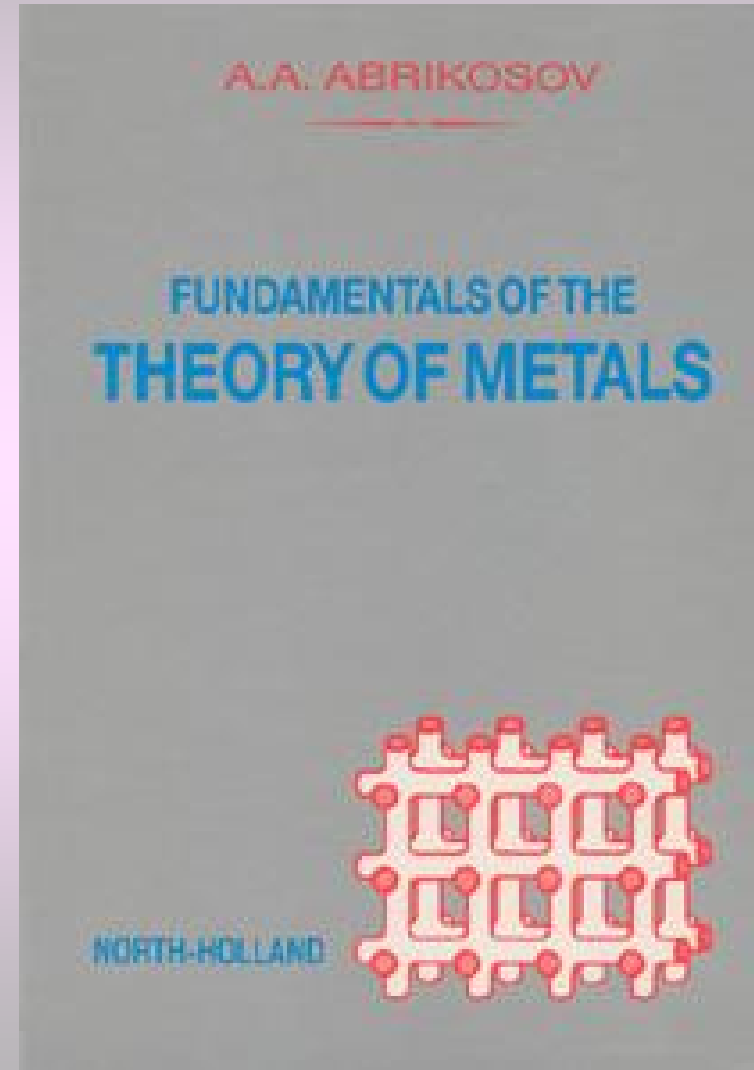
Normal metals in RadioFrequency and the normal skin effect



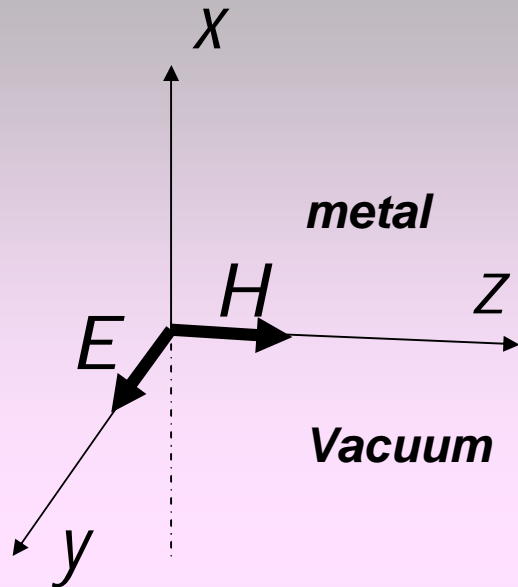
$$H(x, t) = H_0 e^{i(kx - \omega t)}$$

$$k = k_1 + i k_2$$

$$d = \left[\frac{2}{\omega \mu \sigma} \right]^{\frac{1}{2}}$$



THE ELECTROMAGNETIC RESPONSE OF A METAL



For a semi-infinite conductor that fills the $+X$ half-space and has a plane surface at $X = 0$

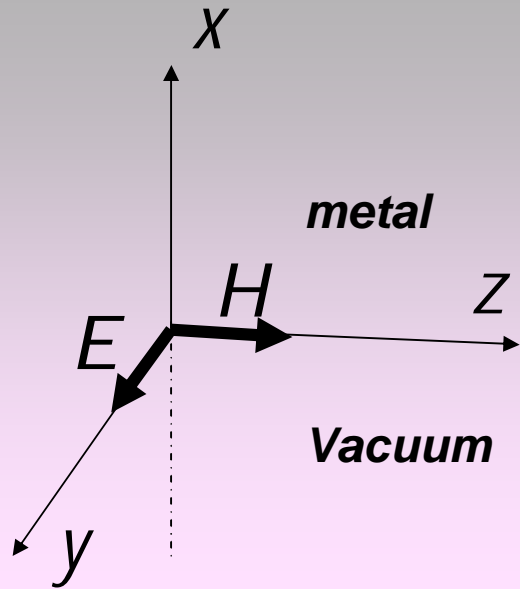
$$H(x) = H(0)e^{i(kx - \omega t)}$$

the **Surface Impedance** is defined as:



$$Z \equiv \frac{E_y(0)}{\int_0^\infty J_y(x) dx} = \frac{4\pi E_y(0)}{c H_z(0)}$$





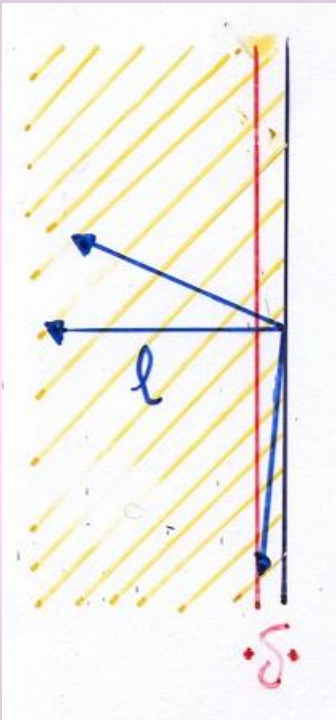
$$Z_S = R_S - iX_S \equiv \frac{E_y(0)}{\int_0^\infty J_y(x) dx} = \frac{4p}{c} \frac{E_y(0)}{H_z(0)}$$

$$R_S = X_S = \left[\frac{m\omega}{2s} \right]^{\frac{1}{2}} = \frac{r}{d}$$

$$d = \left[\frac{2}{\omega m s} \right]^{\frac{1}{2}}$$

The Anomalous Skin Effect

$$\omega \nearrow ; T \searrow \longrightarrow \delta \searrow$$

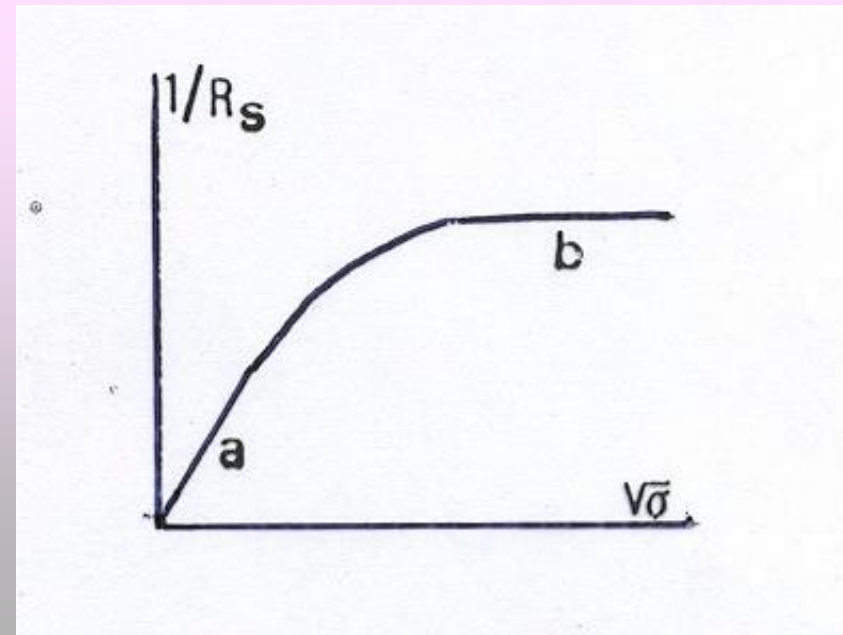


$$\vec{J}(\vec{r}) = \sigma \vec{E}(\vec{r})$$

$$\vec{J}(\vec{r}) = \int_{\mathbf{1}} f(\vec{r}_1 - \vec{r}) \cdot \vec{E}(\vec{r}_1) d\vec{r}_1$$

$$n_{eff} \approx n \left(\frac{d}{\mathbf{1}} \right)$$

$$\sigma_{eff} \approx \sigma \left(\frac{d}{\mathbf{1}} \right)$$



Beijing 2004 - International Conference on High Energy Physics



International Technology Recommendation Panel of the International Committee for Future Accelerators (ICFA)

Front line from left to right:

Akira Masaike, George Kalmus, Volker Soergel, **Barry Barish**, Giorgio Bellettini, Hirotaka Sugawara, Paul Grannis

Back line from left to right:

Gyung-Su Lee, Jean-Eude Augustin, David Plane, Jonathan Bagger, Norbert Holtkamp, Katsunobu Oide



La commissione, presieduta da Barry Barish, aveva il compito di scegliere tra la tecnologia normal-conduttiva o superconduttiva per l'International Linear Collider (ILC)

“...Both the 'warm' technology and the 'cold' superconducting technology would work for a linear collider... Each offers its own advantages, and each represents many years of R&D by teams of extremely talented and dedicated scientists and engineers. At this stage it would be too costly and time consuming to develop both technologies toward construction. ...”

“... We based our decision on a set of criteria that addressed scientific, technical, cost, schedule, operability issues for each technology, as well as their wider impacts on the field and beyond...”

“...On the basis of that assessment, we recommend that the linear collider be based on superconducting rf technology...”

Barry Barish

“...Both the 'warm' technology and the 'cold' superconducting technology would work for a linear collider... Each offers its own advantages, and each represents many years of R&D by teams of extremely talented and dedicated scientists and engineers. At this stage it would be too costly and time consuming to develop both technologies toward construction. ...”

“...On the basis of that assessment, we recommend that the linear collider be based on superconducting rf technology...”

Barry Barish



First ILC Workshop

Towards an International Design of a Linear Collider

November 13th (Sat) through 15th (Mon), 2004

KEK, High Energy Accelerator Research Organization
1-1 Oho, Tsukuba, Ibaraki 305-0801, Japan

Program Committee:

Kaoru Yokoya (KEK), Hitoshi Hayano (KEK),
Kenji Sato (KEK), David Burke (SLAC),
Steve Holmes (FNAL), Gerald Dugan (Cornell),
Nick Walker (DESY), Jean-Pierre Delahaye (CERN),
Gloria Napoli (CEA/Saclay)



International Advisory Committee:

Robert Aymar (CERN), Albrecht Wagner (DESY),
Michael Witmerli (FNAL), Yoji Totsuka (KEK),
Jonathan Dorfan (SLAC), Won Namkung (PAL),
Brian Foster (Oxford), Maury Tigner (Cornell),
Hecheng Chen (IHEP), Alexander Skisinsky (BNP),
Carlos Garcia Canal (JUNLP),
Sachio Komamiya (Tokyo), Paul Grimm (SUNY)

Local Organizing Committee:

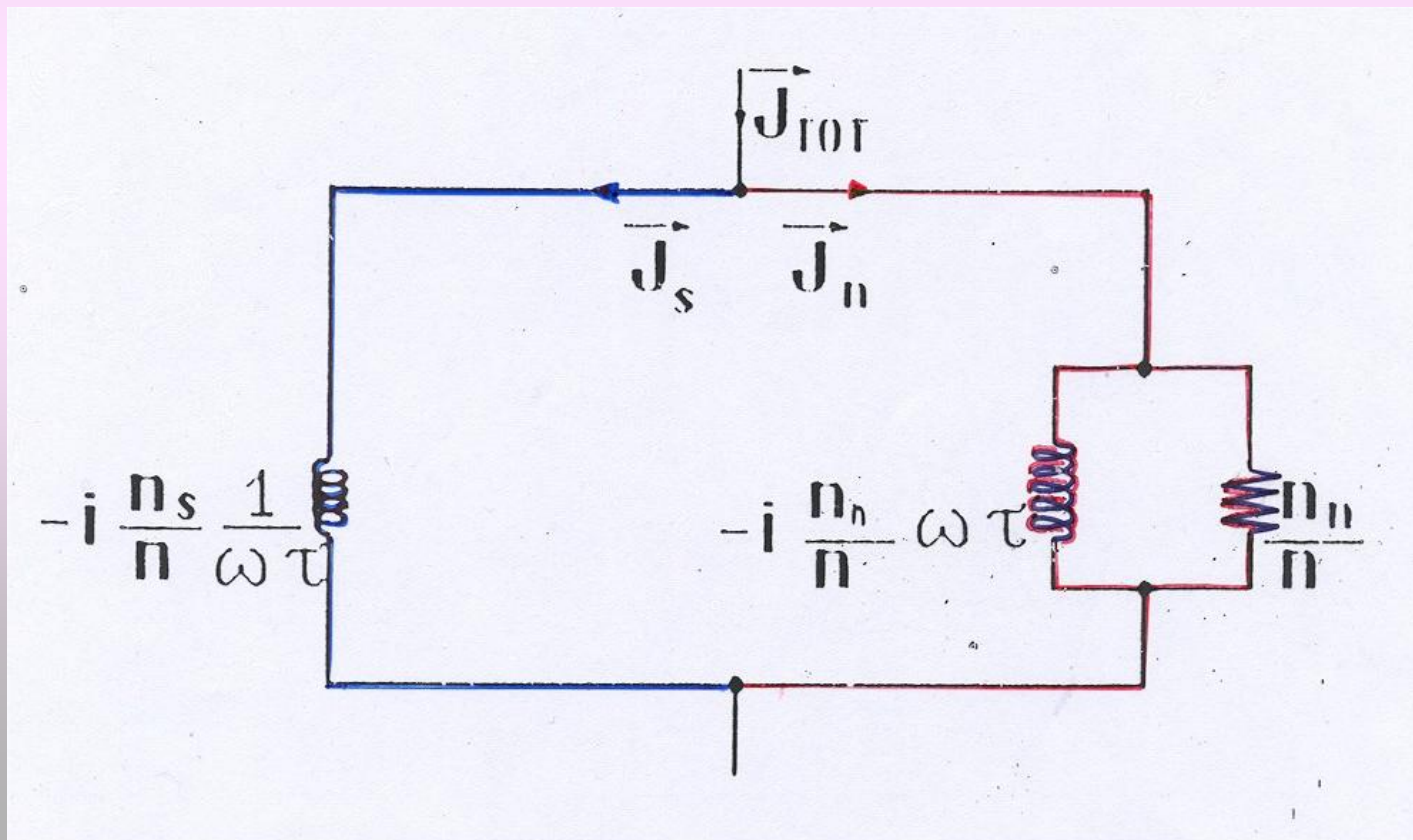
Yoji Totsuka (KEK)(Chair), Fumihiko Takasaki (KEK)(Deputy chair),
Junji Uehara (KEK), Kiyoshi Hada (KEK), Shigeru Karada (KEK),
Nobuniro Terunuma (KEK), Toshiyasu Higo (KEK), Tsureniko Omori (KEK),
Toshiaki Tsuchi (KEK), Akiya Miyamoto (KEK), Masao Kurki (KEK),
Kiyosumi Tsuchiya (KEK), Shuichi Noguchi (KEK), Eiji Kako (KEK)

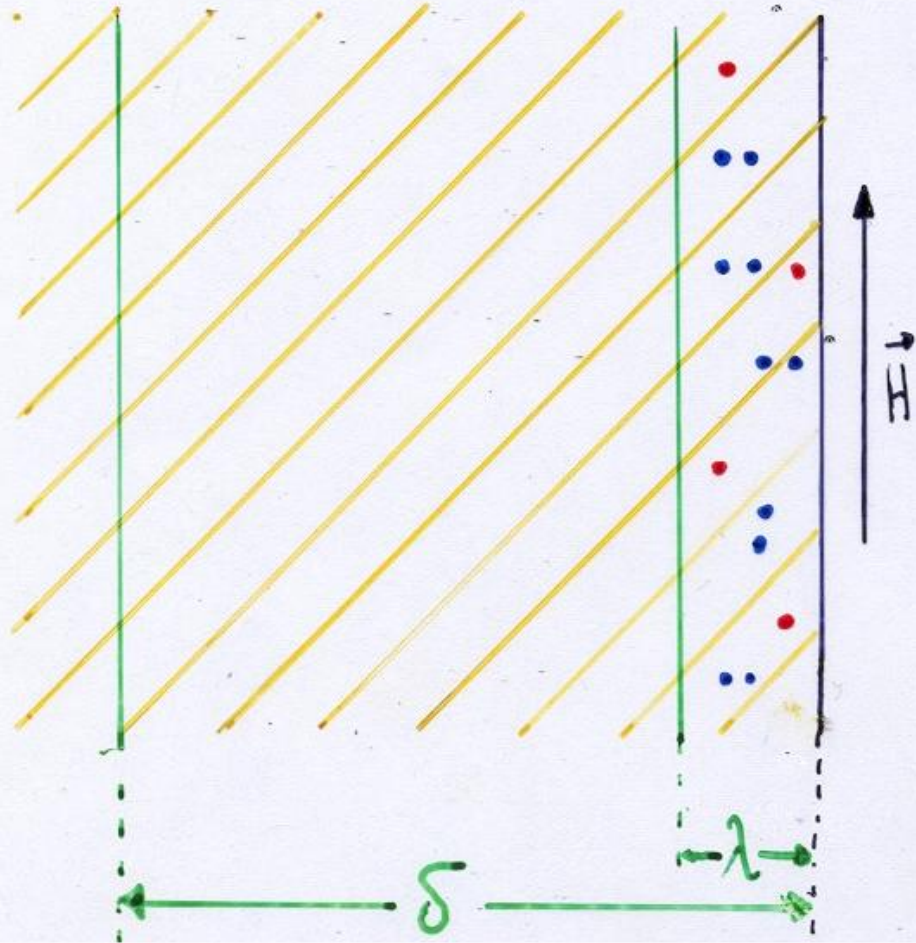
<http://lcdev.kek.jp/ILCWS/>

Superconductors in radiofrequency

$$T = T_c; \quad \omega \neq 0 \quad \text{à} \quad R_s \neq 0$$

$$\vec{J} = \vec{J}_n + \vec{J}_s$$





$$R_S = w^2 l \frac{n_n}{n}$$

$$\frac{n_n}{n} \approx e^{-\frac{\Delta}{k_B T}}$$

Surface Impedance and Surface Resistance



For a normal metal in the normal regime:

$$Z_n = \frac{1 - i}{\sigma_n \delta} = (1 - i) \frac{\rho_n}{\delta}$$

$s_n = 1 / r_n =$ dc conductivity at T

$d =$ skin depth

Extension to Superconductors:

$s_1 - is_2$ in place of s_n

As derived by Nam, for $T < T_c / 2$, R_s can be approximated by:

$$\frac{R_s}{R_n} = \frac{1}{\sqrt{2}} \frac{\frac{s_1}{s_n}}{\left(\frac{s_2}{s_n}\right)^{\frac{3}{2}}}$$

Mattis and Bardeen Integrals



In the framework of the BCS theory, for $\hbar\omega < 2\Delta$, the complex conductivity of a superconductor is:

$$\frac{\mathbf{S}_1}{\mathbf{S}_n} = \frac{2}{\hbar\omega} \int_{\Delta}^{\infty} [f(E) + f(E + \hbar\omega)] g^+(E) dE$$

$$\frac{\mathbf{S}_2}{\mathbf{S}_n} = \frac{1}{\hbar\omega} \int_{\Delta - \hbar\omega, -\Delta}^{\Delta} [1 - 2f(E + \hbar\omega)] g^-(E) dE$$

The two integrals σ_1/σ_n and σ_2/σ_n are easily numerically calculated.

$$\frac{\mathbf{S}_1}{\mathbf{S}_n} = \left[\frac{\frac{2\Delta}{K_B T}}{(1 + e^{-\Delta/K_B T})^2} \right] e^{-\Delta/K_B T} \ln \frac{\Delta}{\hbar\omega}$$

$$\frac{\mathbf{S}_2}{\mathbf{S}_n} = \frac{p\Delta}{W} \tanh \frac{\Delta}{2K_B T}$$

In the normal skin effect regime, for $\hbar\omega \ll 2\Delta$

R_{BCS}



Then, if $T < T_c / 2$

$$R_{BCS} \cong \frac{R_n}{\sqrt{2}} \left(\frac{\hbar w}{p\Delta} \right)^{\frac{3}{2}} \frac{S_1}{S_n} = A \sqrt{r_n} e^{-\frac{\Delta}{K_B T}} (1 + O(\Delta, w, T))$$

Empirically, R_{res} is found to be dependent on r_n too.

Essence of the previous calculations

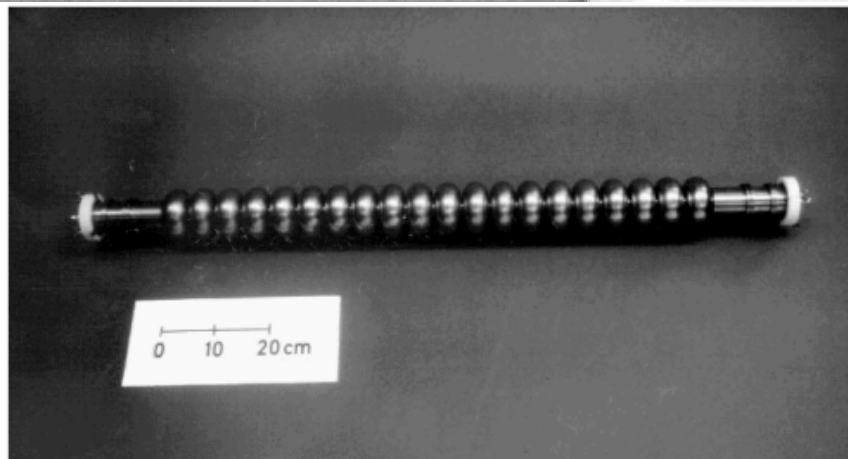
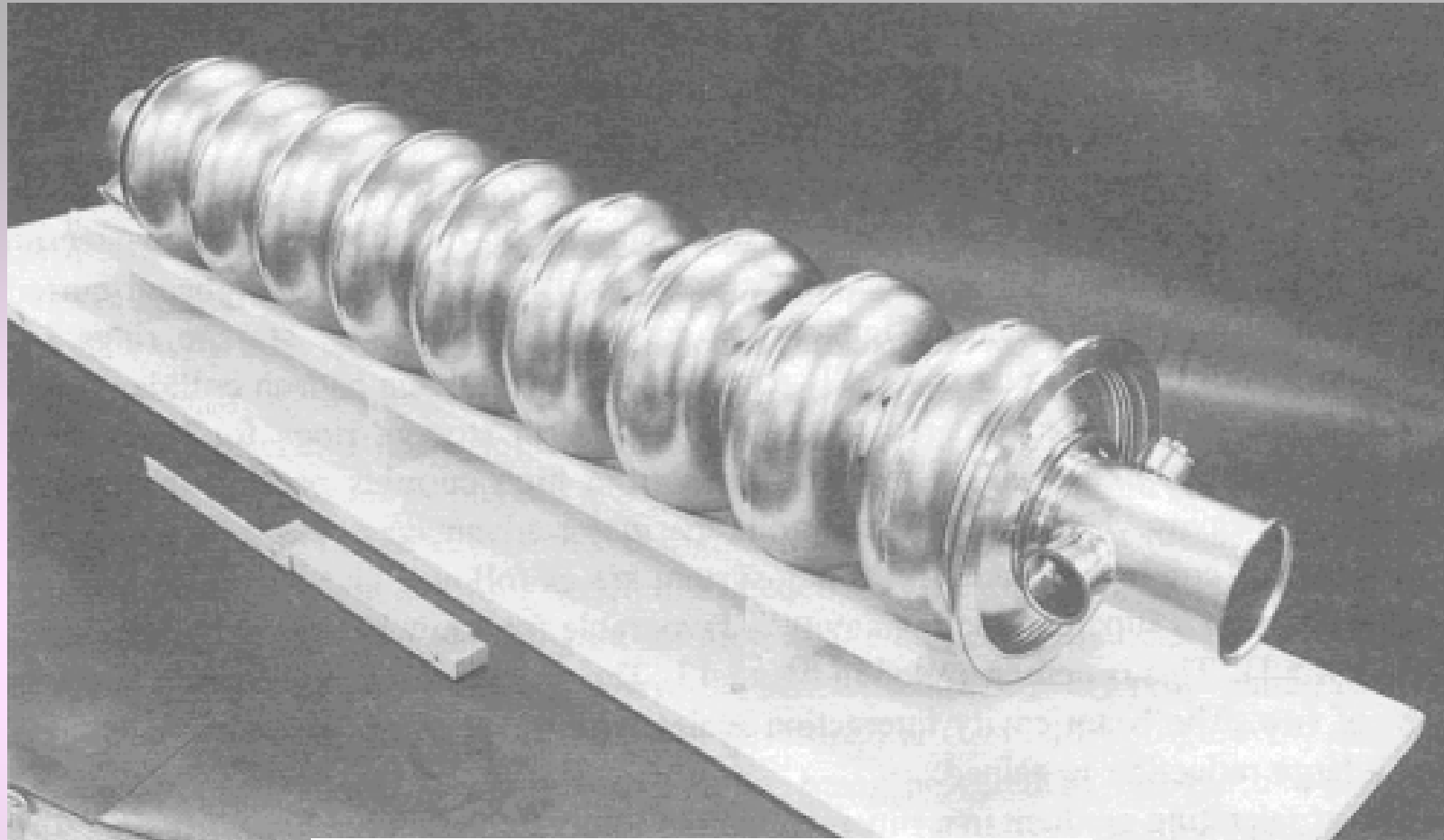
For low rf losses,
a high T_c value is not sufficient



A metallic behaviour
in the normal state is mandatory

Bulk fabrication techniques (Electron cavities)

- E-beam Welding
- Hydroforming
- Electroforming
- Explosive forming
- Spinning





350 MHz half copper cell under NC measuring



The electron beam welding machine



20.000 cavities x
24 Kg di Niobium x
500 €/Kg =

240,000,000 € only of bare Nb

20.000 cavities x

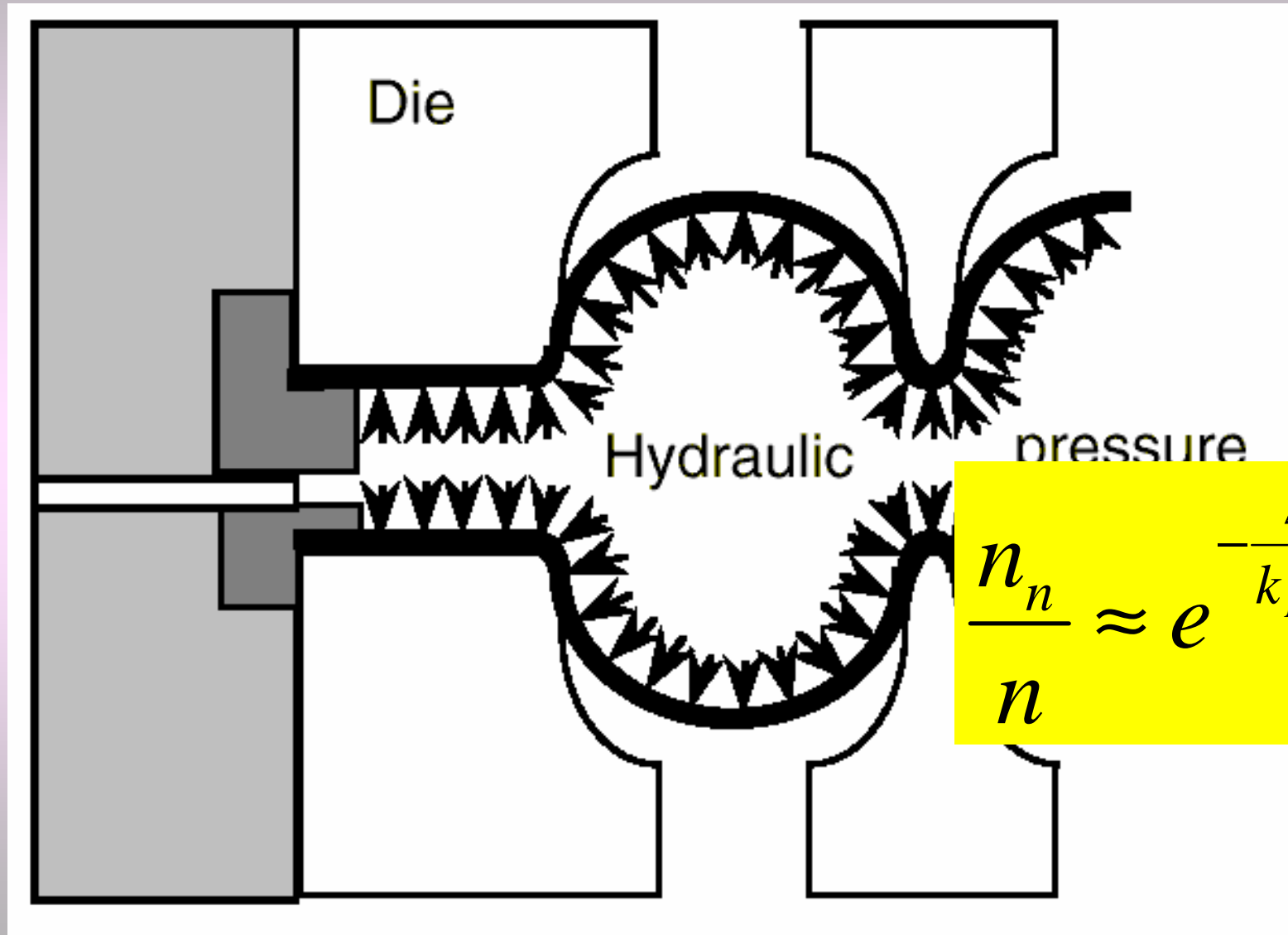
9 cells =

180,000 EB weldings x

12 hours / welding =

100 years of manufacture

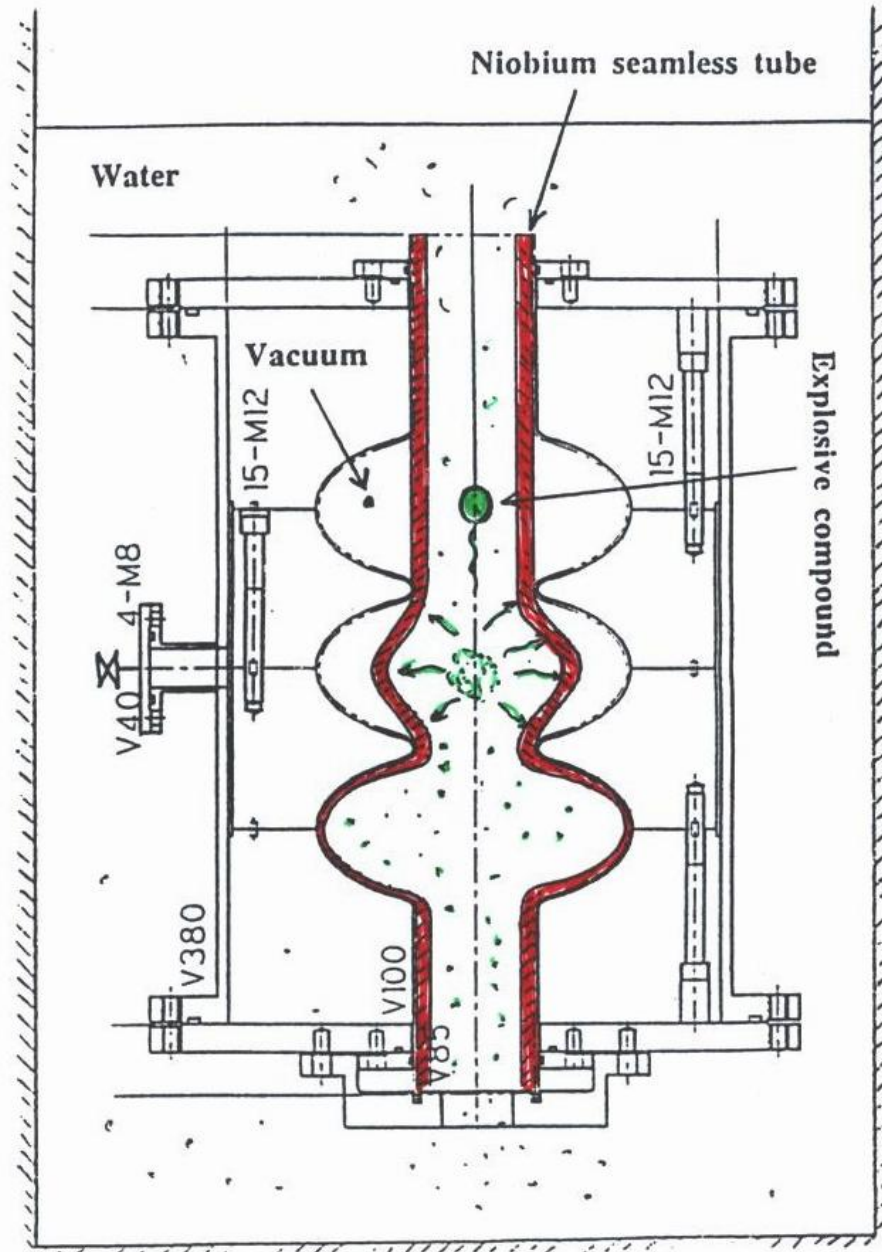
Principle of copper multicell hydroforming at CERN



Hydroflambage

Tube Niobium épaisseur 2 mm - diamètre 52 mm





Idea of the explosive forming method for seamless multi-cell cavities.

Properties of Selected High Explosives*

Explosive	Relative Power, %		Detonation Velocity, fps (m/s)	Energy, ft · lb/lb (kJ/kg)	Detonator Required	Storage Life	Maximum Pressure, ksi (MPa)
	TNT	Form of Charge					
Trinitrotoluene (TNT)	100	Cast	23,000 (7010)	262,000 (780)	J-2*	Moderate	2400 (16 548)
Cyclotrimethylene trinitramine (RDX)	170	Pressed granules	27,500 (8380)	425,000 (1270)	No. 6	Very good	3400 (23 443)
Pentaerythritol tetranitrate (PETN)	170	Pressed granules	27,200 (8290)	435,000 (1300)	No. 6	Excellent	3200 (22 064)
Pentolite (50/50)	140	Cast	25,000 (7620)	317,000 (950)	No. 8	Good	2800 (19 306)
Tetryl	129	Pressed granules	25,700 (7835)		Special**	Excellent	
Composition C-3	115	Hand-shaped putty	26,400 (8045)		No. 6	Good	
40% straight dynamite	94	Cartridge granules	15,500 (4725)	202,000 (605)	No. 8	Fair	970 (6688)
50% straight ditching dynamite	103	Cartridge granules	17,400 (5305)	220,000 (660)	No. 6	Fair	
60% extra dynamite	109	Cartridge granules	12,500 (3810)	240,000 (715)	No. 6	Fair	620 (4275)
Blasting gelatin	99	Cartridge plastic	26,200 (7985)	408,000 (1220)	J-2	Fair	2600 (17 927)
Bituminous coal D permissible explosive		Cartridge granules	4600 (1400)		No. 8	Fair	
Primacord, 40 g/ft		Plastic or cotton cord	20,800 (6340)		No. 6	Excellent	
Mild detonating cord, 10 g PETN/ft		Metal-coated cord	24,000 (7315)		Special†	Excellent	
Detasheet‡		Cut to shape	23,700 (7225)		No. 8	Very good	
Cyadyn 3‡	90	Cartridge granules	7000 (2135)		No. 6	Fair-good	
IRECO DBA-10HV§	20	Slurry (two parts)	11,500 (3505)		Special	Excellent (unmixed components)	

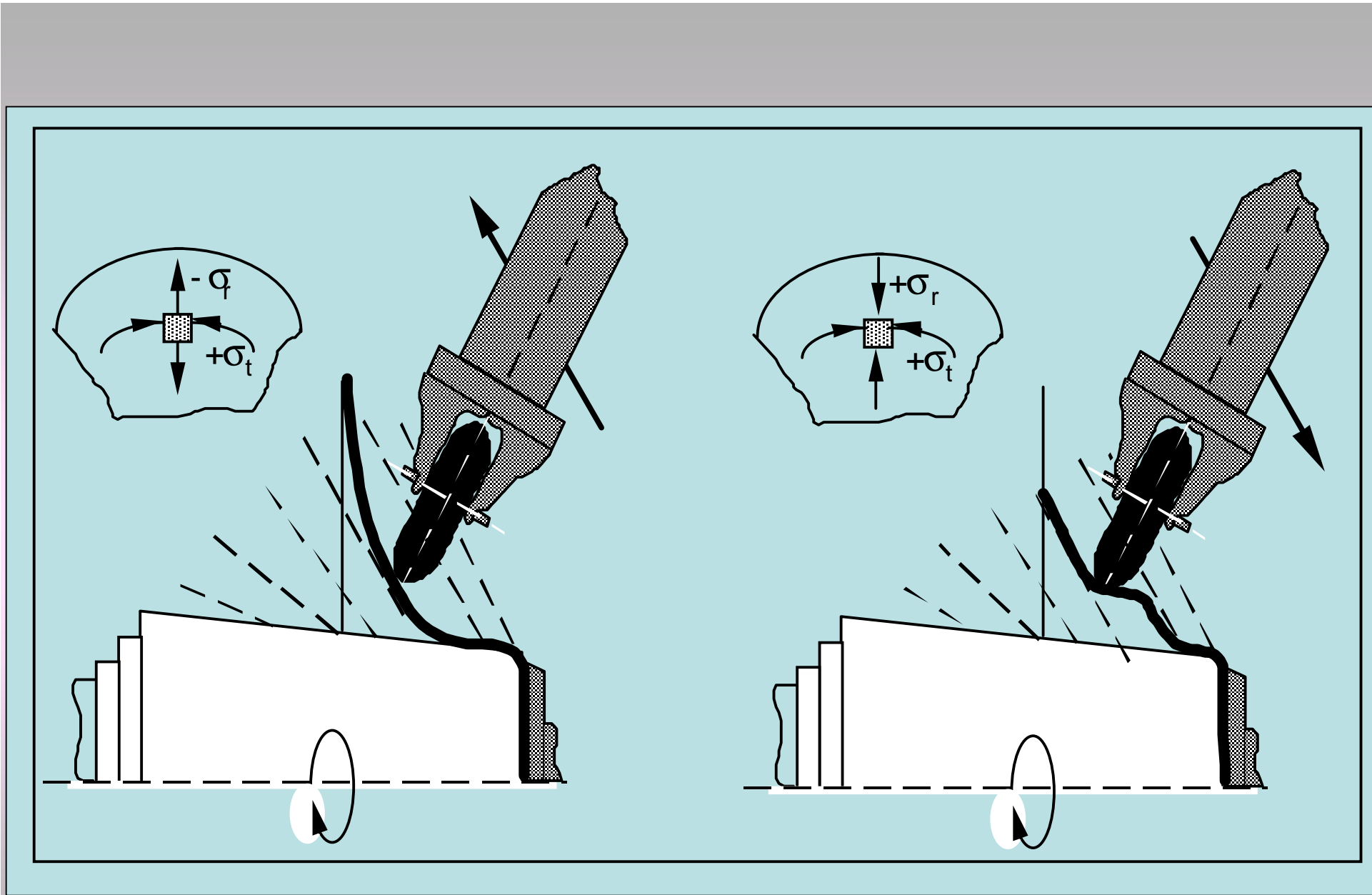
* With booster.

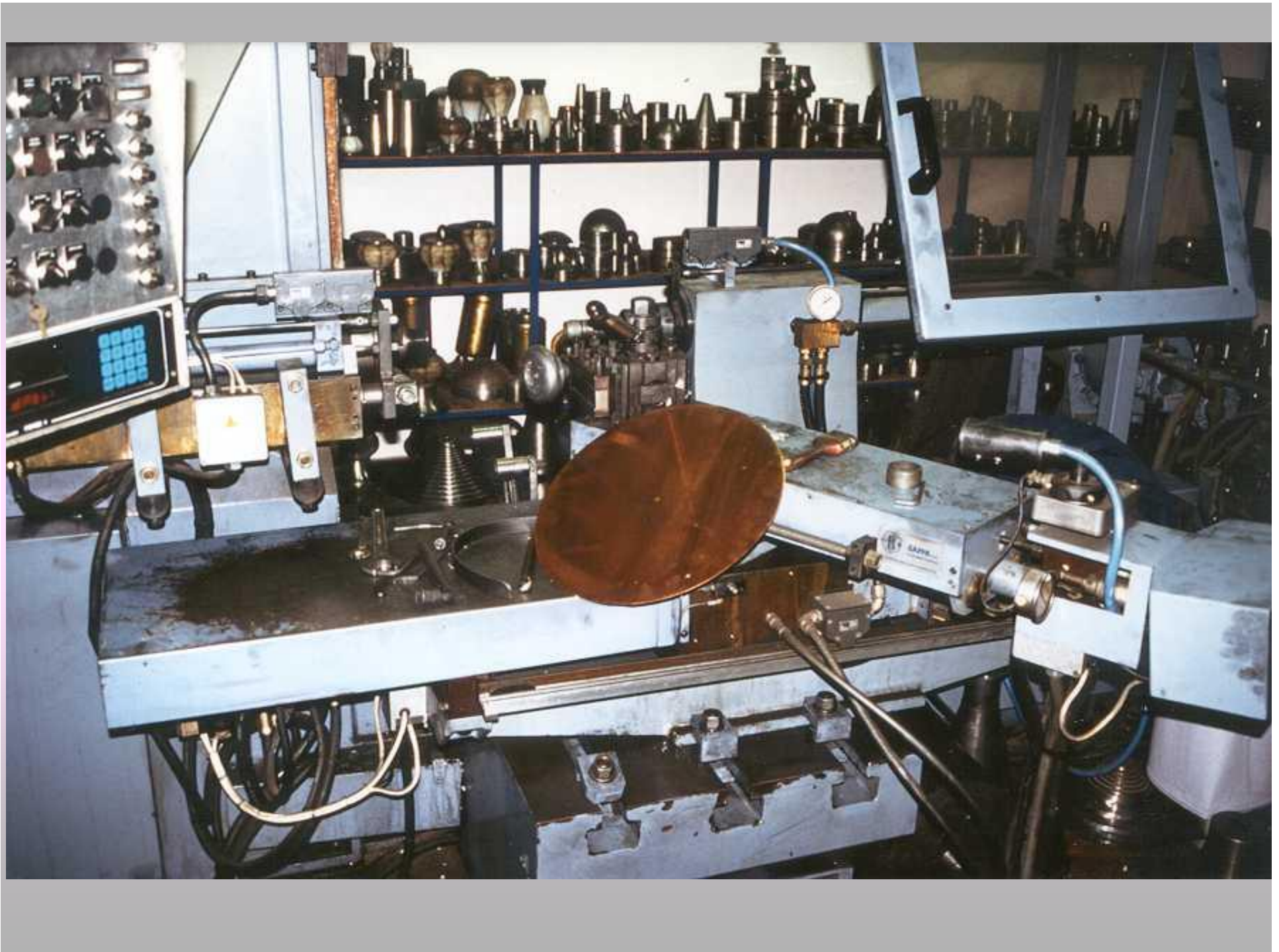
** Special engineer's blasting cap.

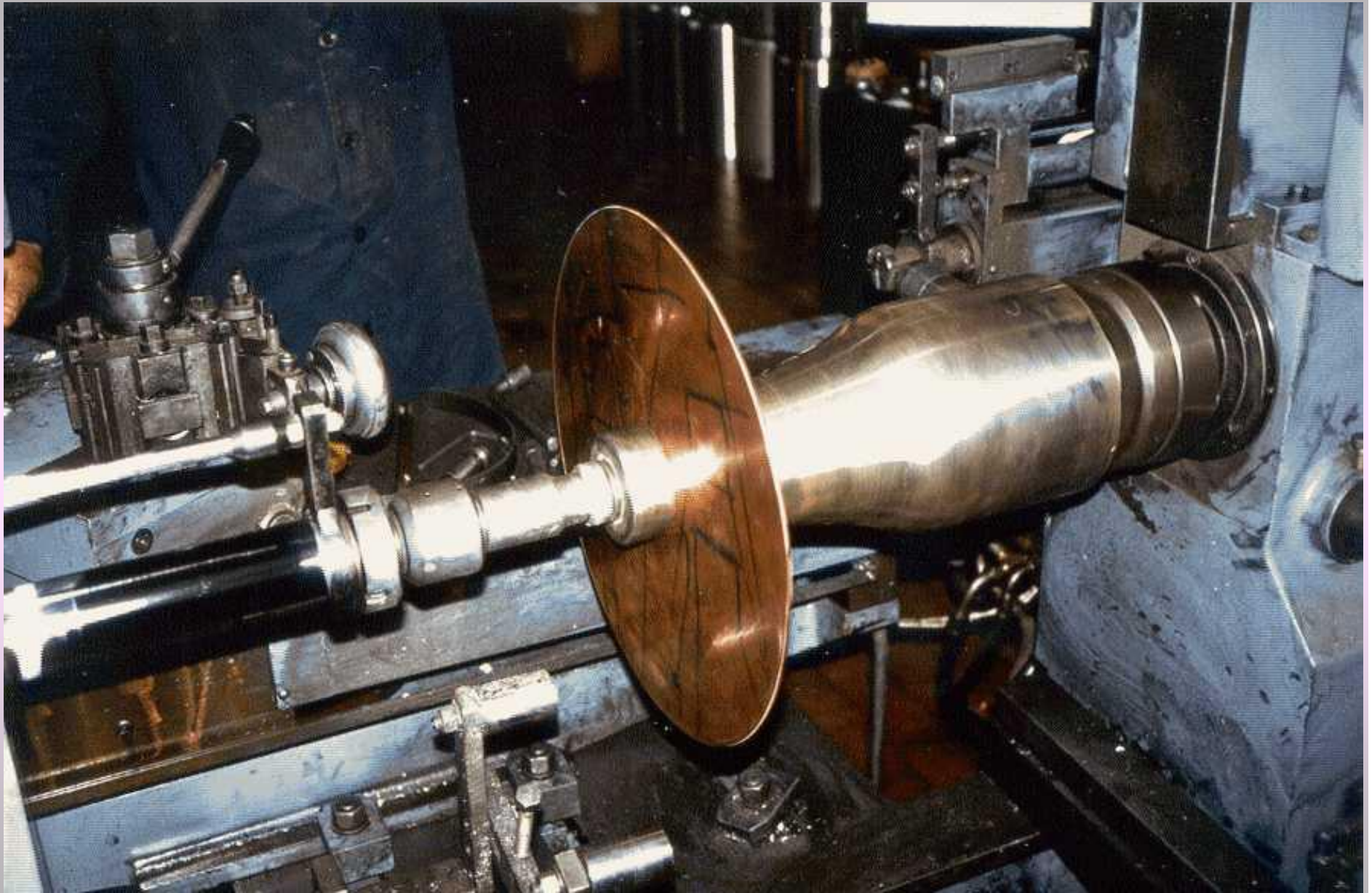
† Registered trademark, E. I. du Pont de Nemours & Company, Inc.

‡ Registered trademark, American Cyanamid Company.

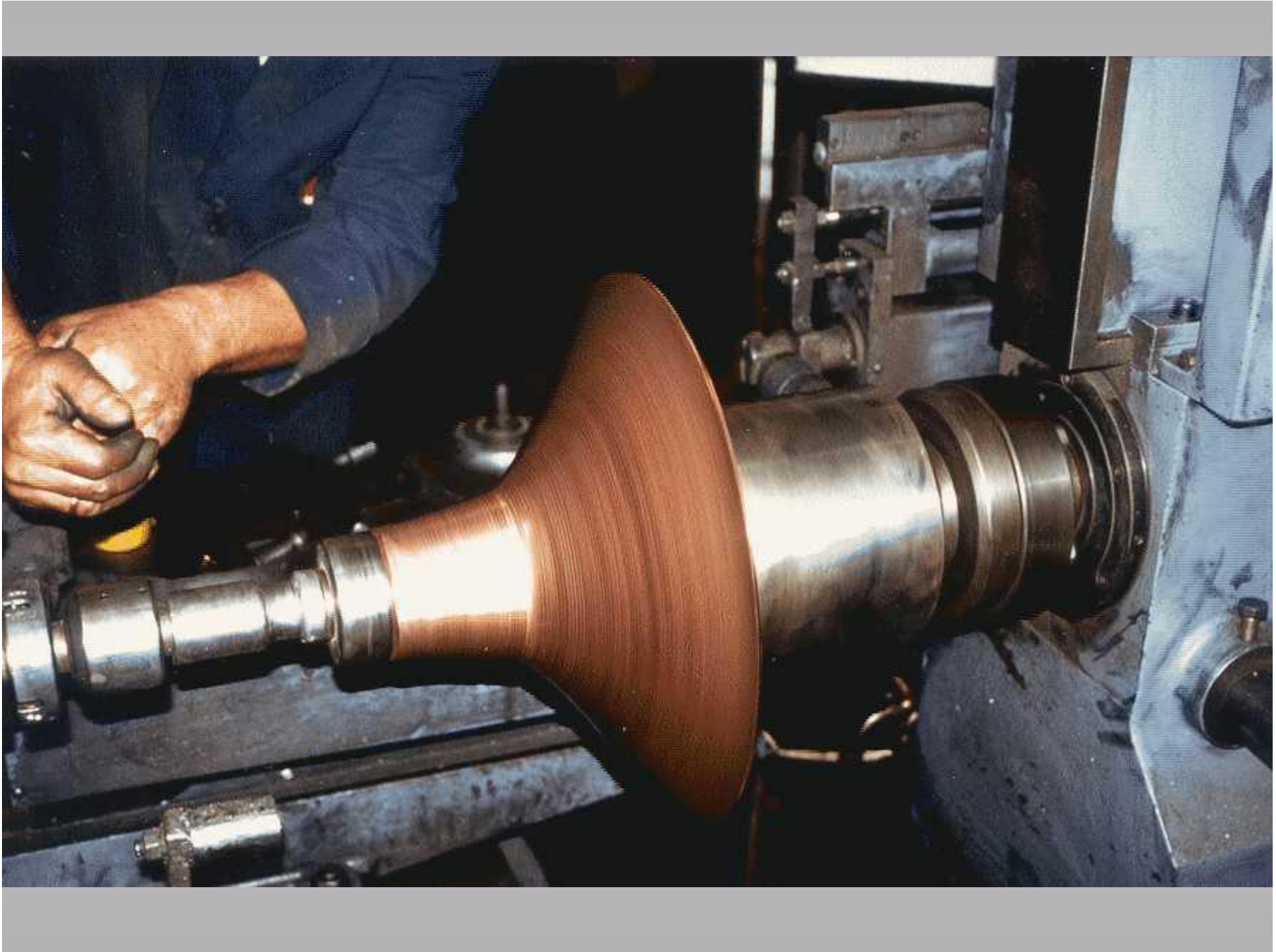
§ Intermountain Research and Engineering Corp.

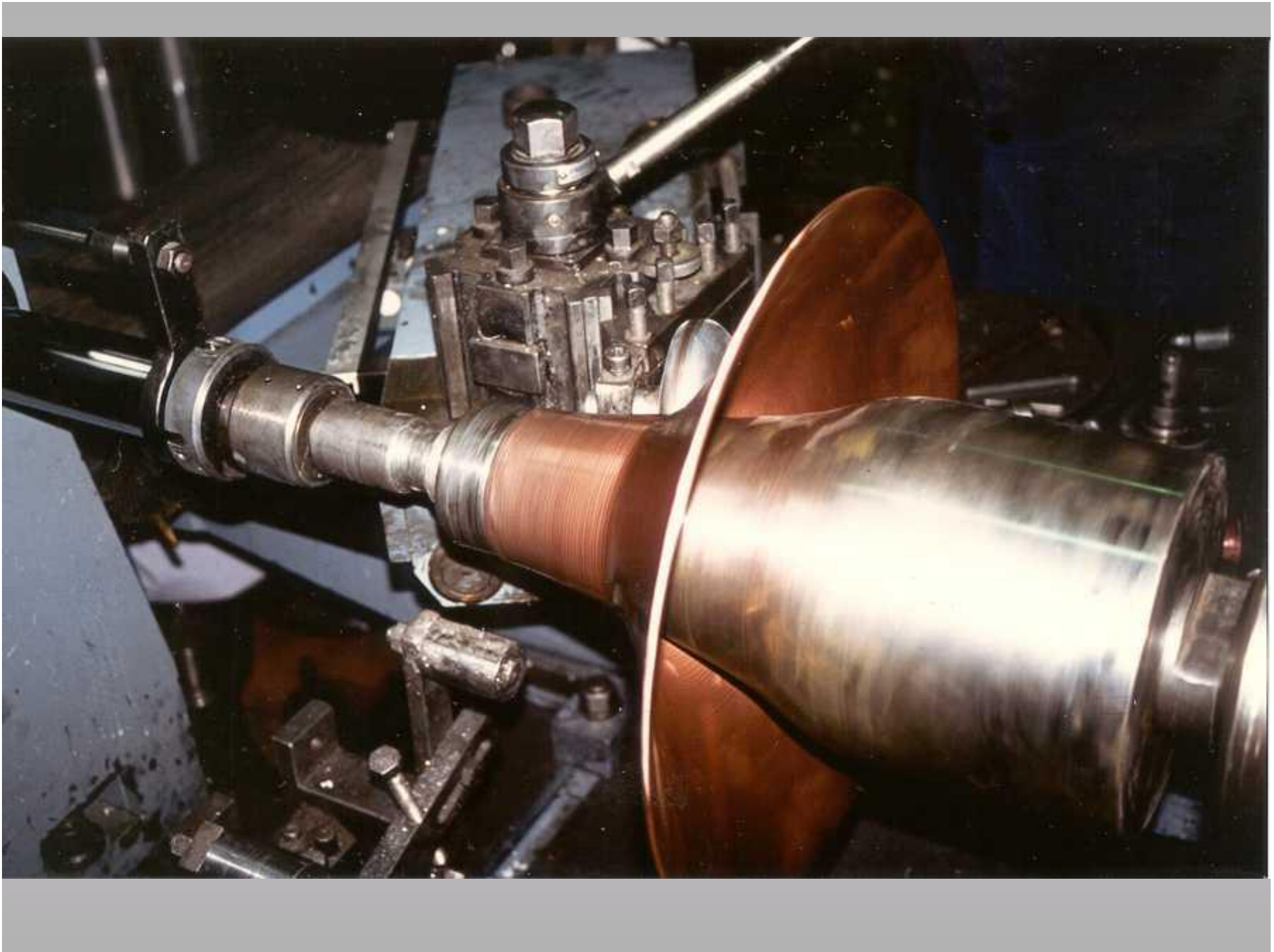


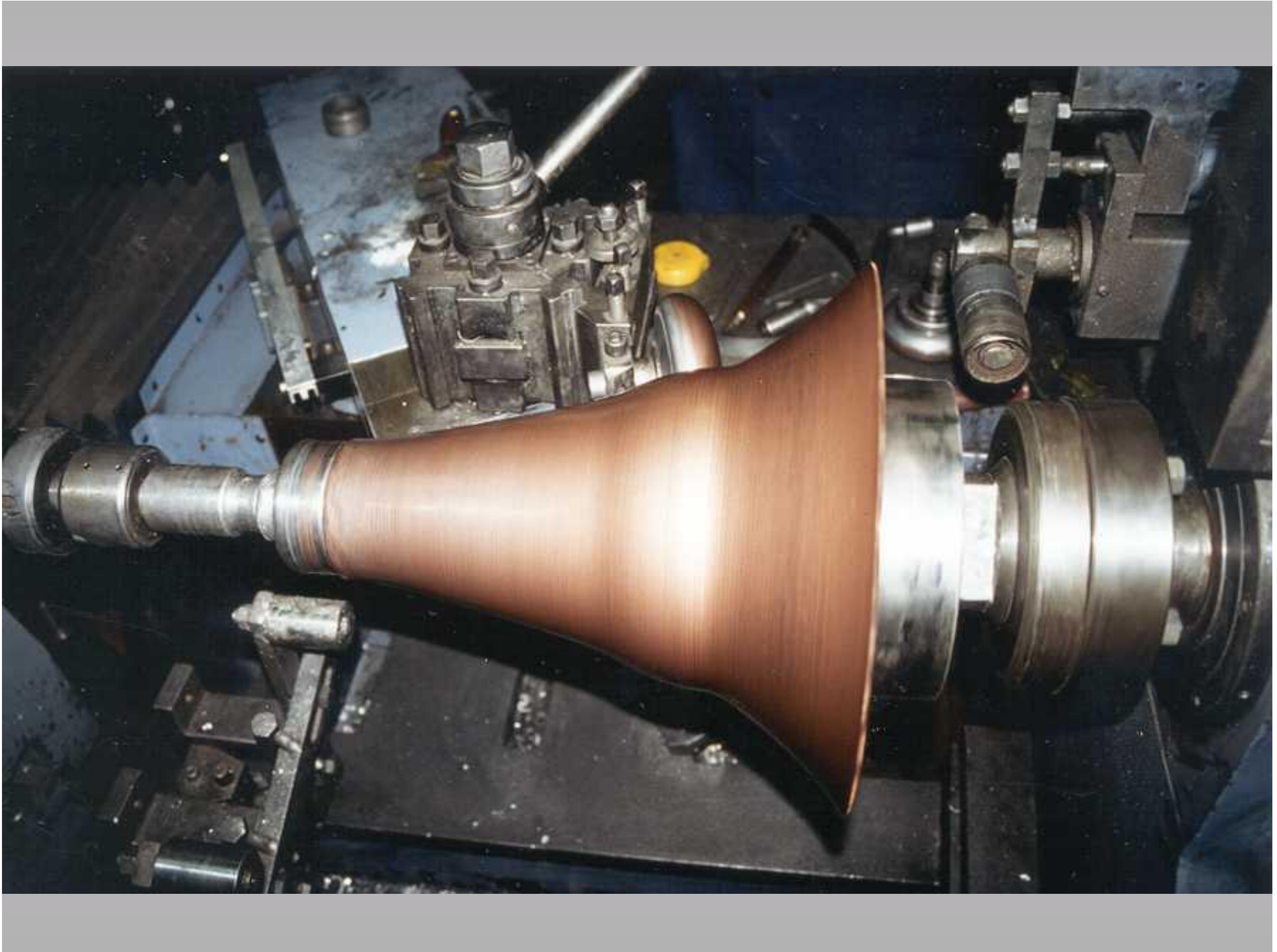


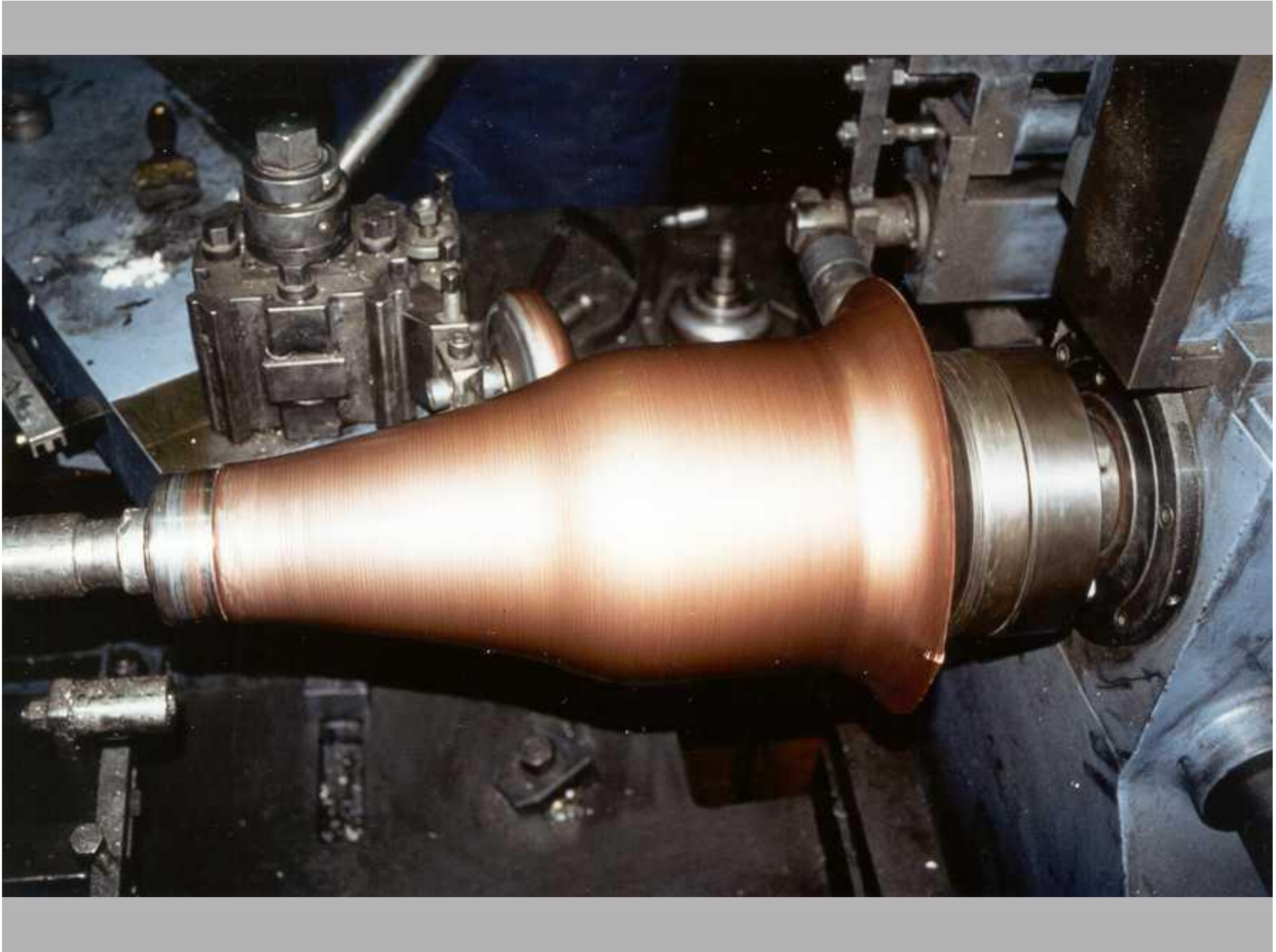


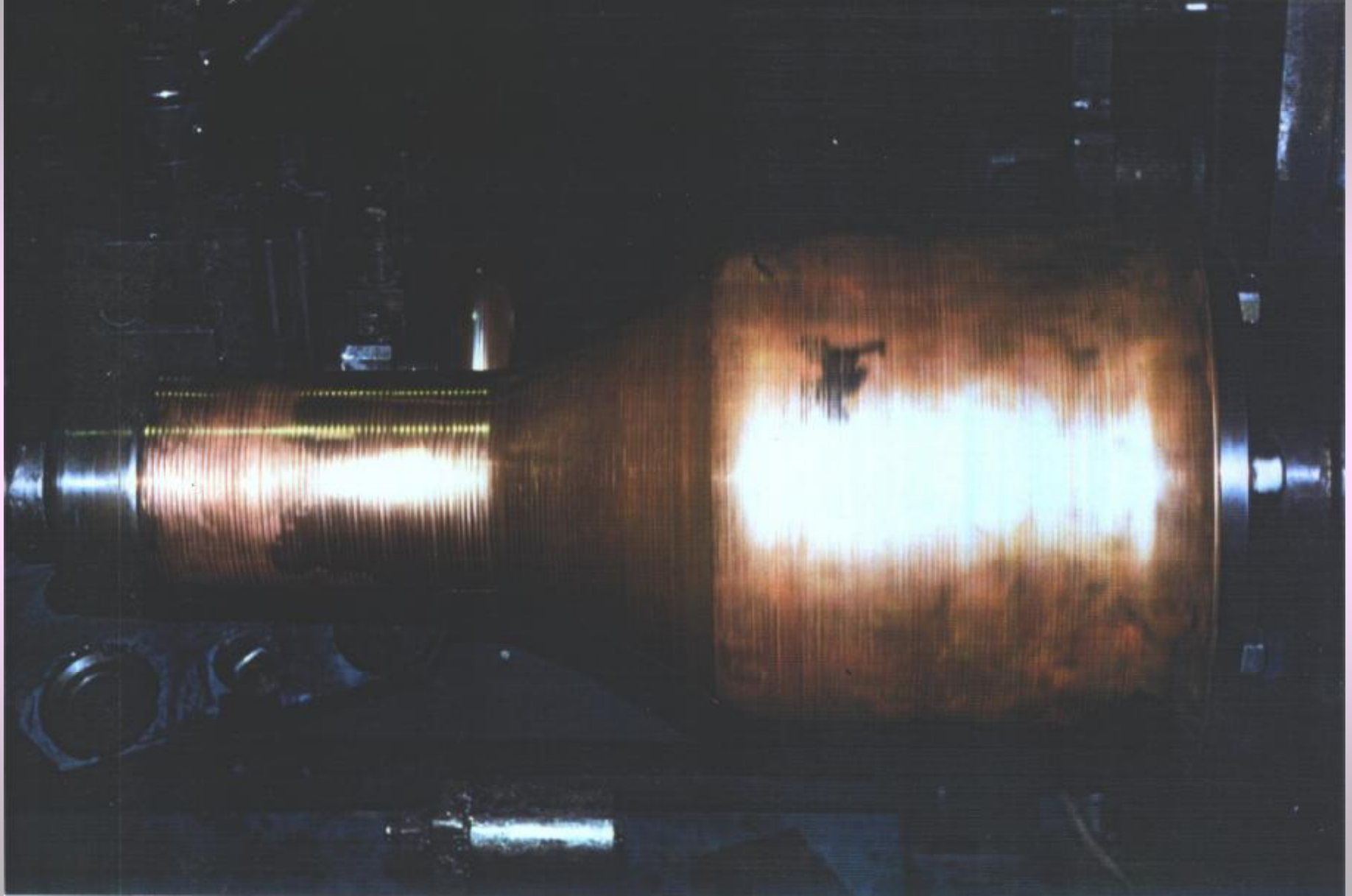




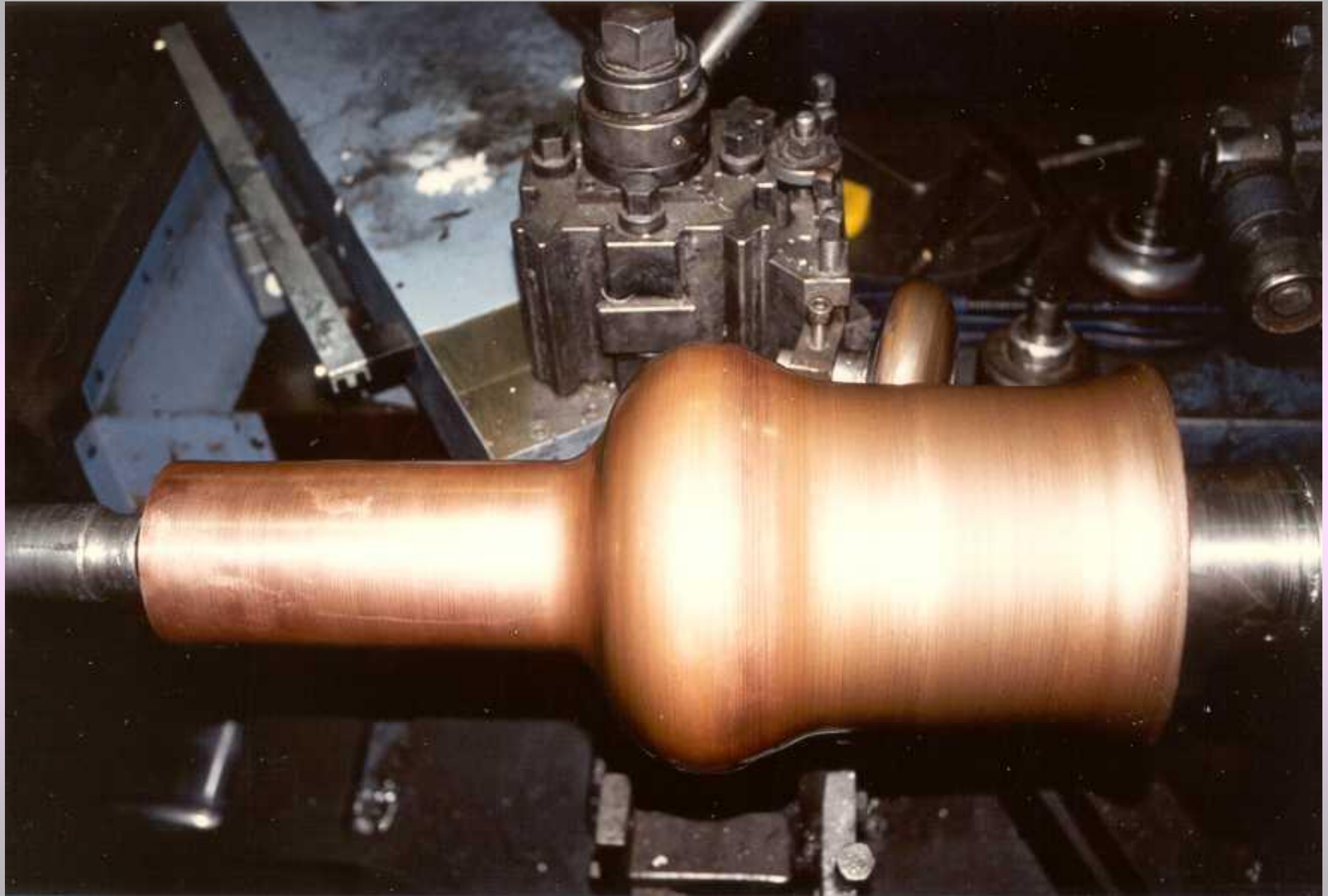


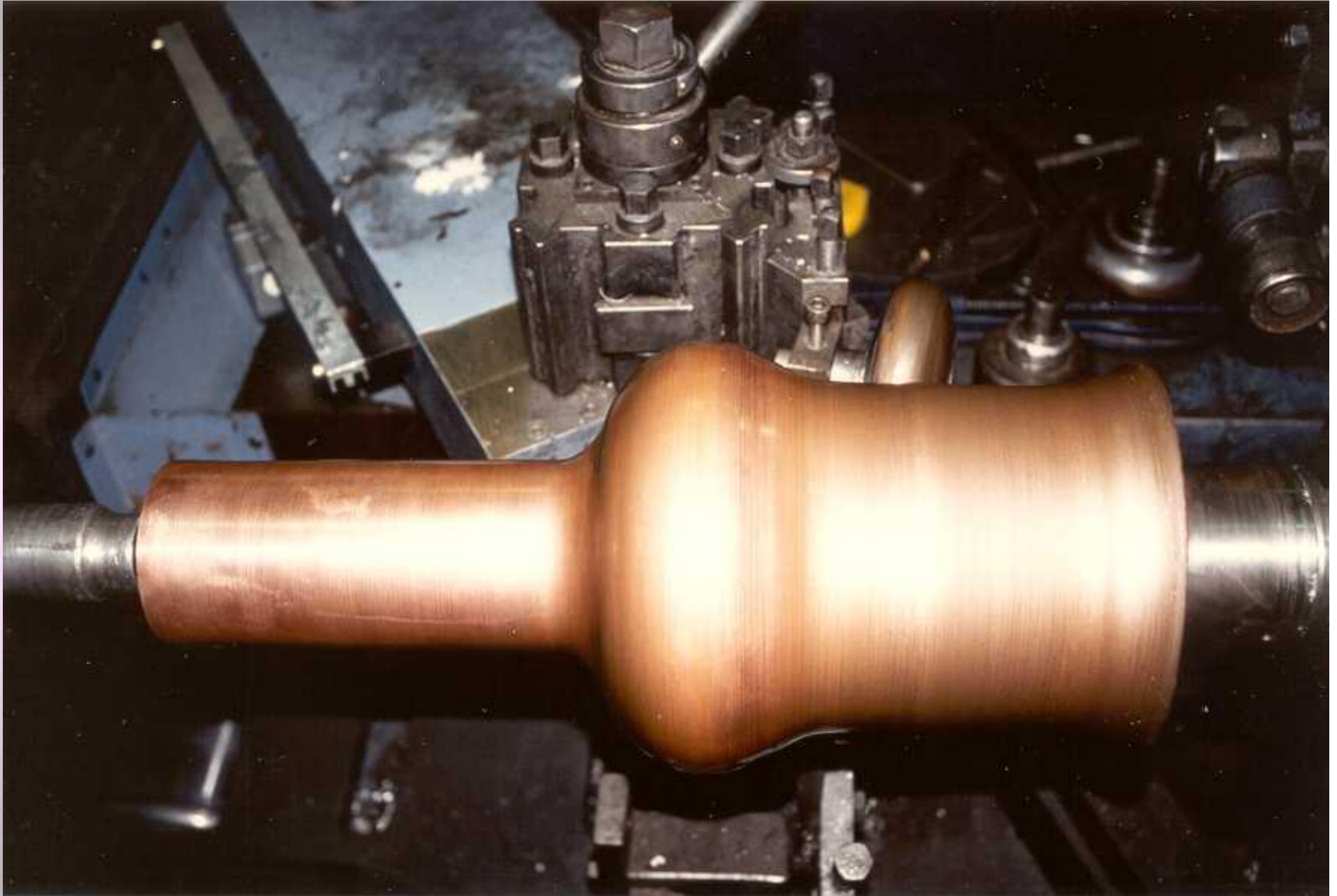


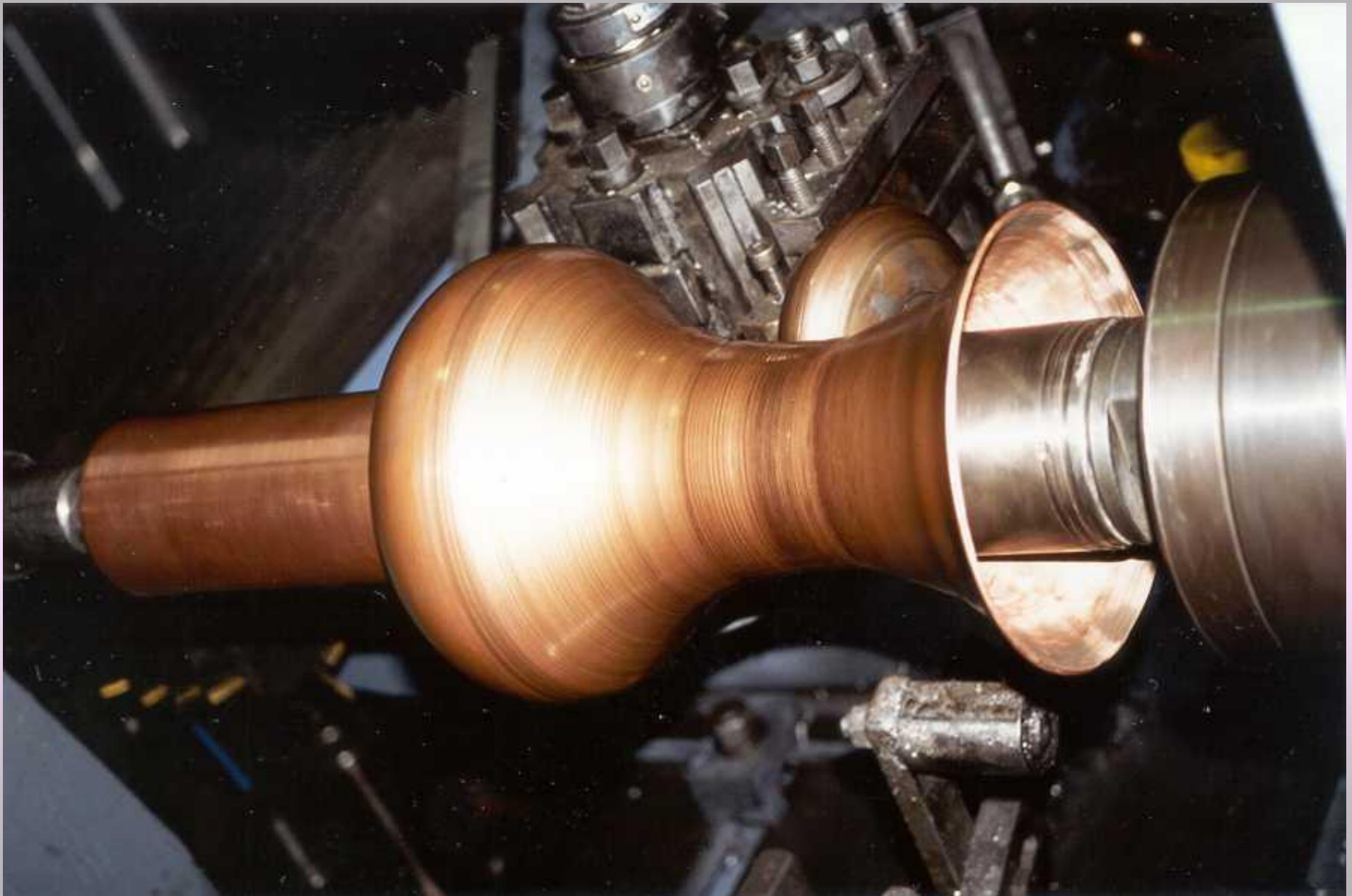


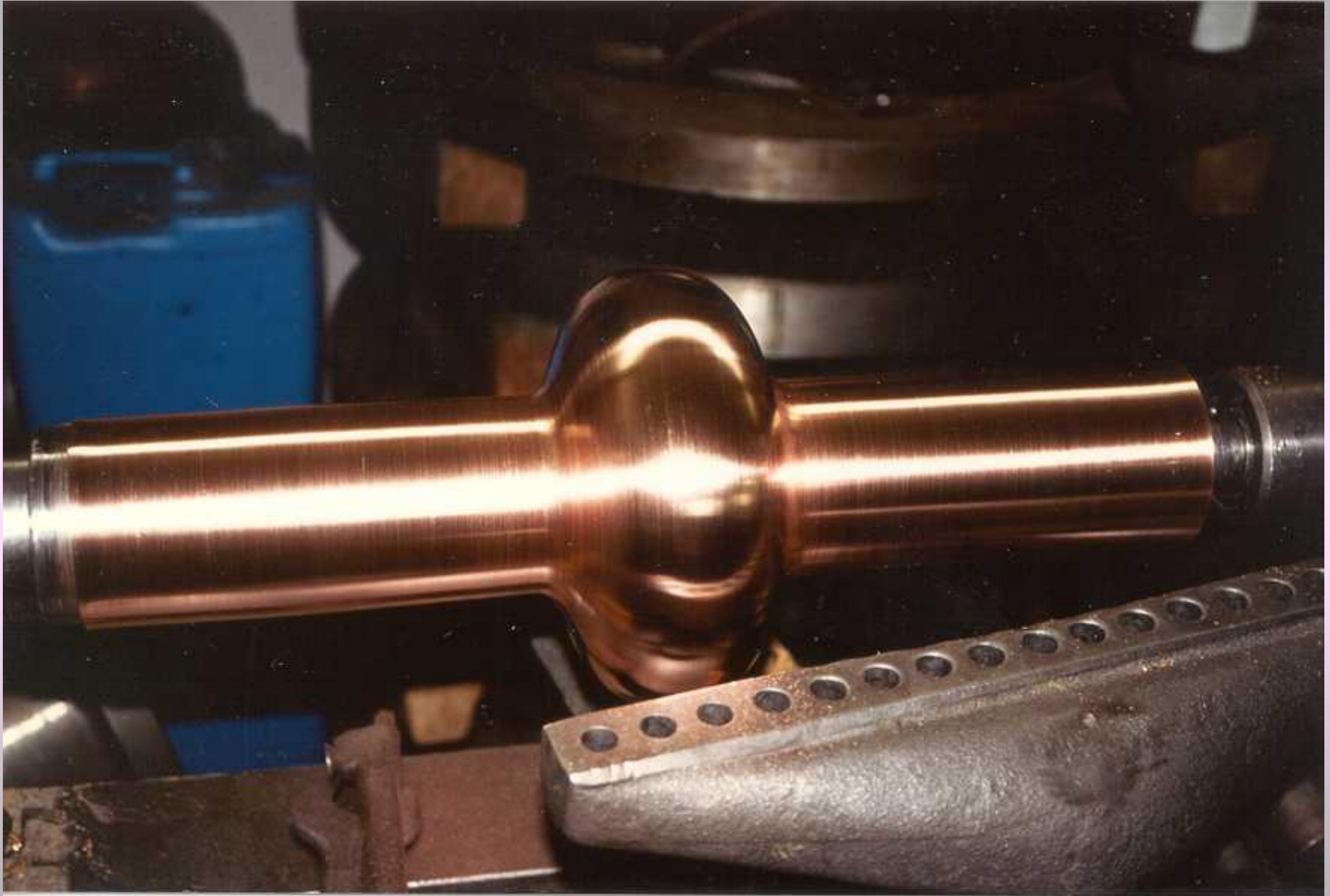


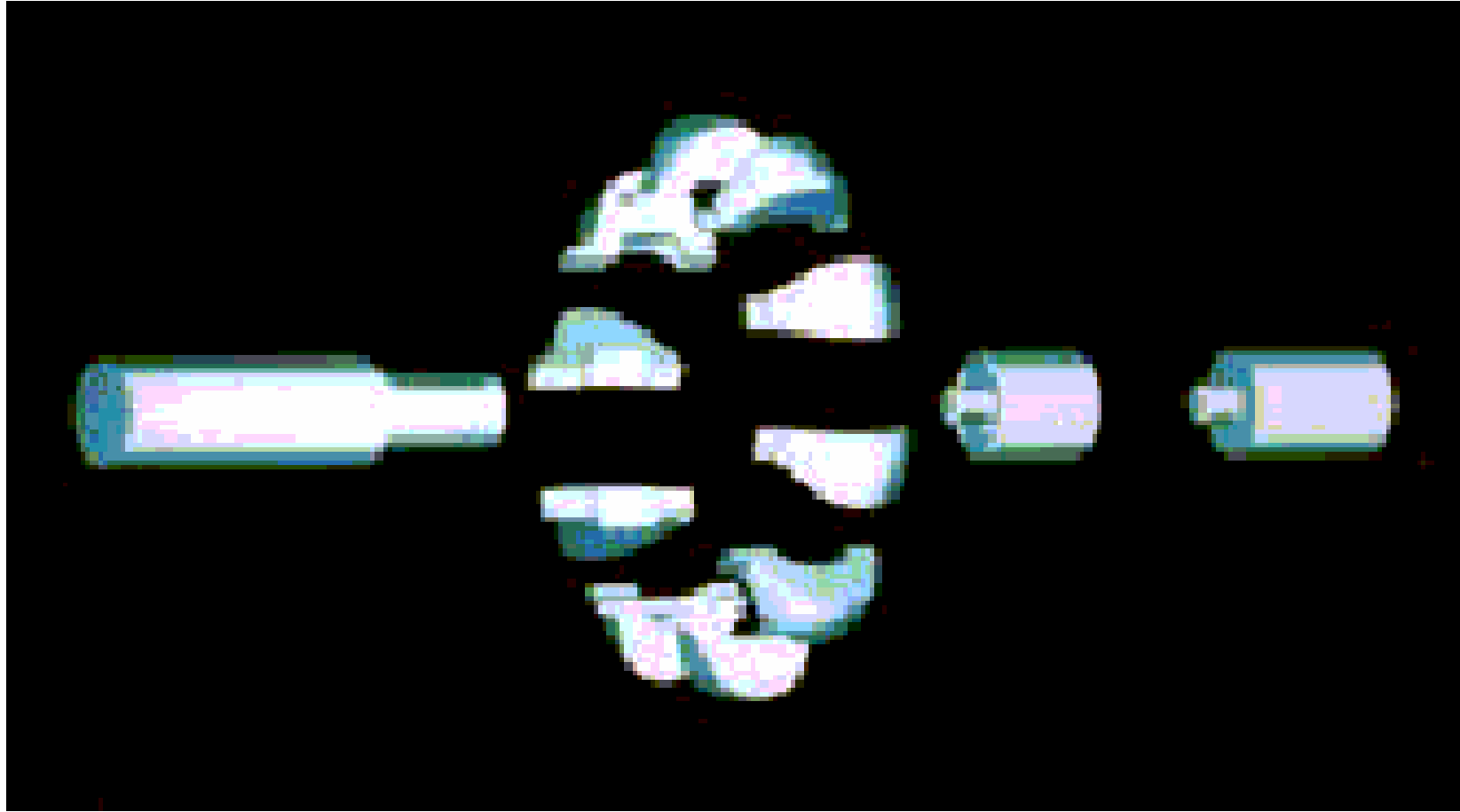


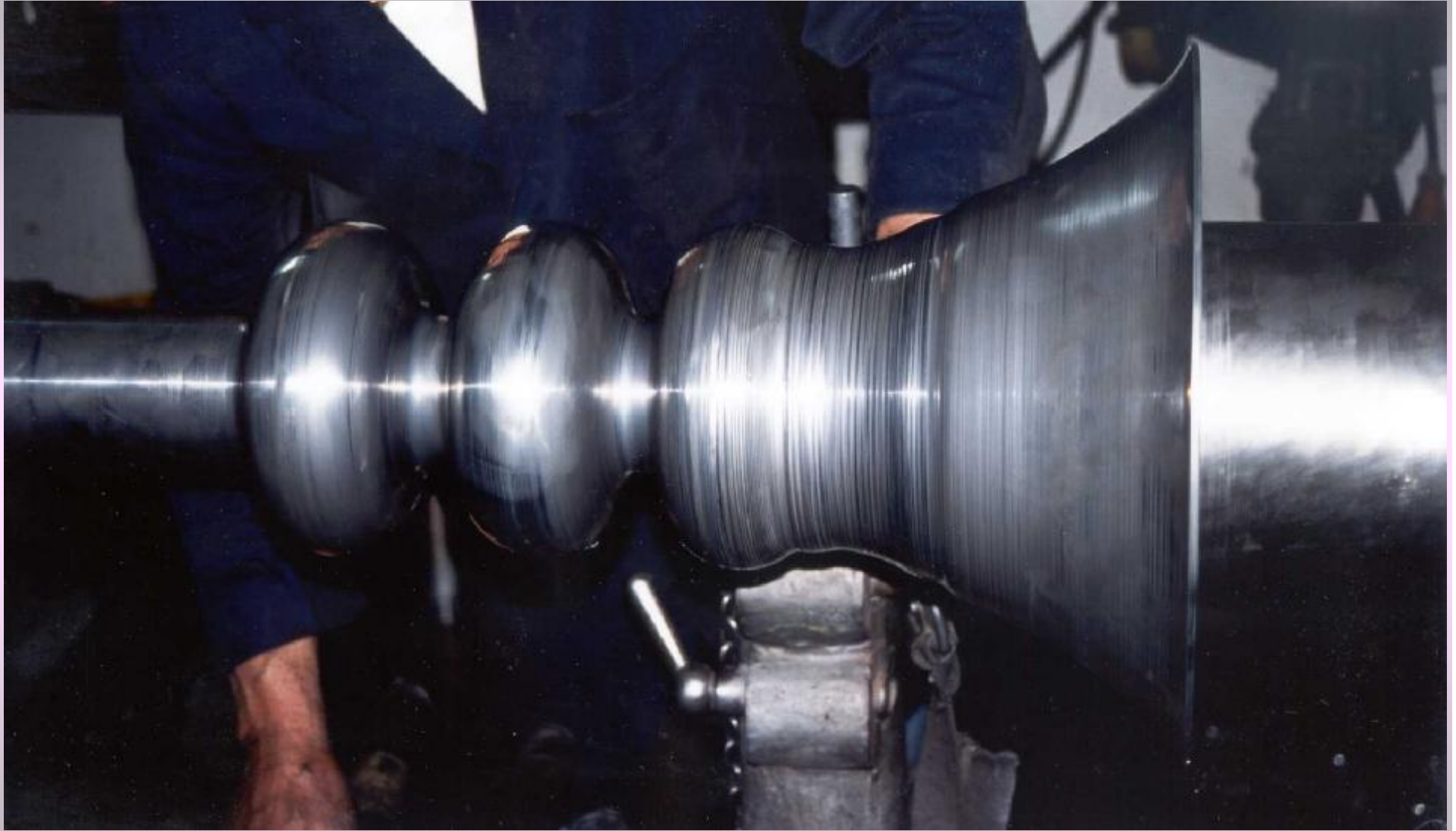


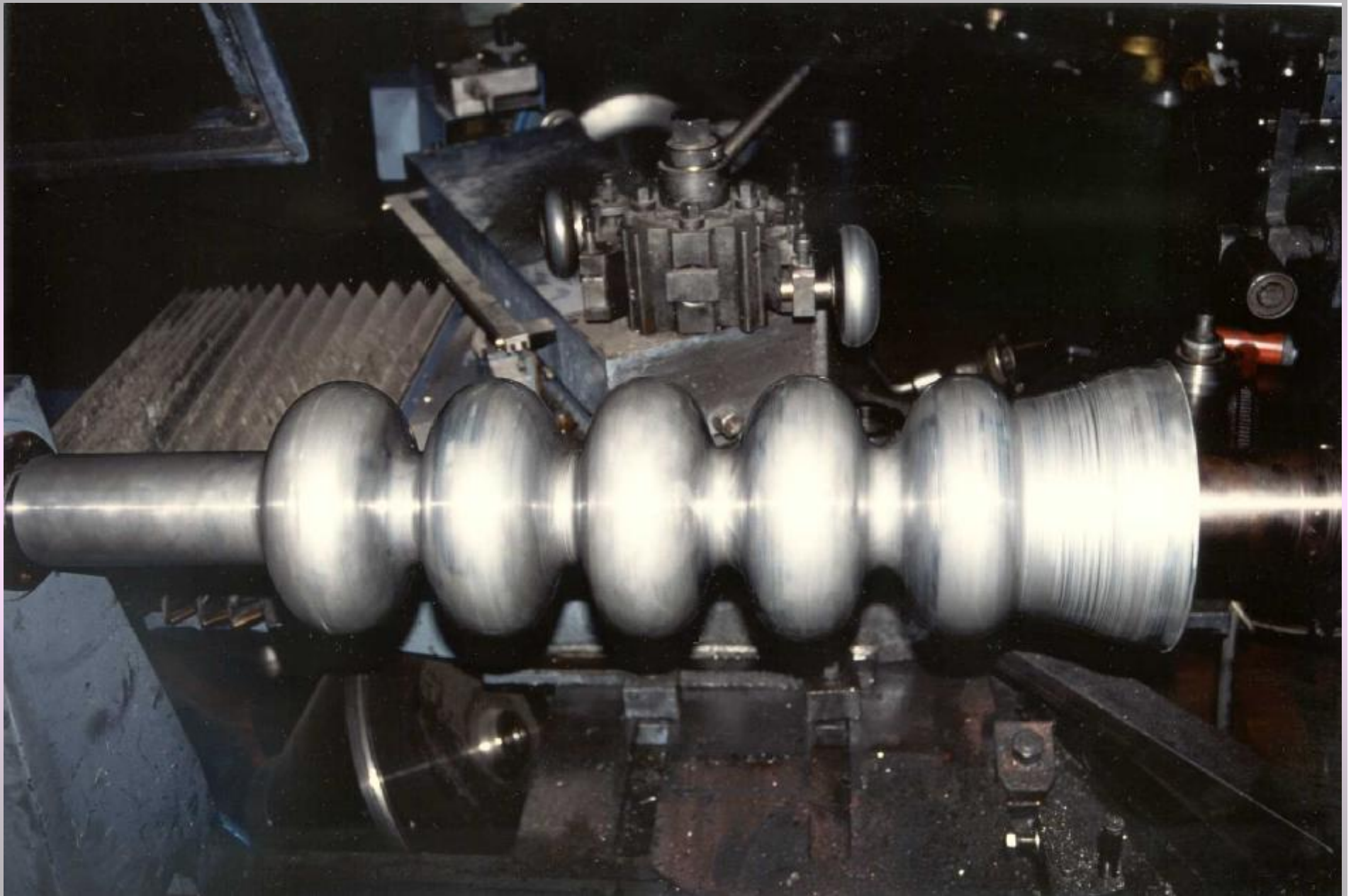


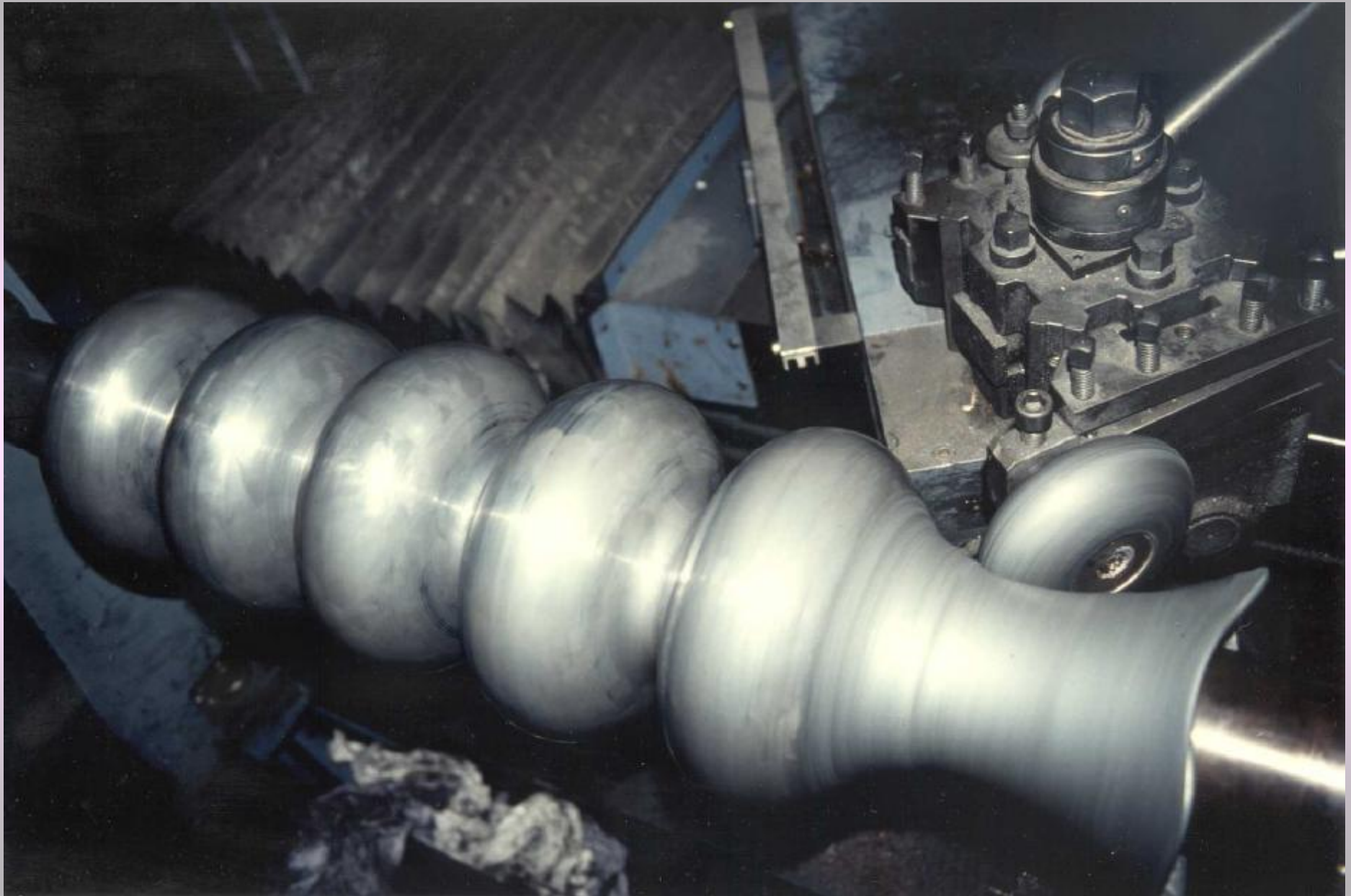




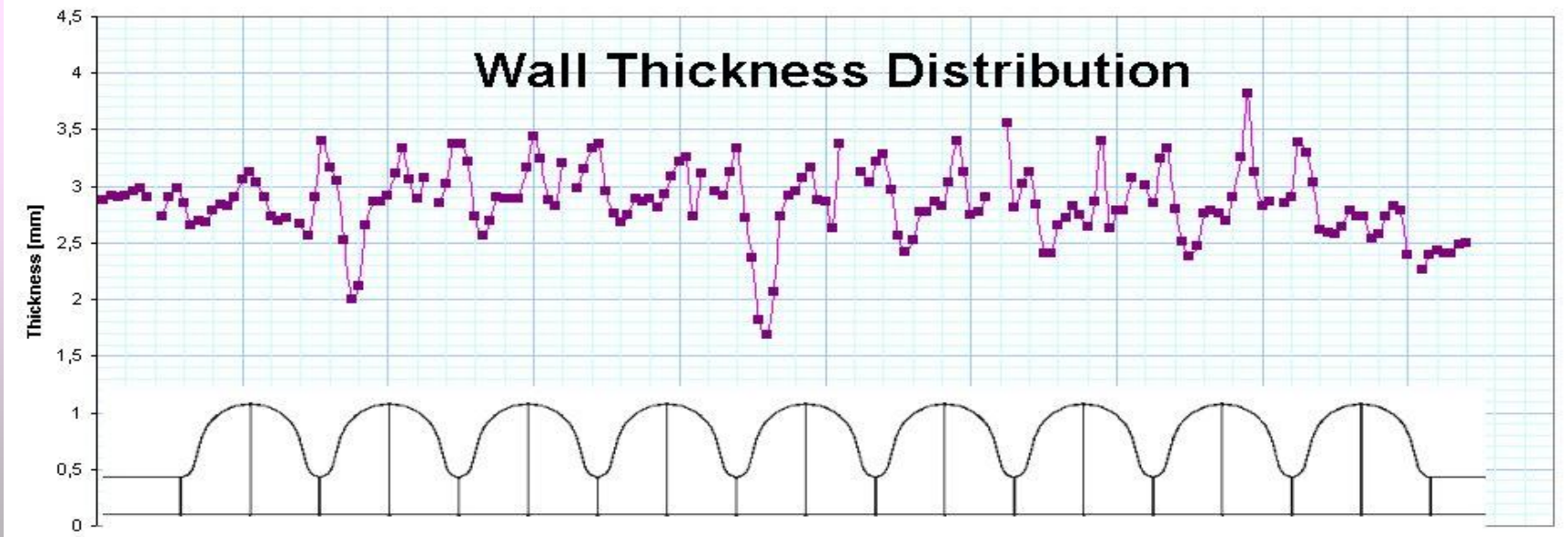
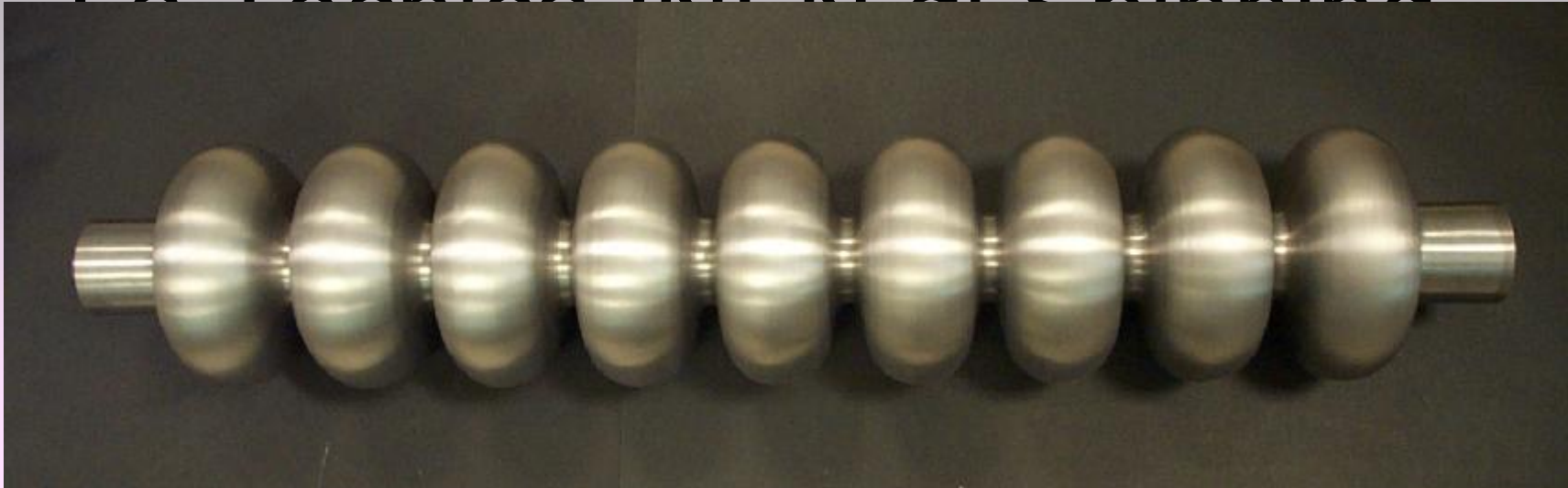


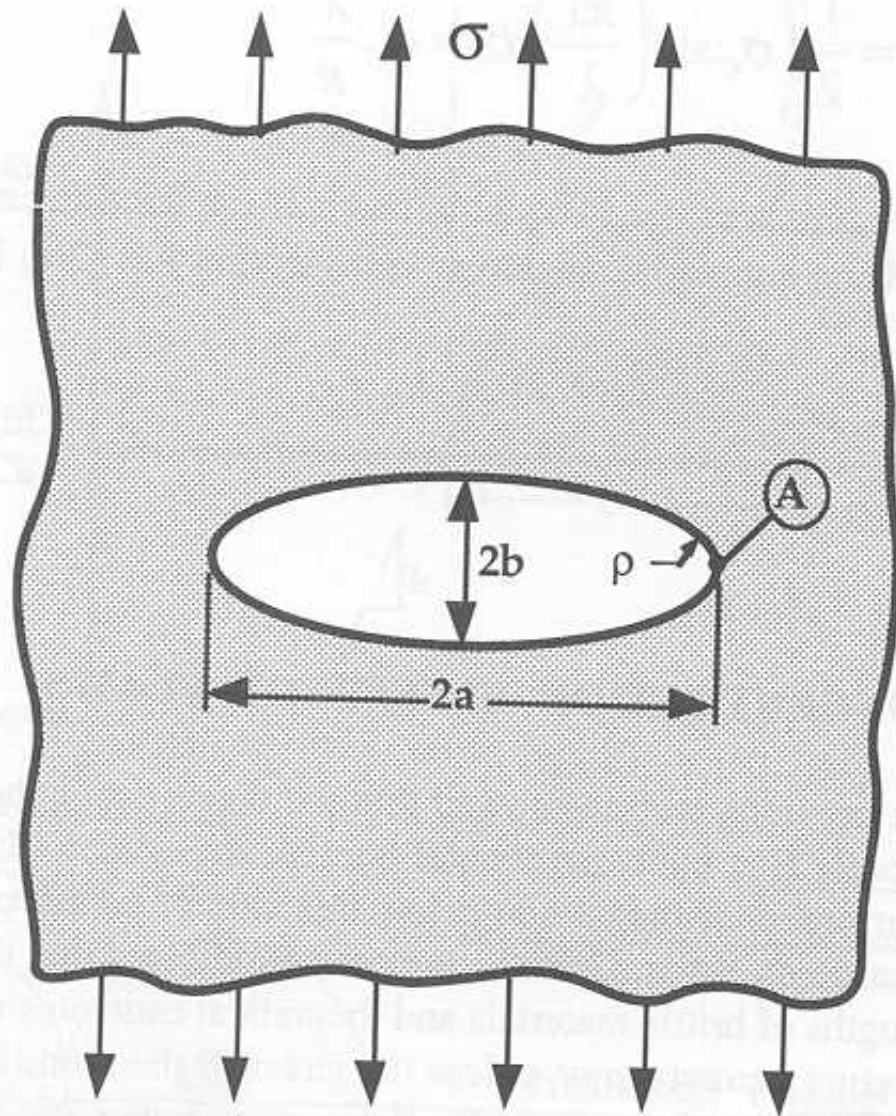






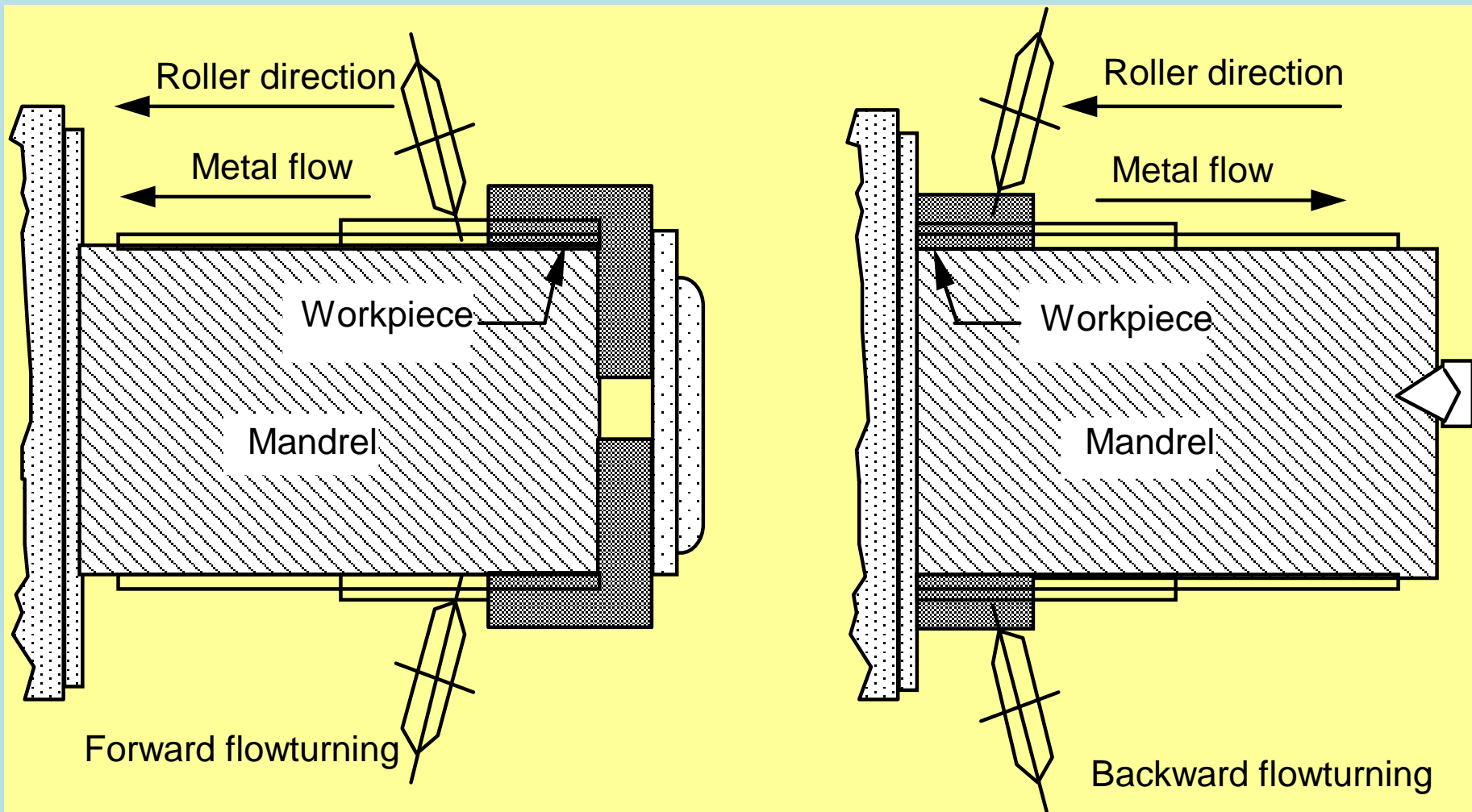
Le Teeorie INFN di Spinning





Elliptical hole in a flat plate.

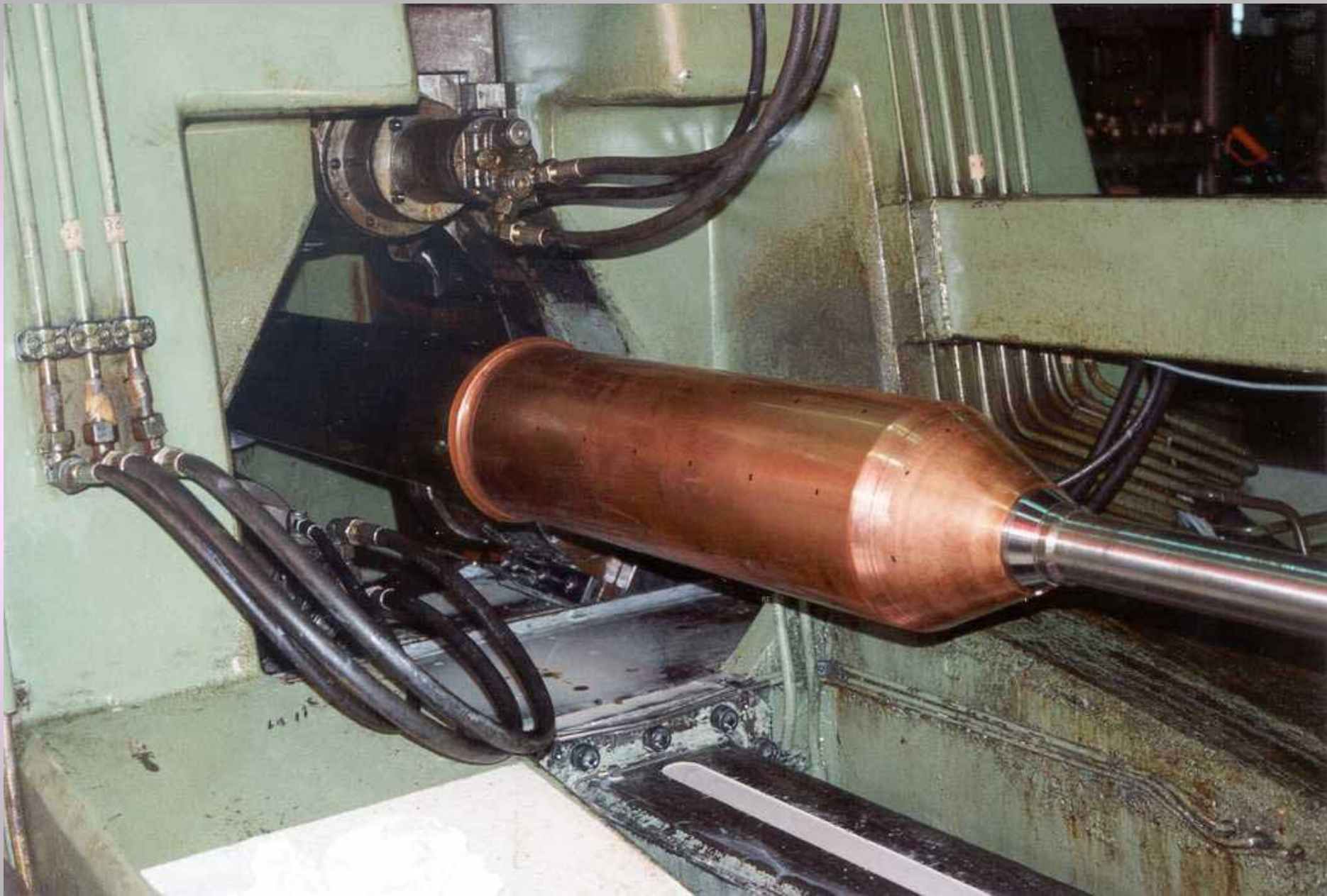
















Blankholder

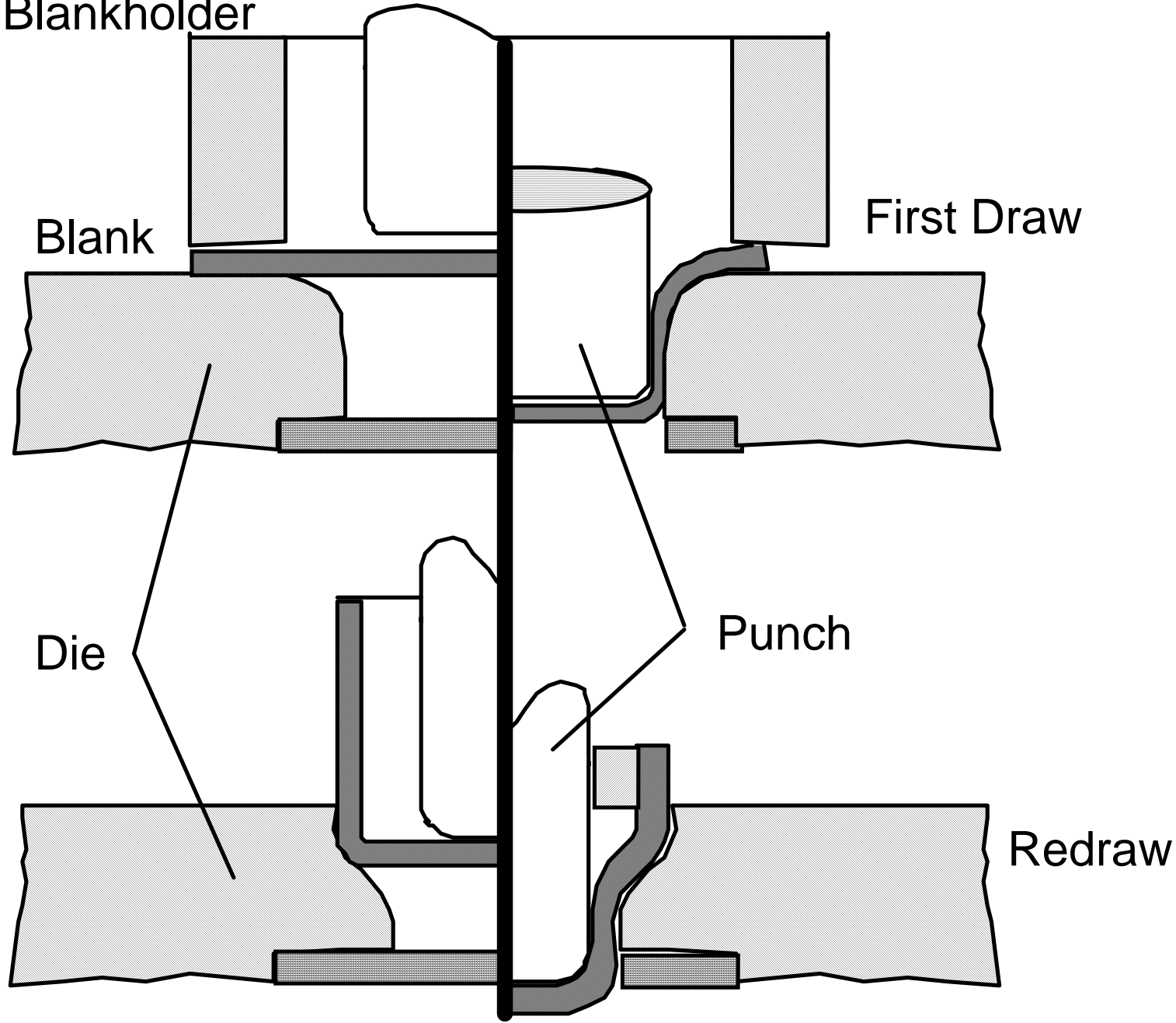
Blank

First Draw

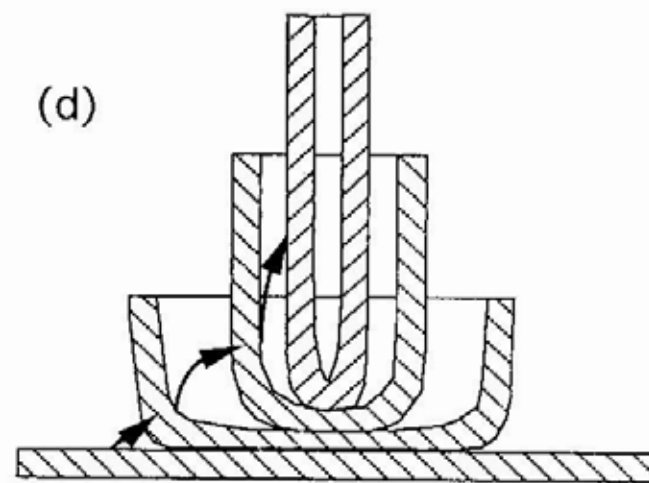
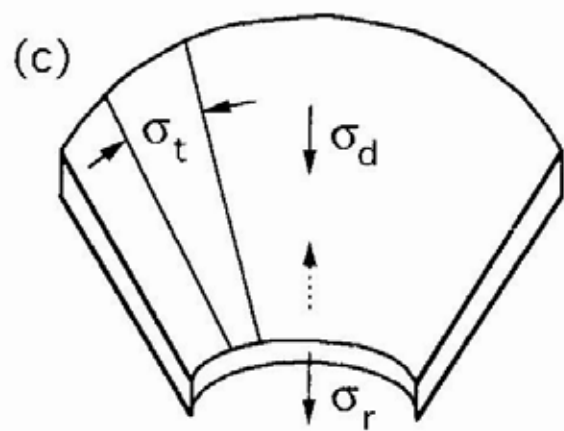
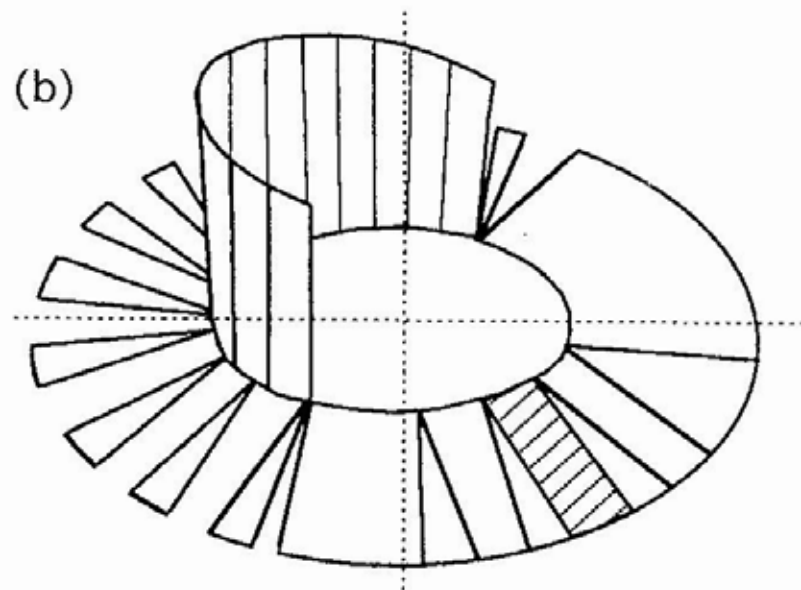
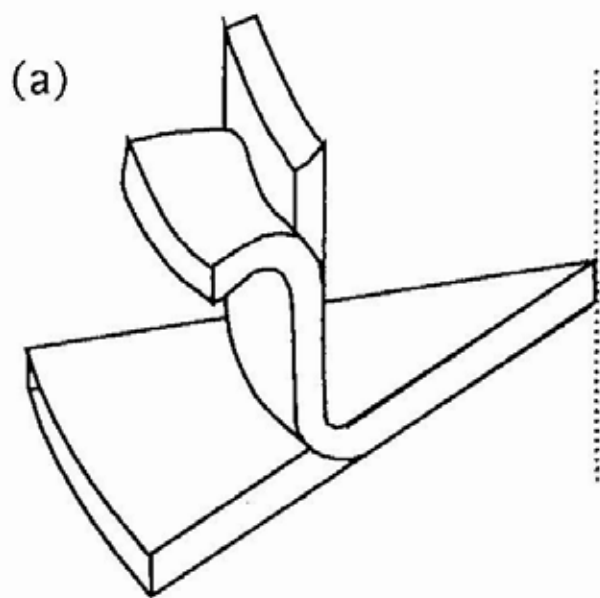
Die

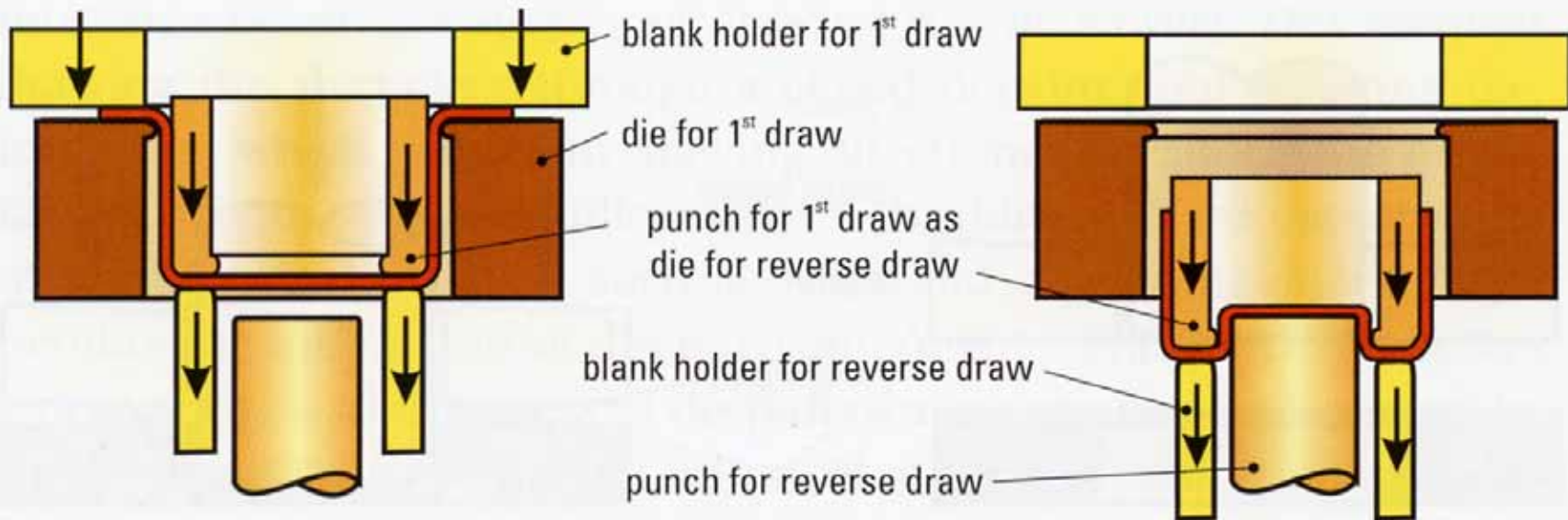
Punch

Redraw







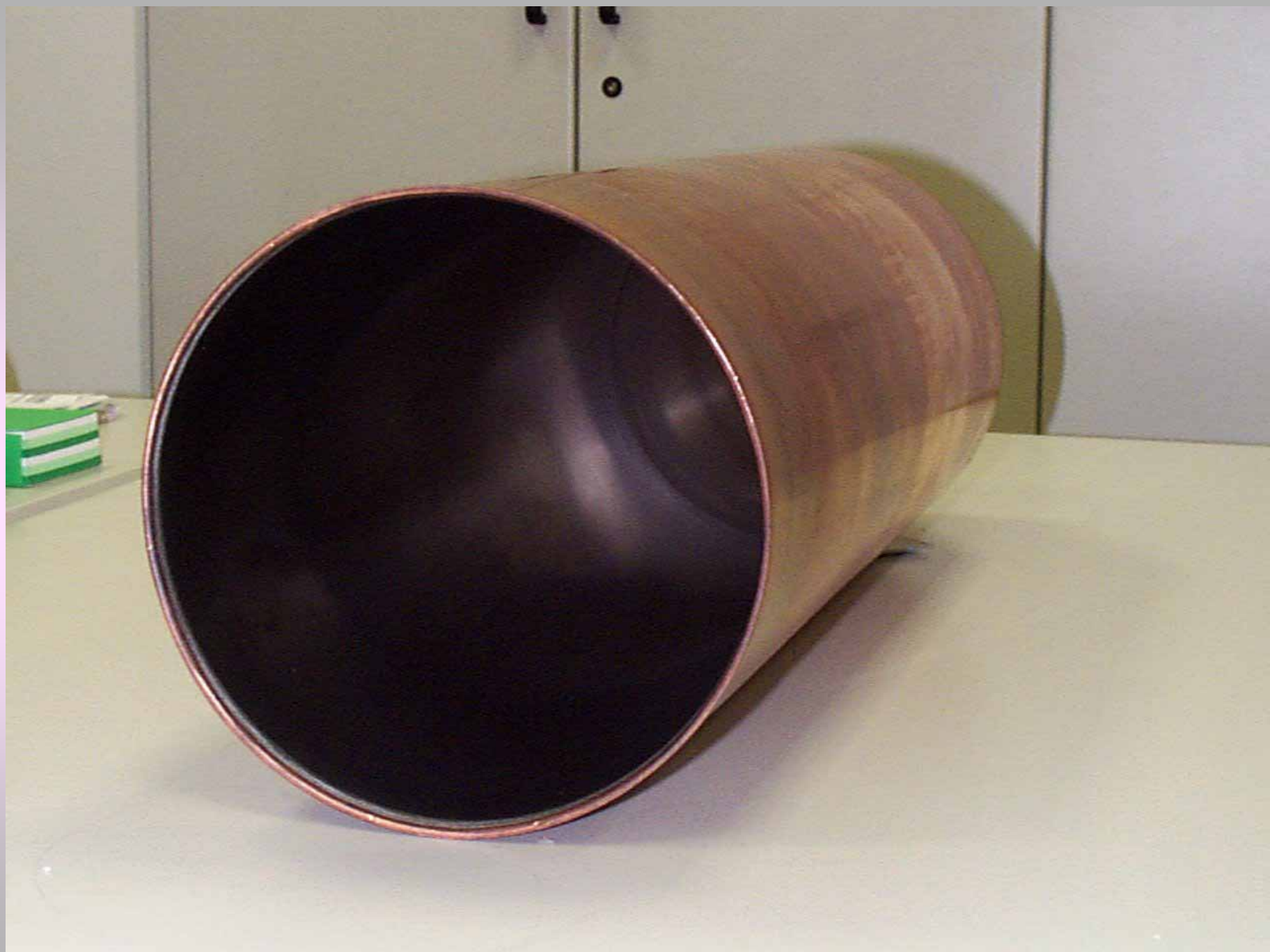






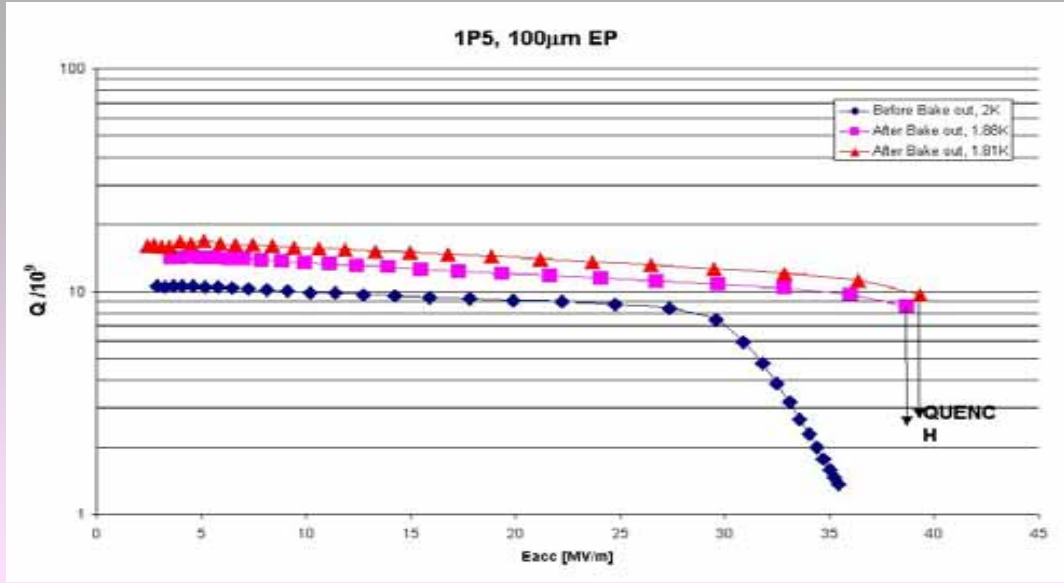




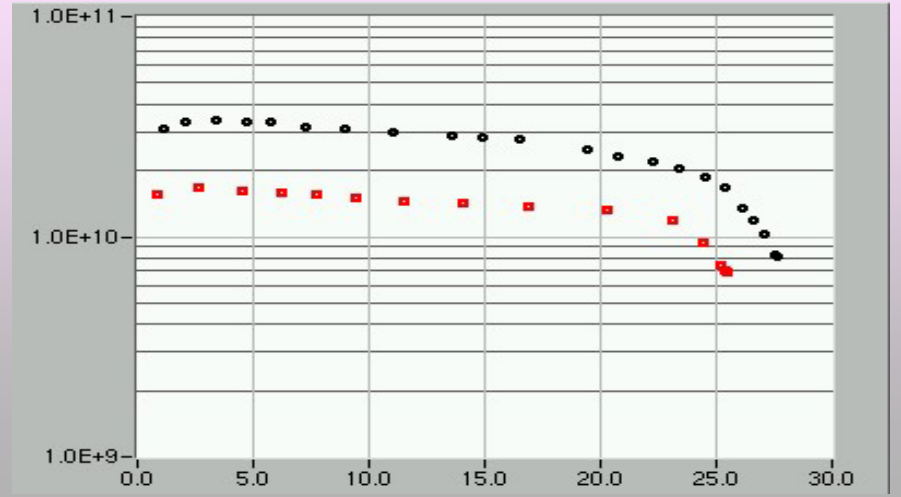








La 3-celle ha lo stesso andamento delle mono prima del trattamento meccanico











Thin film fabrication Techniques

Potential advantages

- Strong reduction of thermal instabilities
- Higher Q values (at 4.2K, BCS ...)
- Reduced magnetic field sensitivity
- Reduced field emission ?
- Possible use of different “substrates”
- Possible use of high T_C superconductors
- Cost !

Lep is operating with 288 4-cell thin film coated 350MHz cavities, the overall cost reduction with respect to bulk is estimated in 27,000,000 US\$

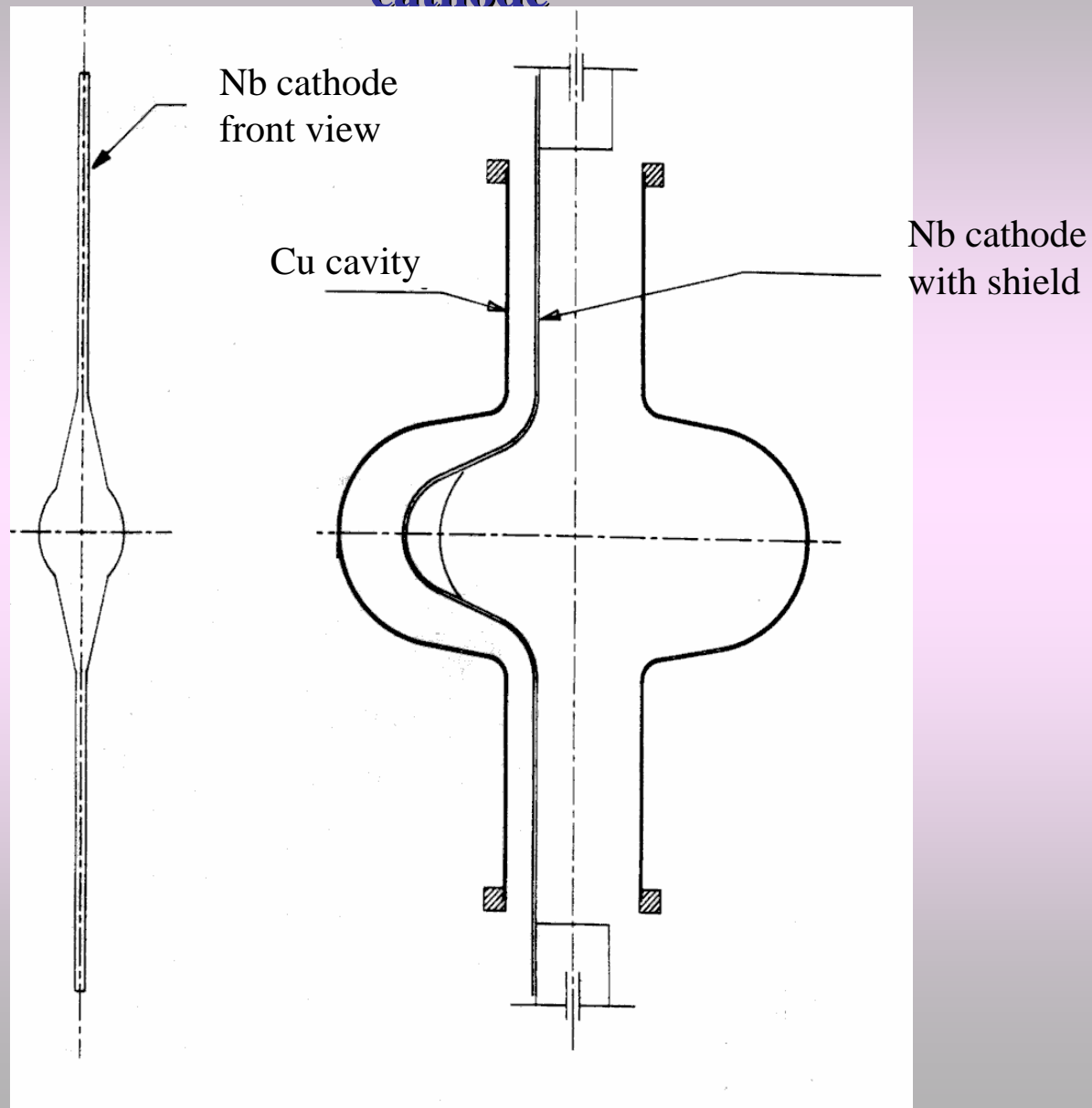
Problems

- Higher “Q - slope”
(especially for “innovative” superconductors)

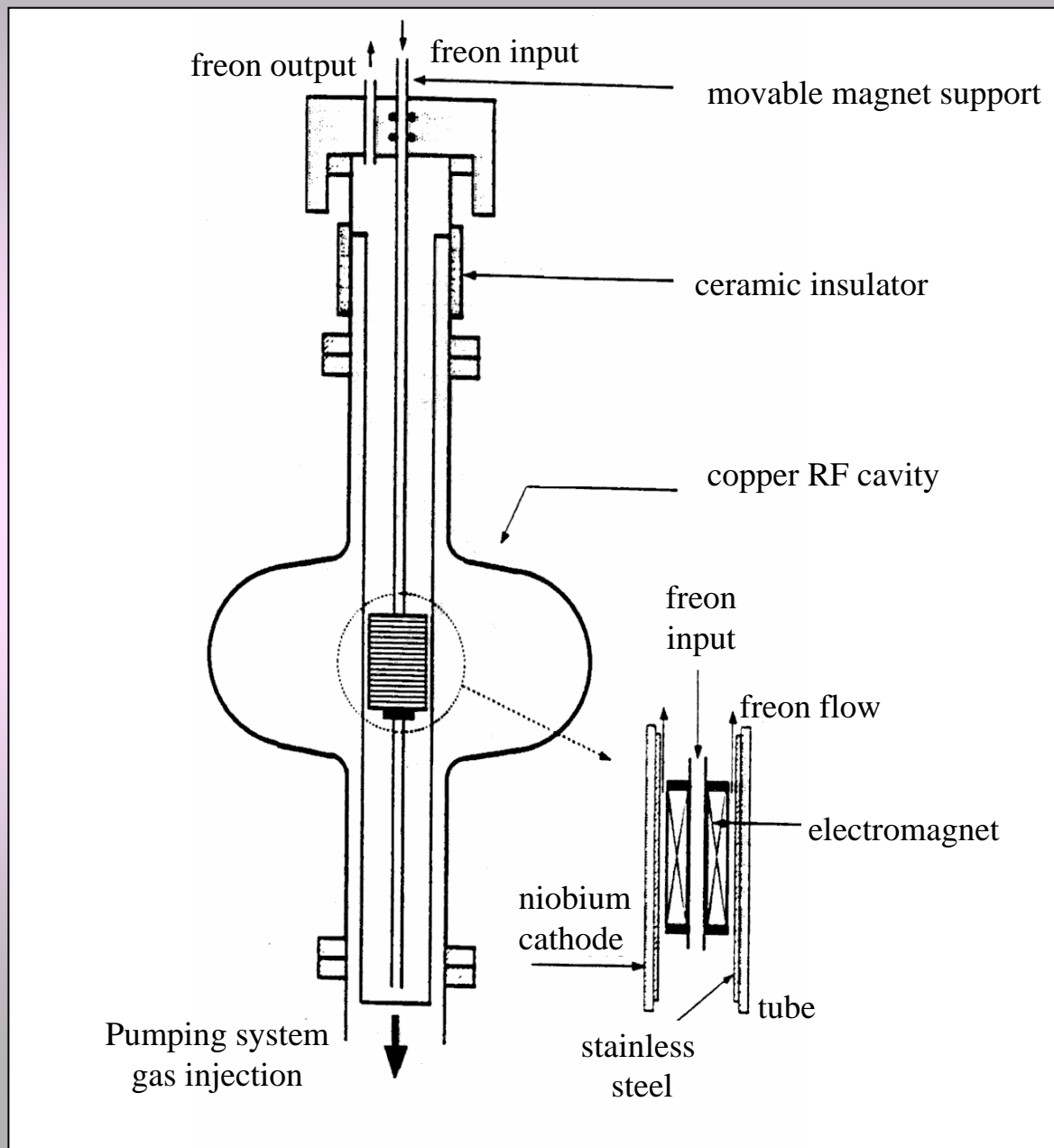
Thermal conductivity of best metals

Material	Purity	RRR	k [W/K cm]		
			4 K	9 K	16 K
Cu (OFHC)	99.995	103	6.5	14.2	22
Al	99.99	88	3.5	8	12.5
Al	99.999	2000	78	140	120
Ag	99.95	160	10.5	22	25
Au	99.95	130	6	12	15
Nb		250	0.4	3.5	3.5
			(0.9)	(6)	
Nb		400	0.7	5	4
			(1)	(8)	
Nb		1000	1.6	9	5

Schematic view of a 500 MHz cavity with diode sputtering cathode



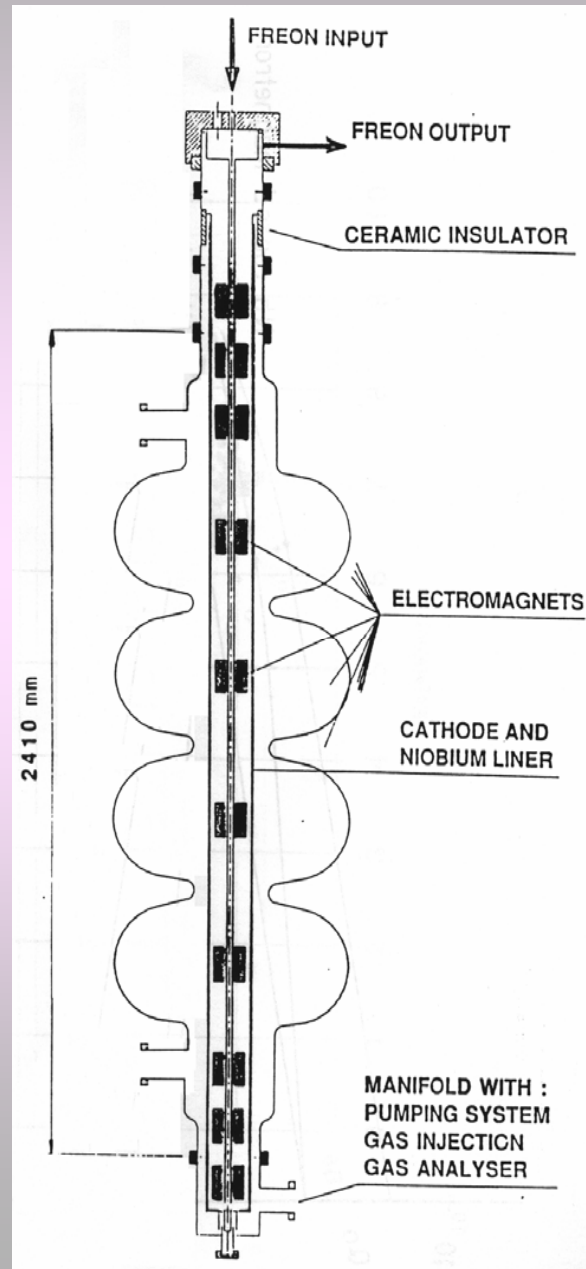
Schematic view of a magnetron sputtering configuration for single-cell cavity

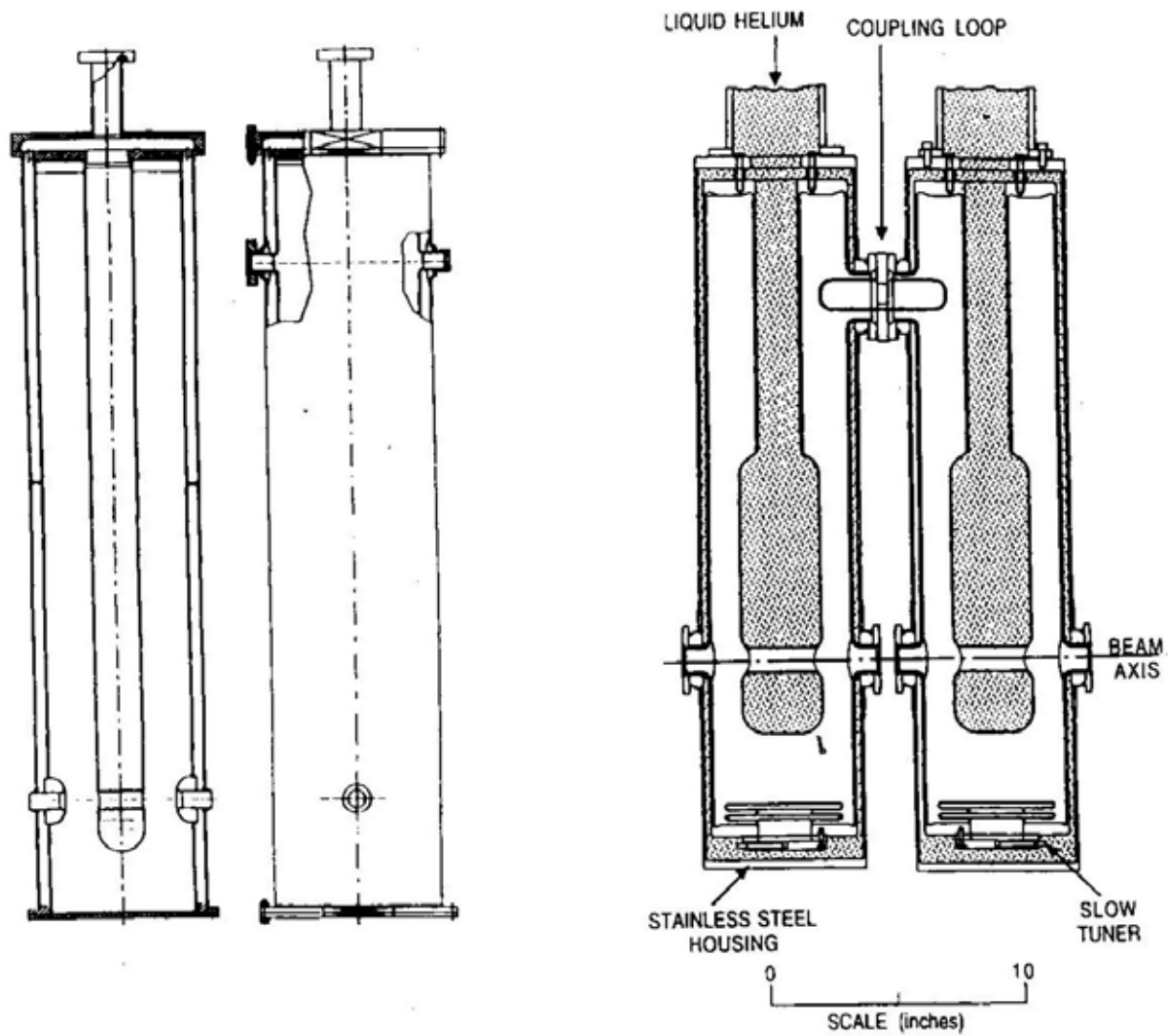




Magnetron insertion into 500 MHz cavity

Magnetron sputtering for 4-cell LEP cavities

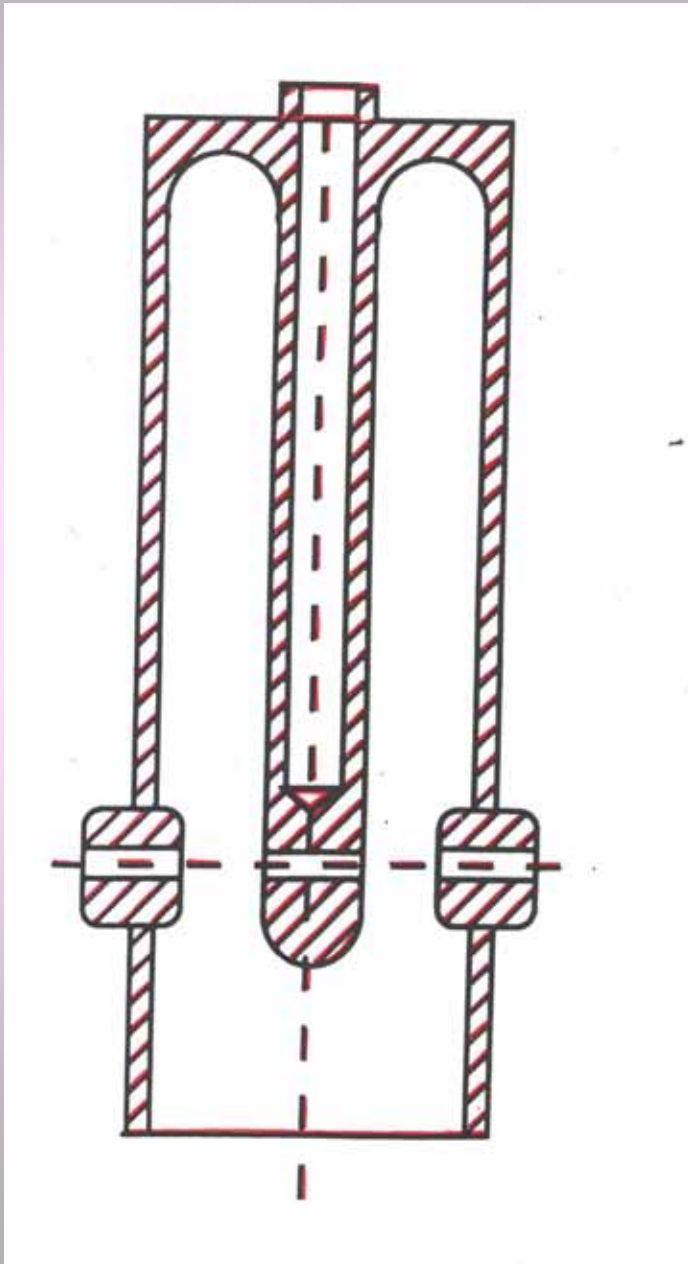




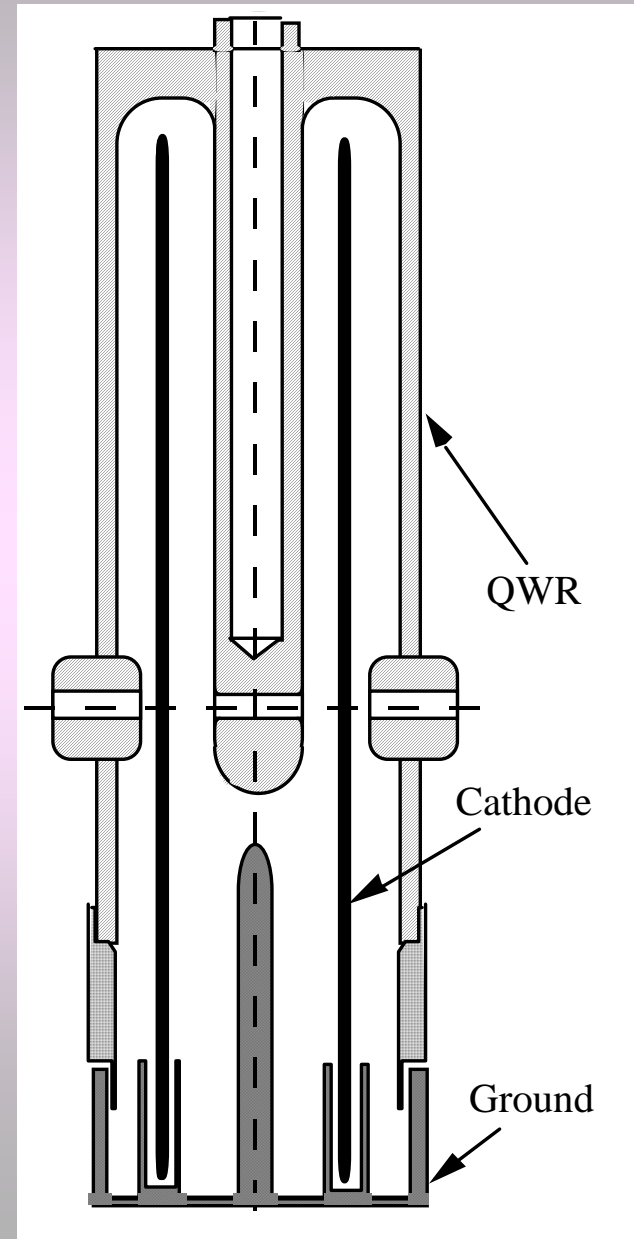
The Legnaro (left) and New Delhi (right) double wall bulk niobium QWRs



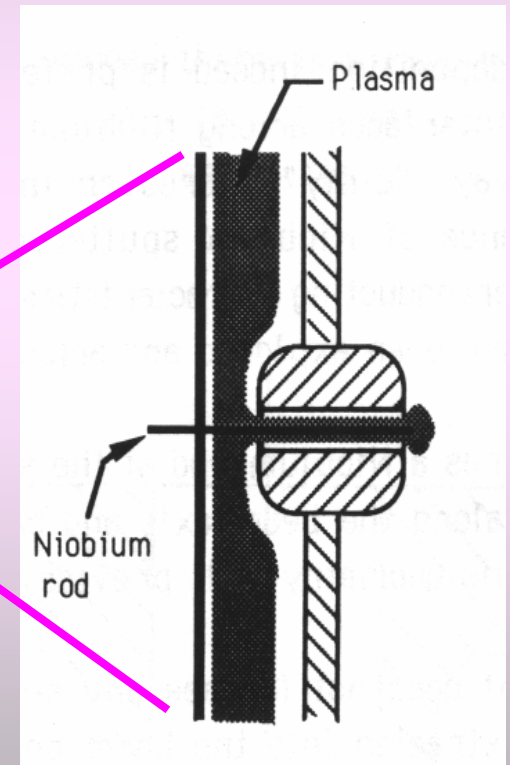
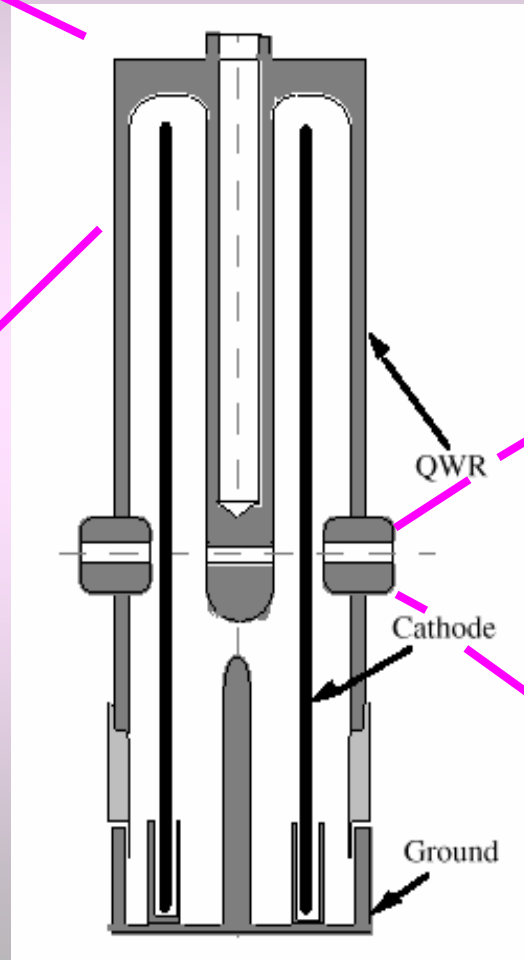
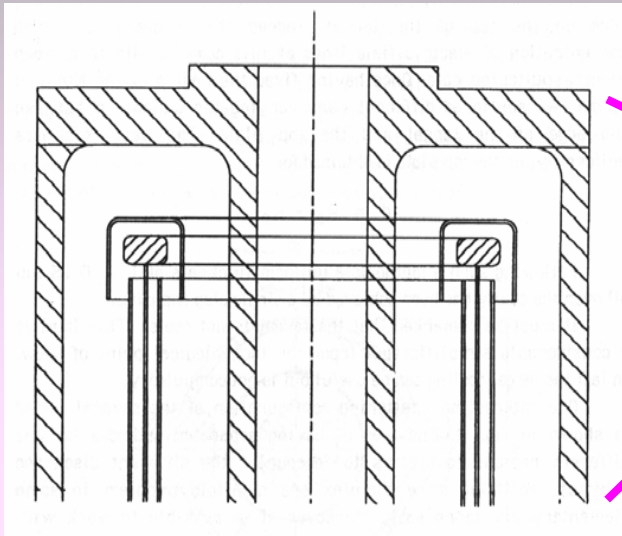
The cavity



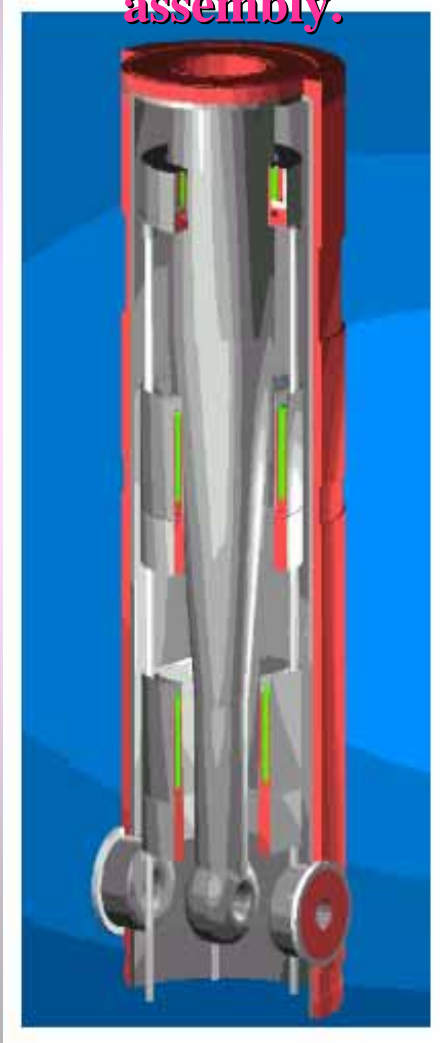
The sputtering configuration



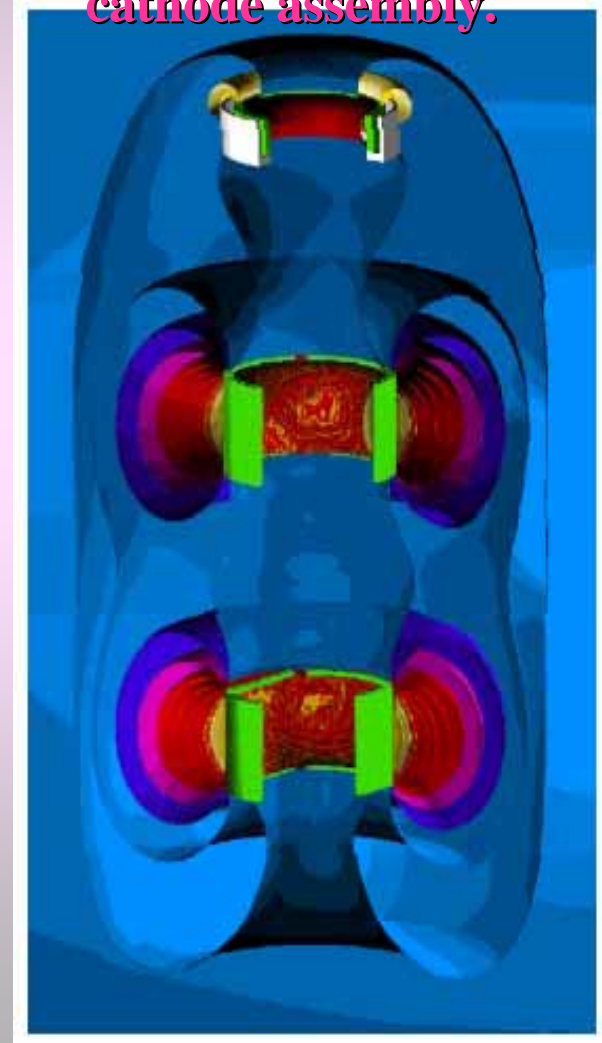
Niobium sputter-coated QWR



**Quarter-wave resonator with
magnetron sputtering
assembly.**



**Calculated magnetic field
distribution in the magnetron
cathode assembly.**





CENTRE
RESEARCH



